



Newfoundland and Labrador Hydro  
Hydro Place, 500 Columbus Drive  
P.O. Box 12400, St. John's, NL  
Canada A1B 4K7  
t. 709.737.1400 | f. 709.737.1800  
nlhydro.com

April 30, 2025

Board of Commissioners of Public Utilities  
Prince Charles Building  
120 Torbay Road, P.O. Box 21040  
St. John's, NL A1A 5B2

Attention: Jo-Anne Galarneau  
Executive Director and Board Secretary

**Re: Quarterly Report on Asset Performance in Support of Resource Adequacy for the Twelve Months Ended March 31, 2025**

Please find enclosed Newfoundland and Labrador Hydro's ("Hydro") Quarterly Report on Asset Performance in Support of Resource Adequacy for the Twelve Months Ended March 31, 2025.<sup>1</sup>

As included in the previous quarterly report, Hydro has included an update on the Muskrat Falls Assets to provide the Board of Commissioners of Public Utilities with additional information. This is provided as Appendix B to this report. Hydro has also provided two investigation reports related to the Labrador-Island Link as Attachment 1 and 2 to this report.

Should you have any questions, please contact the undersigned.

Yours truly,

**NEWFOUNDLAND AND LABRADOR HYDRO**

Shirley A. Walsh  
Senior Legal Counsel, Regulatory  
SAW/rr

Encl.

ecc:

**Board of Commissioners of Public Utilities**  
Jacqui H. Glynn  
Board General

**Island Industrial Customer Group**  
Paul L. Coxworthy, Stewart McKelvey  
Denis J. Fleming, Cox & Palmer  
Glen G. Seaborn, Poole Althouse

**Labrador Interconnected Group**  
Senwung F. Luk, Olthuis Kleer Townshend LLP  
Nicholas E. Kennedy, Olthuis Kleer Townshend LLP

**Consumer Advocate**  
Dennis M. Browne, KC, Browne Fitzgerald Morgan & Avis  
Stephen F. Fitzgerald, KC, Browne Fitzgerald Morgan & Avis  
Sarah G. Fitzgerald, Browne Fitzgerald Morgan & Avis  
Bernice Bailey, Browne Fitzgerald Morgan & Avis

**Newfoundland Power Inc.**  
Dominic J. Foley  
Douglas W. Wright  
Regulatory Email

<sup>1</sup> Formerly titled "Quarterly Report of Generating Units for the Twelve Months Ended []."

# Quarterly Report on Asset Performance in Support of Resource Adequacy

For the Twelve Months Ended March 31, 2025

April 30, 2025

A report to the Board of Commissioners of Public Utilities



## Contents

1.0	Introduction .....	1
2.0	Assumptions Used in Hydro’s Assessment of System Reliability and Resource Adequacy .....	3
3.0	Current Period Overview .....	5
4.0	Hydraulic Unit DAFOR Performance – Regulated Hydro .....	7
	Bay d’Espoir Facility .....	8
	4.1.1 Bay d’Espoir Unit 5 .....	8
	4.1.2 Bay d’Espoir Unit 6 .....	8
	4.1.3 Bay d’Espoir Unit 7 .....	9
	4.2 Granite Canal Facility .....	9
	4.3 Paradise River Facility .....	10
5.0	Hydraulic Unit DAFOR Performance – Muskrat Falls .....	10
	5.1 Muskrat Falls Unit 1 .....	12
6.0	Thermal Unit DAFOR Performance .....	12
	6.1 Holyrood TGS Unit 1 .....	13
	6.2 Holyrood TGS Unit 2 .....	14
7.0	Combustion Turbine DAUFOP Performance .....	15
	7.1 Stephenville Gas Turbine .....	18
	7.2 Holyrood Combustion Turbine .....	19
8.0	Labrador-Island Link EqFOR Performance .....	19

## List of Appendices

Appendix A: Soldiers Pond Synchronous Condensers

Appendix B: Muskrat Falls Asset Update – Reporting period up to March 31, 2025

## List of Attachments

Attachment 1: L3501/2 Failure Investigation OPGW Tower Peaks – Central Newfoundland

Attachment 2: L3501/2 Failure Investigation Ice Storm Southern Labrador

## **1.0 Introduction**

In this report, Newfoundland and Labrador Hydro (“Hydro”) provides data on forced outage rates of its generating facilities and the Labrador-Island Link (“LIL”). The data provided pertains to historical forced outage rates and assumptions Hydro uses in its assessments of resource adequacy. This report covers the performance for the current 12-month reporting period of April 1, 2024 to March 31, 2025 (“current period”).

This report contains forced outage rates for the current period for individual generating units at regulated hydraulic facilities,<sup>1</sup> the Holyrood Thermal Generating Station (“Holyrood TGS”), Hydro’s combustion turbines, and the non-regulated Muskrat Falls Hydroelectric Generating Facility (“Muskrat Falls Facility”). In addition, equivalent forced outage rates are provided for the 900 MW LIL.<sup>2</sup> This report also provides, for comparison purposes, the individual asset forced outage rates for the 12-month reporting period of April 1, 2023 to March 31, 2024 (“previous period”). Further, total asset class data is presented based on the calendar year for the remainder of the ten most recent years—2015 to 2024—with the exception of the Muskrat Falls Facility<sup>3</sup> and the LIL.<sup>4</sup>

The forced outage rates of Hydro’s generating units are calculated using two measures:

- 1)** Derated adjusted forced outage rate (“DAFOR”) for the continuous (base-loaded) units; and
- 2)** Derated adjusted utilization forced outage probability (“DAUFOP”) for the standby units.

DAFOR is a metric that measures the percentage of time that a unit or group of units is unable to generate at its maximum continuous rating due to forced outages or unit deratings. The DAFOR for each unit is weighted to reflect differences in generating unit sizes to provide a combined total and reflect the relative impact a unit’s performance has on overall generating performance. This measure is applied to

---

<sup>1</sup> Regulated hydraulic facilities include the Bay d’Espoir Hydroelectric Generating Facility (“Bay d’Espoir Facility” or “BDE”), the Cat Arm Hydroelectric Generating Station (“Cat Arm Station” or “CAT”), the Hinds Lake Hydroelectric Generating Station (“Hinds Lake Station” or “HLK”), the Upper Salmon Hydroelectric Generating Station (“Upper Salmon Station” or “USL”), the Granite Canal Hydroelectric Generating Station (“Granite Canal Station” or “GCL”), and the Paradise River Hydroelectric Generating Station (“Paradise River Station” or “PRV”).

<sup>2</sup> The LIL has been commissioned and is currently rated at 700 MW. As reported the latest Labrador Island Link update filed April 3, 2025, Hydro has postponed the 900 MW test to the fall of 2025, as the winter testing window is now closed due to system loading conditions.

<sup>3</sup> The final generating unit at the Muskrat Falls Facility was released for commercial operation on November 25, 2021. Annual DAFOR performance data is available beginning in 2022.

<sup>4</sup> The LIL was officially commissioned on April 13, 2023. Annual equivalent forced outage rate (“EqFOR”) data is only available for 2024 year end.

1 hydraulic units and, historically, was used for the thermal units; however, it does not apply to  
2 combustion turbines because of their operation as standby units and their relatively low operating  
3 hours.

4 DAUFOP is a metric that measures the percentage of time that a unit or group of units will encounter a  
5 forced outage and not be available when required. DAUFOP is a measure primarily used for combustion  
6 turbines; however, this measure may be applicable to thermal units, should their operation move  
7 towards standby operation in the future. This metric includes the impact of unit deratings.

8 The forced outage rates include outages that remove a unit from service completely as well as instances  
9 when units are derated. If a unit's output is reduced by more than 2%, the unit is considered derated  
10 under Electricity Canada guidelines. These guidelines require that the derated levels of a generating unit  
11 be calculated by converting the operating time at the derated level into an equivalent outage time.

12 As the LIL is not a generating unit, the above noted forced outage rate measures do not apply to this  
13 asset. Instead, Hydro has determined an appropriate metric to be an EqFOR to measure the  
14 performance of this asset as it relates to the supply of electricity to the Island. This EqFOR measures the  
15 percentage of time that the LIL bipole is unable to deliver its maximum continuous rating<sup>5</sup> to the Island  
16 due to forced outages, derates, or unplanned monopole outages. The effect of deratings and unplanned  
17 monopole outages is converted to equivalent bipole outage time using the same methodology as  
18 outlined above for generating units.

19 In addition to forced outage rates, this report provides details for those outages which occurred in the  
20 current period that contributed materially to forced outage rates exceeding those used in Hydro's  
21 resource adequacy planning analysis for both the near and long-term.

---

<sup>5</sup> The LIL maximum continuous rating is 700 MW at present.

## 2.0 Assumptions Used in Hydro’s Assessment of System Reliability and Resource Adequacy

Hydro continually assesses the reliability of its system and its ability to meet customer requirements, filing both near- and long-term assessments with the Board of Commissioners of Public Utilities.<sup>6</sup>

As part of the ongoing *Reliability and Resource Adequacy Study Review* proceeding, Hydro detailed the process undertaken for determining the forced outage rates most appropriate for use in its near-term reliability assessments and long-term resource adequacy analysis. Table 1 and Table 2 summarize the most recent forced outage rate assumptions, as determined using the forced outage rate methodology.<sup>7</sup> Forced outage rate assumptions will be re-evaluated on an annual basis to incorporate the most recent data available.

**Table 1: Hydro’s Reliability and Resource Adequacy Study Analysis Values – Generating Units (%)**

Asset Type	Measure	Near-Term Analysis Value	Resource Planning Analysis Value
Hydraulic: Regulated	DAFOR	3.60	3.03
Hydraulic: Muskrat Falls	DAFOR	2.30	3.03
Thermal	DAUFOP	20.00 <sup>8</sup>	20.00
Combustion Turbines			
Happy Valley	DAUFOP	4.65	4.65
Hardwoods and Stephenville	DAUFOP	30.00	30.00
Holyrood	DAUFOP	4.90	4.90

A three-year, capacity-weighted average was applied to the regulated hydraulic units (Bay d’Espoir Facility, Cat Arm Station, Hinds Lake Station, Granite Canal Station, Upper Salmon Station, and Paradise River Station) for a near-term analysis, resulting in a DAFOR of 3.60%, while a ten-year, capacity-weighted average was applied for use in the long-term resource planning model, resulting in a DAFOR of

<sup>6</sup> Hydro currently files an assessment of near-term system reliability and resource adequacy annually in November, the Near-Term Reliability Report. Hydro also files an assessment of longer-term system reliability and resource adequacy. The most recent filing was the “2024 Resource Adequacy Plan: An Update to the Reliability and Resource Adequacy Study,” Newfoundland and Labrador Hydro, rev. 2, August 26, 2025 (originally filed July 9, 2024), (“2024 Resource Plan”).

<sup>7</sup> Values indicated for Hydro’s near-term analysis reflect those used in the 2024 Resource Plan and the “Reliability and Resource Adequacy Study Review – 2024 Near-Term Reliability Report – November Report,” Newfoundland and Labrador Hydro, November 20, 2024 (“November 2024 Near-Term Report”).

<sup>8</sup> The Holyrood TGS base assumption is 20.00%. The sensitivity assumption is 34.00%. A sensitivity value of 34.00% was chosen to reflect actual performance at the Holyrood TGS for the 2021–2022 winter operating period.

1 3.03%. The DAFOR value was based on historical data reflective of Hydro’s maintenance program over  
2 the long-term.

3 For the Muskrat Falls Facility, the near-term forced outage rate was based on the forced outage rates of  
4 the units to date, to reflect the possibility of outages early in the lifetime of the Muskrat Falls Facility. In  
5 the long-term resource planning model, the regulated hydroelectric forced outage rate was used, as it is  
6 assumed that these assets will be maintained to the same standards as the remainder of the hydraulic  
7 fleet.

8 Historically, forced outage rates for the three units at the Holyrood TGS have been reported using the  
9 DAFOR metric, which is predominately used for units that operate in a continuous (base-loaded)  
10 capacity. As presented in Hydro’s RRA Study 2022 Update,<sup>9</sup> there are reliability concerns associated with  
11 the operation of the units at the Holyrood TGS in an emergency standby capacity. When considering  
12 standby or peaking operations of units at the Holyrood TGS, DAFOR is no longer the most appropriate  
13 measure of forced outage rates; instead, UFOP<sup>10</sup> and DAUFOP should be considered. Given the  
14 frequency of deratings historically experienced by these units, DAUFOP is a more appropriate measure.

15 Analyses performed for a range of Holyrood TGS DAUFOP assumptions indicate the sensitivity of supply  
16 adequacy to changes in the availability of the Holyrood TGS. From this analysis, a forced outage rate of  
17 20.00% was recommended in the near-term, with a sensitivity value of 34.00%. Hydro will continue to  
18 analyze the operational data to ensure that forced outage rate assumptions for the Holyrood TGS are  
19 appropriate.

20 At present time, the operation of the units at the Holyrood TGS remains base-loaded to ensure the  
21 availability of capacity for the power system, as the LIL is recently commissioned and in the early  
22 operational stages. This will remain the case as Hydro continues to monitor LIL performance and  
23 reliability. If the LIL is found to perform well for an extended period, and system conditions permit,  
24 Hydro will have the opportunity to incrementally remove the Holyrood TGS units from service. To  
25 ensure alignment with the assumptions used in the resource planning model (PLEXOS)<sup>11</sup> while

---

<sup>9</sup> “Reliability and Resource Adequacy Study – 2022 Update,” Newfoundland and Labrador Hydro, October 3, 2022 (“RRA Study 2022 Update”).

<sup>10</sup> Utilization forced outage probability (“UFOP”).

<sup>11</sup> The resource planning model does not differentiate between DAFOR and DAUFOP metrics; rather, it applies a forced outage rate only.

1 appropriately reporting on current period versus historical performance, Hydro will continue to use the  
2 DAFOR performance measure and the 20.00% forced outage rate for the units at the Holyrood TGS.

3 As the combustion turbines in the existing fleet vary in age and condition, each was considered on an  
4 individual basis. For the Happy Valley Gas Turbine, a three-year, capacity-weighted average was applied  
5 to the unit for the near-term analysis while a ten-year capacity-weighted average was applied for use in  
6 the resource planning model. The DAUFOP values were based on historical data to reflect the unit’s past  
7 performance. For the Holyrood Combustion Turbine (“Holyrood CT”) the DAUFOP was calculated based  
8 on a scenario-based approach rather than historical data, due to the unit’s minimal operating time and  
9 resultant small data set. For the Hardwoods and Stephenville Gas Turbines, a fixed DAUFOP consistent  
10 with values considered in Hydro’s previous near-term reliability reports was used for the near-term and  
11 long-term analyses.<sup>12</sup> As presented in Hydro’s 2024 Resource Plan, the Hardwoods and Stephenville Gas  
12 Turbines are proposed for retirement in 2030.

13 Now that the LIL is commissioned, multiple years of operational experience are required to better  
14 inform the long-term selection of a bipole forced outage rate. In the interim, the bipole forced outage  
15 rate will be addressed with a range of upper and lower limits as additional scenarios in the analysis -  
16 currently 10% and 1%, respectively. As LIL performance statistics become available in the coming years,  
17 the forced outage rate range may be narrowed. However, the current base-case assumption is a 5% LIL  
18 forced outage rate.

**Table 2: Hydro’s Reliability and Resource Adequacy Study Analysis Values – LIL (%)**

Asset Type	Measure	Base Planning Analysis Value	Range of Planning Analysis Values
LIL	EqFOR	5	1–10

### 19 **3.0 Current Period Overview**

20 Table 3 presents an overview of the current period performance, compared to previous period  
21 performance and most recent Planning Analysis values.

---

<sup>12</sup> “Reliability and Resource Adequacy Study Review – 2024 Near-Term Reliability Report – November Report,” Newfoundland and Labrador Hydro, November 20, 2024.

**Table 3: DAFOR and DAUFOP Overview (%)**

<b>Asset Type</b>	<b>Measure</b>	<b>1-Apr-2023 to 31-Mar-2024</b>	<b>1-Apr-2024 to 31-Mar-2025</b>	<b>Near-Term Planning Analysis Value</b>	<b>Resource Planning Analysis Value</b>
Hydraulic: Regulated	DAFOR	6.15	2.13	3.60	3.03
Hydraulic: Muskrat Falls Facility	DAFOR	0.79	2.28	2.30	3.03
Thermal	DAFOR/DAUFOP <sup>13</sup>	43.07	31.92	20.00	20.00
<b>Combustion Turbines</b>					
Happy Valley	DAUFOP	23.38	0.00	4.65	4.65
Hardwoods/Stephenville	DAUFOP	43.32	28.20	30.00	30.00
Holyrood	DAUFOP	5.71	8.57	4.90	4.90

1 As shown in Table 3, regulated hydraulic DAFOR and thermal performance improved for the current  
 2 period, while the Muskrat Falls Facility DAFOR performance declined for the current period, when  
 3 compared to the previous period.

4 The DAUFOP performance for the Hardwoods and Stephenville Gas Turbines and the Happy Valley Gas  
 5 Turbine have improved in the current period, while the Holyrood CT has declined in the current period,  
 6 compared to the previous period.

7 Table 4 presents LIL data for the current and the previous period. Since the previous filing, the  
 8 performance of the LIL has improved slightly, with no significant impacts to the EqFOR because of any  
 9 operational events that have occurred.

<sup>13</sup> The resource planning model does not differentiate between DAFOR and DAUFOP; rather, it requires the selection of a forced outage rate percentage.

**Table 4: EqFOR Overview (%)**

Asset Type	Measure	1-Apr-2023 to 31-Mar-2024	1-Apr-2024 to 31-Mar-2025	Base Planning Analysis Value	Range of Planning Analysis Values
LIL	EqFOR	2.70 <sup>14</sup>	0.86 <sup>15</sup>	5	1–10

## 4.0 Hydraulic Unit DAFOR Performance – Regulated Hydro

Detailed results for the current period and the previous period are presented in Table 5 and Chart 1. These results are compared to Hydro’s near-term and resource planning analysis values for forced outage rates, as used in the 2024 Resource Plan and the November 2024 Near-Term Report. Any individual unit with forced outage rates which exceed the established near-term and/or resource planning analysis values is discussed herein.

**Table 5: Hydraulic Weighted DAFOR – Regulated Hydro**

Generating Unit	Maximum Continuous Unit Rating (MW)	12 Months Ended Mar 2024 (%)	12 Months Ended Mar 2025 (%)	Near-Term Analysis Value (%)	Resource Planning Analysis Value (%)
<b>All Hydraulic Units – Weighted</b>	<b>954.4</b>	<b>6.15</b>	<b>2.13</b>	<b>3.60</b>	<b>3.03</b>
<b>Hydraulic Units</b>					
BDE Unit 1	76.5	0.00	0.00	3.60	3.03
BDE Unit 2	76.5	0.16	0.00	3.60	3.03
BDE Unit 3	76.5	0.00	2.75	3.60	3.03
BDE Unit 4	76.5	0.24	0.71	3.60	3.03
BDE Unit 5	76.5	0.00	5.09	3.60	3.03
BDE Unit 6	76.5	34.56	8.53	3.60	3.03
BDE Unit 7	154.4	0.00	3.88	3.60	3.03
CAT Unit 1	67	0.24	0.84	3.60	3.03
CAT Unit 2	67	0.00	0.07	3.60	3.03
HLK Unit	75	0.88	1.41	3.60	3.03
USL Unit	84	53.90	0.34	3.60	3.03
GCL Unit	40	2.54	3.55	3.60	3.03
PRV Unit	8	0.33	7.87	3.60	3.03

<sup>14</sup> The LIL was not commissioned until April 14, 2023.

<sup>15</sup> This EqFOR is calculated on a base LIL capacity of 700 MW. On a base capacity of 900 MW, the EqFOR is calculated to be approximately 2.56%. Following the completion of the 900 MW test, all calculations will be adjusted to reflect the change in assumptions.

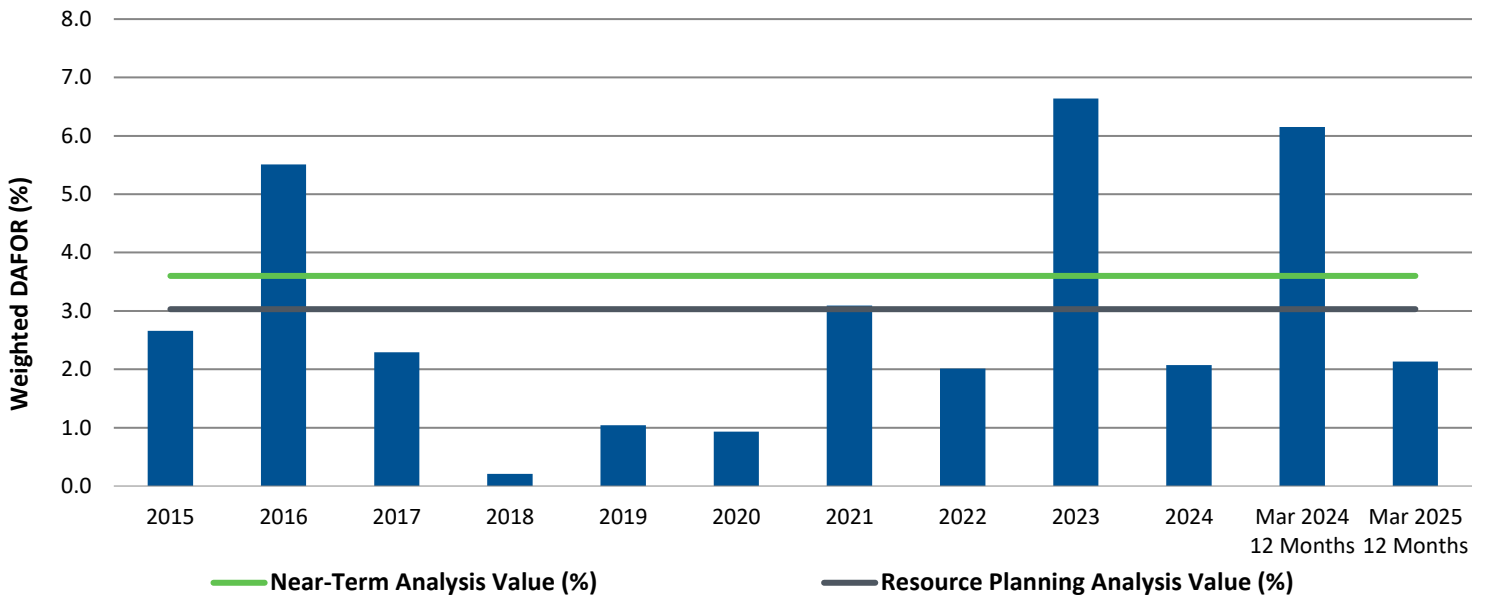


**Chart 1: Hydraulic Weighted DAFOR – Regulated Hydro**

**1 Bay d’Espoir Facility**

**2 4.1.1 Bay d’Espoir Unit 5**

3 Considering individual hydraulic unit performance, the Bay d’Espoir Unit 5 DAFOR of 5.09% is above the  
 4 resource planning analysis value of 3.03% and the near-term planning analysis value of 3.60% for an  
 5 individual hydraulic unit. The DAFOR was materially impacted in the current period by a forced  
 6 extension to the planned annual outage, which occurred in May 2024, as previously reported.<sup>16</sup> The unit  
 7 has been operating without issue since it returned to service on May 25, 2024.

**8 4.1.2 Bay d’Espoir Unit 6**

9 Considering individual hydraulic unit performance, the Bay d’Espoir Unit 6 DAFOR of 8.53% is above the  
 10 resource planning analysis value of 3.03% and the near-term planning analysis value of 3.60% for an  
 11 individual hydraulic unit. As previously reported, this increase in DAFOR was primarily the result of the  
 12 forced extension to the planned outage, which occurred in May 2024 as a result of foreign material  
 13 impact to several stator bars.<sup>17</sup> To return the unit to service and allow the necessary preparation time

<sup>16</sup> “Quarterly Report on Asset Performance in Support of Resource Adequacy for the Twelve Months Ended June 30, 2024,” Newfoundland and Labrador Hydro, sec. 4.1.1, pp. 8-9.

<sup>17</sup> Ibid, sec. 4.1.2, pp. 9-10.

1 for a larger work scope, all affected stator bars were repaired and the unit returned to operation on  
2 May 30, 2024.

3 Again, as previously reported, given the new age of this asset, the extent of damage and the significant  
4 operational stresses imposed on the damaged bars, the appropriate long-term solution recommended  
5 by the original equipment manufacturer to prevent premature aging and failure of the asset was to  
6 proceed with the replacement of approximately 10 stator bars at the next available outage opportunity.

7 A scheduled outage on Unit 6 commenced on July 5, 2024 to complete approved capital replacement  
8 work in the switchyard to replace a circuit breaker (B3T6); Hydro completed the necessary work to  
9 replace the affected stator bars and the unit was returned to service on August 23, 2024.

#### 10 **4.1.3 Bay d’Espoir Unit 7**

11 The Bay d’Espoir Unit 7 DAFOR of 3.88% for the current period is above the resource planning analysis  
12 value of 3.03% and the near-term planning analysis value of 3.60% for an individual hydraulic unit. This  
13 increase in DAFOR was the result of a forced outage, which occurred on August 2, 2024, when leaks  
14 were discovered in the generator bearing coolers following the completion of the scheduled annual  
15 outage on Unit 7, as previously reported.<sup>18</sup> As of December 2024, all coolers currently installed on the  
16 unit are new.

#### 17 **4.2 Granite Canal Facility**

18 The Granite Canal unit DAFOR of 3.55% for the current period is above the resource planning analysis  
19 value of 3.03% but is below the near-term planning analysis value of 3.60% for an individual hydraulic  
20 unit. This increase in DAFOR is primarily the result of seven forced outages in the current period.

21 The unit experienced three forced outages due to vibration that occurred during operation in the  
22 hydraulic rough zone, resulting in trips to the unit. These outages occurred on September 13, 2024,  
23 October 19, 2024 and December 22, 2024, and in all instances, Operations staff were dispatched to site  
24 to inspect the plant for anomalies and return the unit to service.

25 Additionally, there were four forced outages that were a result of high bearing oil level alarms. These  
26 outages occurred on November 2, 2024, November 24, 2024, December 5, 2024, and finally from

---

<sup>18</sup> “Quarterly Report on Asset Performance in Support of Resource Adequacy for the Twelve Months Ended September 30, 2024”, Newfoundland and Labrador Hydro, October 31, 2024.

1 January 24–28, 2025. In the first three instances, inspections were completed and no anomaly was  
2 discovered with the unit. During the January 2025 outage, the unit was removed from service after a  
3 high oil level alarm was received on the generator thrust/guide bearing assembly. It was discovered that  
4 air had been entering the oil piping, resulting in a false high-level reading on the transducer.  
5 Modifications were made to the piping layout to prevent air from entering the assembly, and monitoring  
6 of oil level readings over time confirmed the situation has been resolved.

### 7 **4.3 Paradise River Facility**

8 The Paradise River unit DAFOR of 7.87% is above the resource planning analysis value of 3.03% and the  
9 near-term planning analysis value of 3.60% for an individual hydraulic unit. This increase in DAFOR was  
10 the result of two forced outages, as previously reported. The first, a leak in the penstock expansion joint  
11 located in the lower level of the plant. The packing in the expansion joint was replaced in the affected  
12 area and the unit was returned to service on August 24, 2024. The second, from December 5–7, 2024  
13 when the unit was made unavailable due to a low bearing oil level alarm.

## 14 **5.0 Hydraulic Unit DAFOR Performance – Muskrat Falls**

15 Detailed results for the current period and the previous period are presented in Table 6 and Chart 2.  
16 These results are compared to Hydro’s near-term and resource planning analysis values for forced  
17 outage rates, as used in the 2024 Resource Plan and the November 2024 Near-Term Report. Overall, the  
18 plant performance for the Muskrat Falls Facility shows a decline over the previous period, with the  
19 performance of all individual units meeting the established near-term and resource planning analysis  
20 values, with the exception of Muskrat Falls Unit 1, which is discussed below.

**Table 6: Hydraulic Weighted DAFOR – Muskrat Falls**

Generating Unit	Maximum Continuous Unit Rating (MW)	12 Months Ended Mar 2024 (%)	12 Months Ended Mar 2025 (%)	Near-Term Analysis Value (%)	Resource Planning Analysis Value (%)
<b>Muskrat Falls Units - weighted</b>	<b>824</b>	<b>0.79</b>	<b>2.28</b>	<b>2.30</b>	<b>3.03</b>
<b>Muskrat Falls Units</b>					
Muskrat Falls 1	206	2.38	7.74	2.30	3.03
Muskrat Falls 2 <sup>19</sup>	206	0.94	0.74	2.30	3.03
Muskrat Falls 3	206	0.11	0.13	2.30	3.03
Muskrat Falls 4	206	0.01	0.02	2.30	3.03

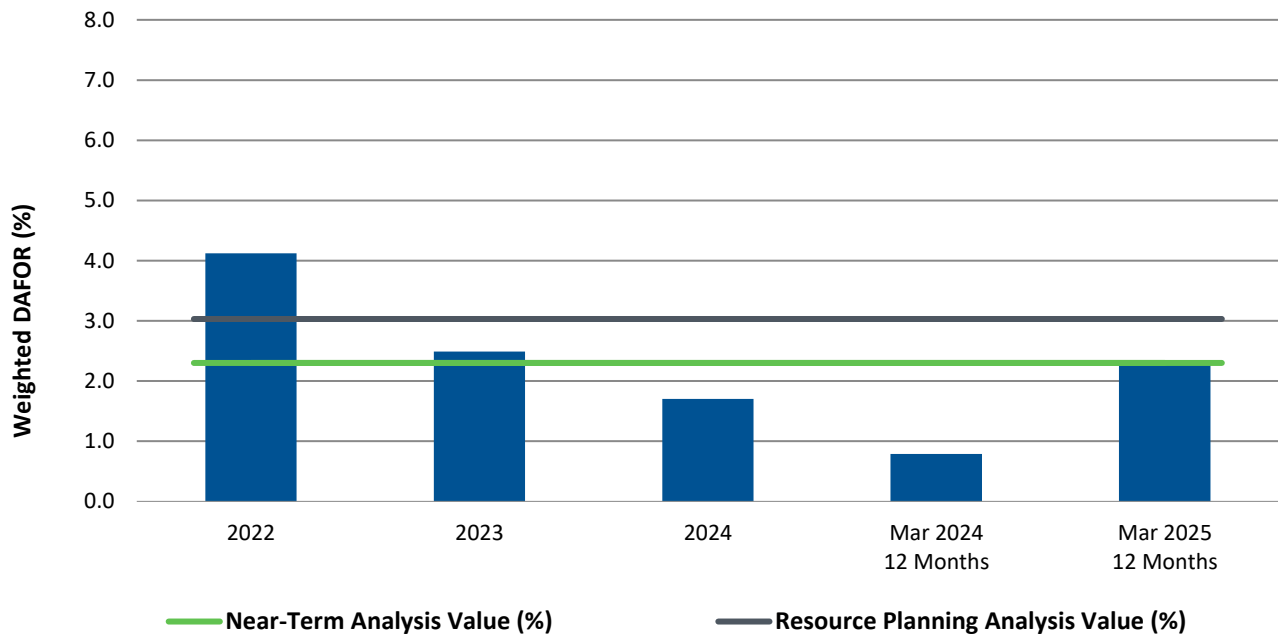


**Chart 2: Hydraulic Weighted DAFOR – Muskrat Falls**

<sup>19</sup> Muskrat Falls Unit 2 was taken offline on a planned outage for major turbine repairs on October 16, 2024, and is expected to return to service in July 2025.

## 5.1 Muskrat Falls Unit 1

The Muskrat Falls Unit 1 DAFOR of 7.74% is above the resource planning analysis value of 3.03% and the near-term planning analysis value of 2.30% for an individual Muskrat Falls unit. As previously reported,<sup>20</sup> this increase in DAFOR was the result of the forced extension of the planned outage, which lasted from September 29 to October 16, 2024 as a result of concrete which had dislodged from the intake and travelled through the unit.<sup>21</sup>

Since the last Rolling 12 report, the unit experienced another forced outage on March 12, 2025, when the unit tripped due to loss of turbine wicket gate position feedback. Further investigation revealed the cause of the trip to be an unseated PLC card in the Governor Control cabinet. The unit was returned to service on March 16, 2025, and has operated reliably since that time.

## 6.0 Thermal Unit DAFOR Performance

Detailed results for the current and previous periods are presented in Table 7 and Chart 3. These results are compared to Hydro’s near-term and resource planning analysis values for forced outage rates, as used in the 2024 Resource Plan and the November 2024 Near-Term Report. Any individual unit with forced outage rates which exceed the established near-term and/or resource planning analysis values is discussed herein.

**Table 7: Thermal Weighted DAFOR**

Generating Unit	Maximum Continuous Unit Rating (MW)	12 months Ended Mar 2024 (%)	12 months Ended Mar 2025 (%)	Near-Term Planning and Resource Planning Analysis Value (%)
<b>All Thermal Units – Weighted</b>	<b>490</b>	<b>43.07</b>	<b>31.92</b>	<b>20.00</b>
<b>Thermal Units</b>				
Holyrood TGS Unit 1	170	9.05	77.01	20.00
Holyrood TGS Unit 2	170	84.22	22.77	20.00
Holyrood TGS Unit 3	150	23.22	3.41	20.00

<sup>20</sup> “Quarterly Report on Asset Performance in Support of Resource Adequacy for the Twelve Months Ended December 31, 2024”, Newfoundland and Labrador Hydro, January 31, 2025, sec. 5.1, pp. 11-12.

<sup>21</sup> Final repairs to the intake civil works are planned during the Unit 1 annual outage in 2025.

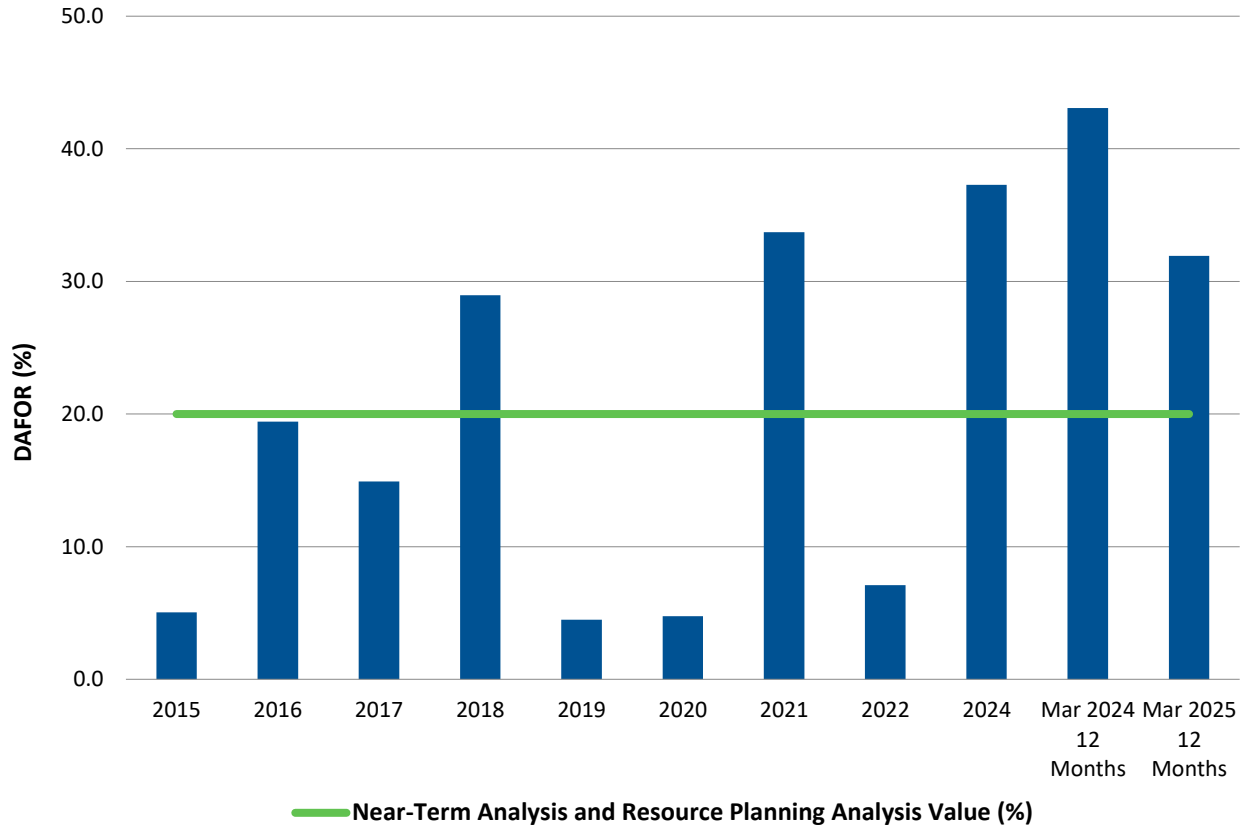


**Chart 3: Thermal DAFOR**

1 For the current period, the weighted DAFOR for all thermal units of 31.92% is above the  
 2 term and resource planning analysis values. The individual unit DAFOR outcome for the current period  
 3 of 3.41% for Unit 3 at the Holyrood TGS is below the 20.00% analysis value. The performance of Unit 1  
 4 and Unit 2 at the Holyrood TGS is discussed in Section 0 and 6.2.

5 **6.1 Holyrood TGS Unit 1**

6 Considering individual thermal unit performance, the DAFOR of 77.01% for Unit 1 at the Holyrood TGS is  
 7 above the near-term and resource planning analysis value of 20.00% for a unit at the Holyrood TGS, and  
 8 shows a decline in performance over the previous period. This elevated DAFOR is the result of a forced  
 9 extension to the planned unit outage to overhaul the Unit 1 turbine and replace the L-0 and L-1 blades  
 10 at the General Electric (“GE”) shop in the United States.<sup>22</sup> The blades were replaced; however, it was

---

<sup>22</sup> “2024 Capital Budget Application,” Newfoundland and Labrador Hydro, rev. September 21, 2023 (originally filed July 12, 2023), sch. 6, prog. 2.

1 found that additional work was required to restore the bearing journals, which resulted in extension to  
2 the outage. All work was completed and the rotor was shipped back to Holyrood site in late 2024. Start-  
3 up activities in January 2025 were delayed due to issues found with the turbine stop valve, which were  
4 resolved and the unit brought online on February 12, 2025. Following return to service, an issue with the  
5 main steam controls valves prevented movement beyond 56% opening, which resulted in a forced  
6 derating to 105 MW. This derating remained until March 10, 2025 when a planned outage was taken to  
7 investigate and correct the issue with the control valves. The unit returned to operation on  
8 March 17, 2025 at full capacity.

## 9 **6.2 Holyrood TGS Unit 2**

10 Considering individual thermal unit performance, the DAFOR of 22.77% for Unit 2 at the Holyrood TGS is  
11 above the near-term and resource planning analysis value of 20.00%, and shows an improvement in  
12 performance over the previous period. As previously reported,<sup>23</sup> a planned unit outage began in 2023 to  
13 overhaul the Unit 2 turbine and replace the L-0 blades at the GE shop in the United States.<sup>24</sup> Subsequent  
14 turbine rotor inspection at the GE shop identified additional and unexpected cracking on the L-1 blades,  
15 resulting in the required replacement of that set of blades.<sup>25</sup> The unit was reassembled in early 2024 and  
16 was officially released for service on May 17, 2024.

17 The elevated DAFOR in the current period has been impacted by the aforementioned forced outage  
18 extension, which lasted approximately eight months, including six weeks in the current period. Since the  
19 previous filing, Holyrood Unit 2 experienced one additional outage which materially impacted the  
20 DAFOR performance. The outage occurred from January 7–12, 2025, due to an issue with the hydraulic  
21 ram that is used to control the amount of steam that is entering the turbine. The ram was rebuilt and  
22 the unit returned to service.

---

<sup>23</sup> Supra, f.n. 16, sec 6.1, p. 13.

<sup>24</sup> Approved in Board Order No. P.U. 17(2022).

<sup>25</sup> These are the low pressure next-to-last stage (“L-1”) blades, a separate stage of blades from the last stage (“L-0”) blades.

## 1 **7.0 Combustion Turbine DAUFOP Performance**

2 DAUFOP Performance for the Hardwoods, Stephenville and Happy Valley Gas Turbines as well as the  
3 Holyrood Combustion Turbine for the period are presented in the charts and tables below.

4 The combined DAUFOP for the Hardwoods and Stephenville Gas Turbines was 28.20% for the current  
5 period, as shown in Table 8 and Chart 4. This is below the near-term and resource planning analysis  
6 value of 30.00%.

7 The Stephenville Gas Turbine DAUFOP for the current period is 53.69%, which is above the near-term  
8 and resourcing planning assumption of 30.00%. The Hardwoods Gas Turbine DAUFOP for the current  
9 period is 0.00%, which is below the near-term and resource planning assumption of 30.00%. On a per-  
10 unit basis, both units have improved performance when compared to the previous period. As the forced  
11 outage rate for the Stephenville Gas Turbine exceeds the established near-term and resource planning  
12 analysis values, a discussion on same is included in Section 0.

**Table 8: Hardwoods/Stephenville Gas Turbine DAUFOP**

<b>Gas Turbine Units</b>	<b>Maximum Continuous Unit Rating (MW)</b>	<b>12 months Ended Mar 2024 (%)</b>	<b>12 months Ended Mar 2025 (%)</b>	<b>Near-Term Planning and Resource Planning Analysis Value (%)</b>
<b>Gas Turbines</b>	<b>100</b>	<b>43.32</b>	<b>28.20</b>	<b>30.00</b>
Stephenville	50	73.11	53.69	30.00
Hardwoods	50	12.31	0.00	30.00

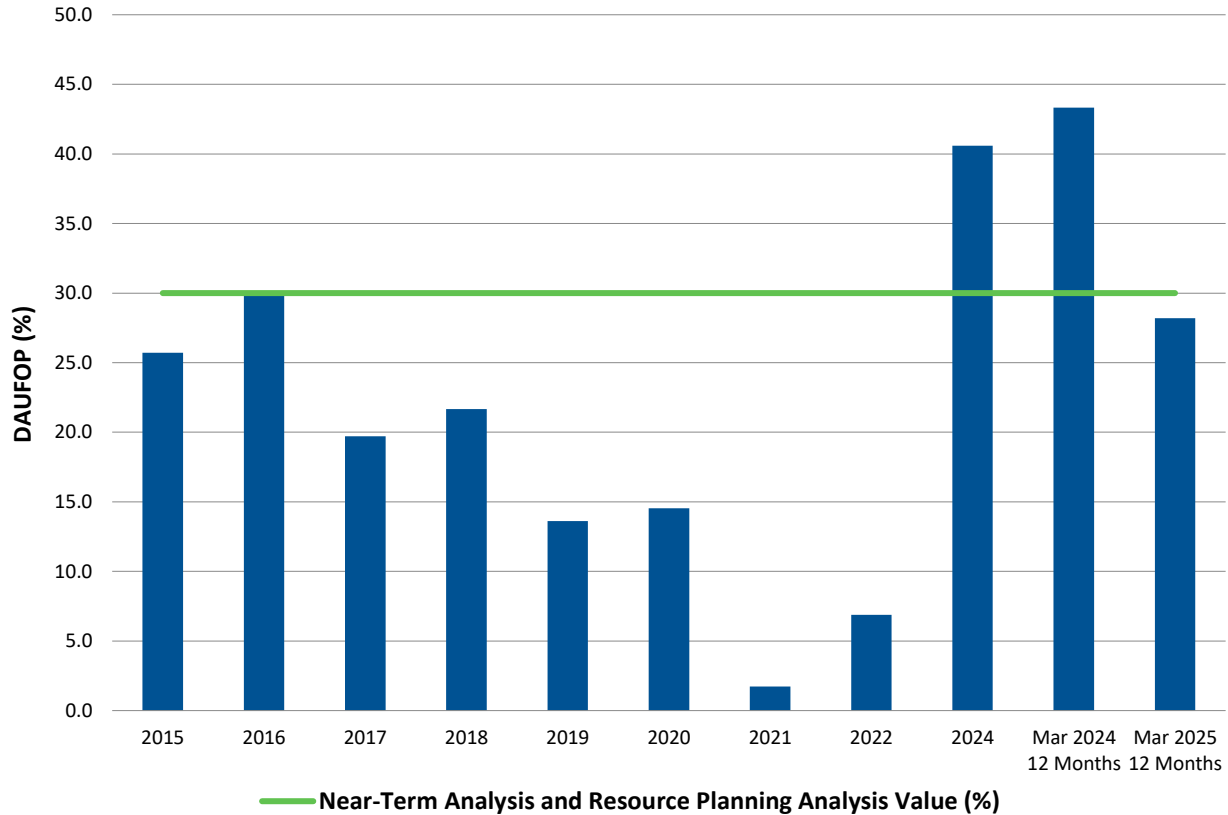


**Chart 4: Gas Turbine DAUFOP: Hardwoods/Stephenville Units**

- 1 The DAUFOP for the Happy Valley Gas Turbine was 0.00% for the current period, as shown in Table 9
- 2 and Chart 5. This is below the near-term and resource planning analysis value of 4.65% and indicates an
- 3 improvement in performance over the previous period.

**Table 9: Happy Valley Gas Turbine DAUFOP**

Gas Turbine Unit	Maximum Continuous Unit Rating (MW)	12 months Ended Mar 2024 (%)	12 months Ended Mar 2025 (%)	Near-Term Planning and Resource Planning Analysis Value (%)
Happy Valley	25	23.38	0.00	4.65

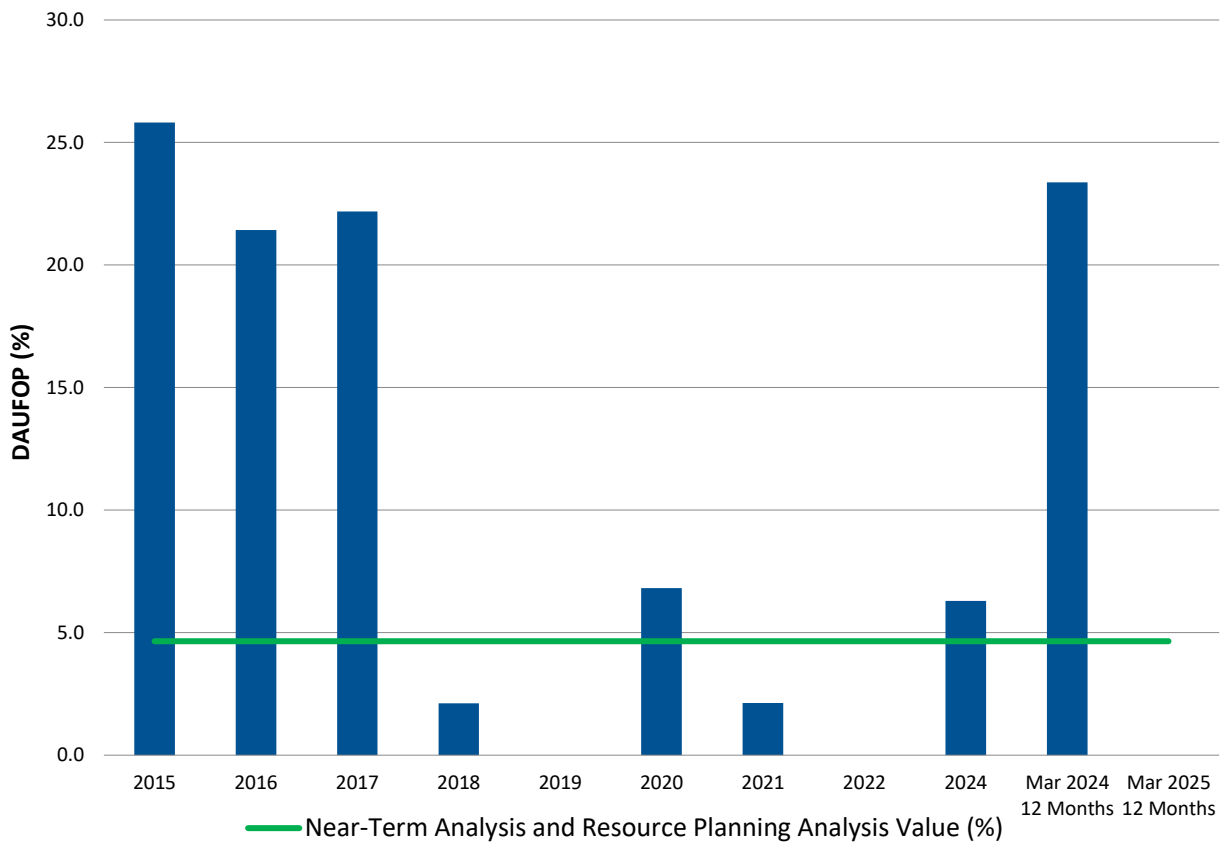


**Chart 5: Gas Turbine DAUFOP: Happy Valley Unit**

1 The Holyrood Combustion Turbine DAUFOP of 8.57% for the current period is above the near-term and  
 2 resource planning analysis value of 4.90%, and indicates a decline in performance when compared to  
 3 the previous period, as show in Table 10 and Chart 6. As the forced outage rate for the Holyrood CT  
 4 exceeds the established near-term and resource planning analysis values, a discussion on same is  
 5 included in Section 7.2.

**Table 10: Holyrood Combustion Turbine DAUFOP**

Combustion Turbine Unit	Maximum Continuous Unit Rating (MW)	12 Months Ended Mar 2024 (%)	12 Months Ended Mar 2025 (%)	Near-Term Planning and Resource Planning Analysis Value (%)
Holyrood	123.5	5.71	8.57	4.90

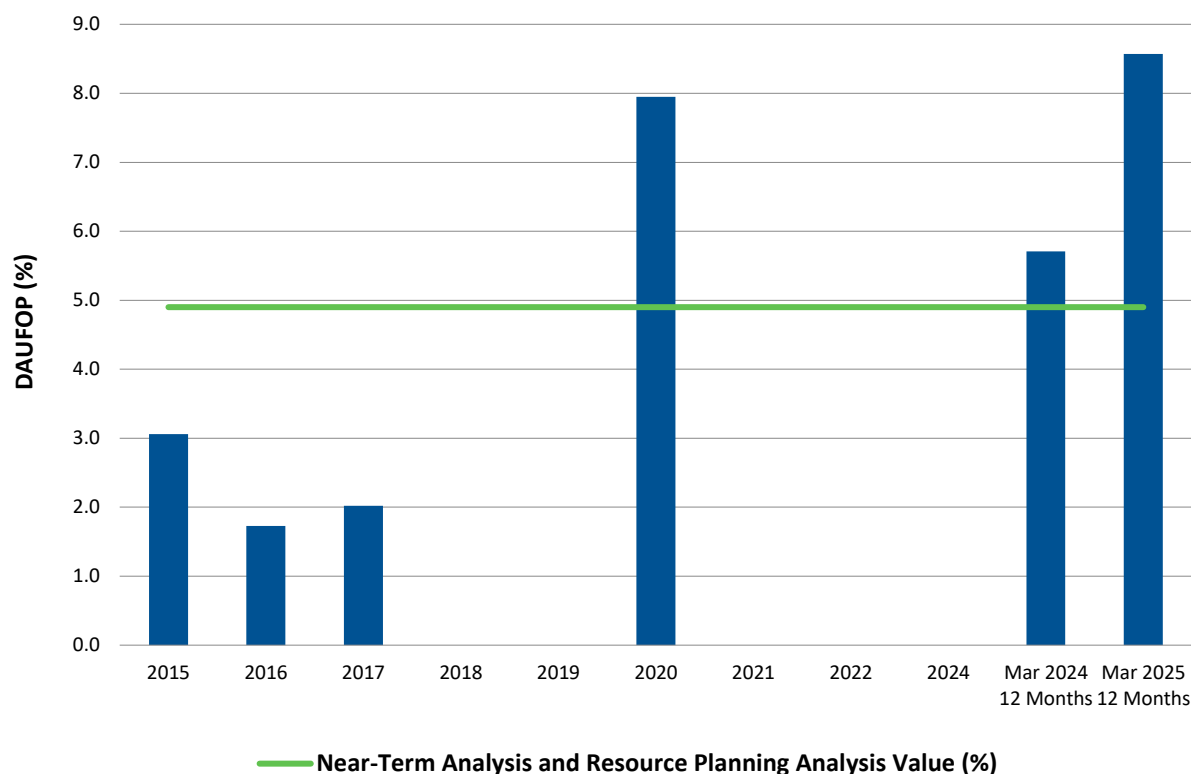


**Chart 6: Combustion Turbine DAUFOP– Holyrood Unit**

**1 7.1 Stephenville Gas Turbine**

2 The Stephenville Gas Turbine DAUFOP was 53.69% for the current period, which is above the near-term  
 3 and resource planning analysis value of 30.00%. This decline in performance is a result of the failure of  
 4 the alternator cooling fan, as previously reported, which occurred on July 14, 2023.<sup>26</sup>

<sup>26</sup> Additional information was provided in the “2023–2024 Winter Readiness Planning Report,” Newfoundland and Labrador Hydro, December 11, 2023, sec. 2.2, p. 8 and sec. 7.4.1, p. 38.

1 Commissioning was successfully completed and the unit returned to service on September 27, 2024.

2 **7.2 Holyrood Combustion Turbine**

3 The Holyrood CT DAUFOP was 8.57% for the current period, which is above the near-term and resource  
4 planning analysis value of 4.90%. This decline in performance is the result of two forced outages in the  
5 current period. The unit was unavailable from February 12–14, 2025 due to a failed blade path  
6 thermocouple. The second outage occurred February 25–26, 2025 due to a failed jacking oil pump. Both  
7 outages were resolved by replacing the failed components.

8 **8.0 Labrador-Island Link EqFOR Performance**

9 The EqFOR for the LIL was 0.86% for the current period, as shown in Table 11. This is slightly below the  
10 range of values used by Hydro in the resource planning analysis scenarios.

**Table 11: LIL EqFOR (%)**

<b>Asset Type</b>	<b>Measure</b>	<b>12 Months Ended Mar 2024 (%)</b>	<b>12 Months Ended Mar 2025 (%)</b>	<b>Base Planning Analysis Value</b>	<b>Range of Planning Analysis Values</b>
LIL	EqFOR	2.70 <sup>27</sup>	0.86	5	1–10

11 The availability of the three Soldiers Pond synchronous condensers (“SC”) is critical to the reliable  
12 delivery of electricity to the Island Interconnected System via the LIL. No operational issues concerning  
13 the Soldiers Pond SCs resulted in outages or derating to the LIL in the current period.

14 A fulsome update on the total number of hours of operation for the Soldiers Pond SCs for the rolling 12-  
15 month period is provided in in Appendix A of this report.

---

<sup>27</sup> This includes the forced outage hours accumulated from April 1, 2024, to April 7, 2024, as the outage began in the current reporting period on March 30, 2024, as reported in the first quarter of 2024 LIL Quarterly Update, and was resolved prior to filing.

# Appendix A

## Soldiers Pond Synchronous Condensers



**Table A-1: Quarterly Rolling 12-Month Operating Hours for Soldiers Pond Synchronous Condensers**

<b>Unit</b>	<b>Operating Hours<sup>1</sup></b>	<b>% Availability<sup>2</sup></b>
SC1	7,627.02	86.8%
SC2	8,258.70	94.0%
SC3	8,313.95	94.7%

- 1 Further information on the operation of the Soldiers Pond Synchronous Condensers is provided in
- 2 Appendix B.

---

<sup>1</sup> Hydro has provided its best estimate of operating hours for each unit for the 12 months ended March 31, 2025 based on an assumption of 24/7 operation of all three SCs, and known outages (both planned and unplanned) recorded in its database.

<sup>2</sup> Synchronous Condenser availability is calculated on the basis of the unit's operating hours, and therefore assumes that the unit is operating when available.

# Appendix B

## Muskrat Falls Assets Update

Reporting period up to March 31, 2025



## 1 1.0 Introduction

2 The Muskrat Falls Assets, made up of the LIL, the Labrador Transmission Assets (“LTA”) including the  
3 Soldiers Pond Synchronous Condensers, and Muskrat Falls have all been commissioned in recent years  
4 and are in the early years of their asset lifespan.

5 As is normal for the early operation of assets, Hydro has encountered some challenges with equipment  
6 due to manufacturing issues or defective components. Such issues are expected early in the  
7 equipment’s life. Equipment failure rates plotted over time generally exhibit a ‘bathtub-shaped curve.’  
8 Incidents of failure tend to be high when equipment is new and again near the end of the equipment’s  
9 useful life, depending on equipment type. In addition to routine ongoing preventative maintenance  
10 activities and sustaining capital programs for each of these assets, there are a number of one-off capital  
11 projects, corrective maintenance activities and engineering studies ongoing with the purpose of  
12 addressing and repairing these early life issues, with the ultimate goal of improving asset reliability over  
13 time to expected levels.

14 Hydro provides the following update to the Board on the status of these activities and other information  
15 as requested by the Board.

## 16 2.0 Muskrat Falls Hydroelectric Generating Facility

17 Muskrat Falls was commissioned in November 2021. The plant continues to outperform similar units  
18 across Canada. As reported in its most recent Rolling 12 report, the Muskrat Falls total plant DAFOR  
19 performance through the end of the first quarter of 2025 was 2.30%, which was significantly better than  
20 the Electricity Canada average of 5.27% for similar units across Canada.

### 21 2.1 Capital Projects

#### 22 *Muskrat Falls – Repair Unit 2 Turbine*

23 As recommended by the original equipment manufacturer (“OEM”) and reported by The Liberty  
24 Consulting Group in its June 2023 monitoring report, vibration issues observed on Unit 2 require  
25 permanent corrective action, including full unit dismantling, to be completed under warranty by the  
26 turbine OEM. There have been no issues with vibration, or the identification of other characteristics  
27 through internal inspections, which would indicate a problem similar to that of Unit 2 on Units 1, 3, or 4.

1 This project is to repair the Unit 2 turbine, which will result in the unit being unavailable for the 2024–  
2 2025 winter season. The expected return to service date for this generating unit is now mid-July 2025 to  
3 allow for additional turbine blade repair; the issue is anticipated to be resolved following completion of  
4 this project.

### 5 **3.0 Soldiers Pond Synchronous Condensers**

6 Hydro continues to address the remaining items that were noted in punchlist reports submitted with the  
7 commissioning certificate and outstanding warranty claims.

#### 8 **3.1 Operations Items**

##### 9 ***Brush Gear***

10 Hydro’s Engineering team, with the OEM for the brush equipment and synchronous condensers, has  
11 been working to identify the root cause of the brush performance issues. Multiple actions have been  
12 taken to improve the reliability of the brush gears for the 2024–2025 winter, including:

- 13 • 12 brushes per ring removed (24 total) on each unit to increase the current density (heat) on  
14 remaining brushes in an effort to improve patina development<sup>1</sup> and overall brush gear  
15 performance;
- 16 • Maintaining the machine hall temperature near 20°C;
- 17 • Nord-lock washers installed on holders to lessen the likelihood of brush holders vibrating loose  
18 and contacting the running face of the slip ring;
- 19 • Humidity levels being measured and trended by Hydro’s Engineering team to ensure brushes are  
20 operating in ideal conditions to support patina development;
- 21 • Managing system voltages to increase load on synchronous condensers (i.e., increase current  
22 density); and

---

<sup>1</sup> During operation a protective film, or patina, is automatically formed on the surface of the slip ring, at the interface point between the brush face and ring surface. When formed properly, this film reduces brush wear to the lowest possible level, and is essential to ensure optimum operation of the brushes.

- 1       • Regular inspections performed to identify changes in performance, allowing for early  
2       intervention prior to damages.

3       In spring 2024, the existing slip ring was removed from synchronous condenser 1 (“SC1”), and sent for  
4       machining to correct a runout causing excessive brush vibration. At this time, a modified brush with the  
5       ability to operate in a higher vibration environment was also provided by the OEM and installed. These  
6       modifications have resulted in improved performance to date. Hydro’s Engineering and Operations  
7       teams will continue to monitor the overall impact of these changes, with the potential to complete this  
8       work on SC2 and SC3 in 2025. Additionally, GE has been working with a different brush gear  
9       manufacturer, and has proposed a different brush assembly with a more robust spring design to lessen  
10      the likelihood of spring failure. This design will be installed on SC3 for performance evaluation in early  
11      spring 2025.

#### 12      ***Forced Outages***

13      Outside of planned outages, the Soldiers Pond Synchronous Condensers have been in operation at all  
14      times during the quarter, with the exception of one trip on Synchronous Condenser 3 as a result of  
15      troubleshooting activities on the exciter; the unit returned to service within an hour. There was no  
16      customer impact

## 17      **4.0 Labrador-Island Link**

18      Since commissioning in April 2023, LIL has been in service and successfully providing power to the  
19      provincial grid. Since the last update, the LIL has been operating at various power transfer levels up to  
20      620 MW, as required by the system. In total, approximately 902 GWh were delivered over the LIL from  
21      January 1, 2025 to March 31, 2025. Hydro continues to ensure the availability of generation at the  
22      Holyrood Thermal Generating Station; however, energy and capacity delivered over the LIL are used to  
23      minimize thermal generation whenever possible.

24      In the early stages of its operation, as is normal for the operation of assets early in life, the current  
25      reliability of the LIL is anticipated to be lower than in the long-term, due to failures associated with new  
26      assets (e.g., due to manufacturing issues or defective components). In addition to routine ongoing  
27      corrective and preventative maintenance activities and sustaining capital programs, there are a number  
28      of capital projects identified to repair these issues.

1 **4.1 Operations Items**

2 **Forced Outages**

3 During the quarter, the LIL experienced six forced outages as follows:

<b>Outage Date</b>	<b>Description/Cause</b>	<b>Customer Impact</b>	<b>Investigation Status</b>
January 13, 2025	LIL tripped Bipole due to over current protection. There was an issue with electrode line (which required repairs). In order to isolate, the Neutral Bus Ground Switch was closed and due to software issue, it resulted in a bipole trip. It was discovered that a software issue resulted in the trip.	<ul style="list-style-type: none"> <li>No Customer Impact</li> </ul>	Investigation complete. Corrective action identified for implementation in software update. <sup>2</sup>
January 18, 2025	LIL Pole 2 tripped due to SF6 low alarm on wall bushing of Transformer T5.	<ul style="list-style-type: none"> <li>No Customer Impact</li> </ul>	Investigation complete. Corrective actions implemented.
January 22, 2025	LIL Pole 2 Tripped following a Cable 2 Low Pressure alarm at the Shoal Cove Transition Compound. Cable 3 attempted to switch from the faulted Pole 2 to the healthy Pole 1; however, the cable connect sequence failed.	<ul style="list-style-type: none"> <li>UFLS event on the island of approximately 78MW estimated 21,484 customers impacted.<sup>3</sup></li> <li>Customers were returned to service within 1 hour.</li> </ul>	Investigation ongoing. Faulty components that caused the trip were replaced.
February 12, 2025	LIL pole 1 tripped due to a Pressure Relief Device operating on Soldiers Pond Transformer T4. Trip was due to ice falling from overhead bus and hitting pressure relief device.	<ul style="list-style-type: none"> <li>No Customer Impact</li> </ul>	Investigation ongoing.

---

<sup>2</sup> Software update was planned for April 2025 however was not completed due to issues identified during commissioning. Troubleshooting and remediation underway.

<sup>3</sup> In the LIL Q1 2025 Quarterly Update, Hydro reported that there were no customer impacts as a result of this trip in error.

**Quarterly Report on Asset Performance in Support of Resource Adequacy  
for the Twelve Months Ended March 31, 2025, Appendix B**

---

March 6, 2025	LIL Pole 2 tripped following a “Operator In Control” transition from Muskrat Falls to Soldiers Pond. This was related to a software issue.	• No Customer Impact	Investigation ongoing.
March 21, 2025	LIL Pole 1 tripped due to a failed SF6 gauge on a valve hall wall bushing in Soldiers Pond.	• No Customer Impact	Investigation ongoing. Faulty SF6 gauge was replaced.

---

1    **Cable Switching**

2    As reported in Hydro’s final 2024–2025 Winter Readiness Report,<sup>4</sup> new equipment was successfully  
3    installed to mitigate cable switching transients at the LIL Transition Compounds in mid-October 2024.

4    Since the Winter Readiness Report, Hydro has identified an icing issue with transition compound  
5    disconnects that can impact cable switching in winter conditions. Hydro is working with GE to engineer a  
6    solution to resolve this issue. In the interim, Hydro is developing operating procedures to ensure reliable  
7    operation in winter conditions, including high power testing.

8    **Replacement of Direct Current Current Transformers (“DCCT”)**

9    In 2023, the OEM and Hydro determined that very low air temperatures at Muskrat Falls Converter  
10    Station were influencing the measurement accuracy of DCCTs, resulting in false protection trips and  
11    power control issues on the LIL. The OEM identified the root cause of the issue to be a manufacturing  
12    defect with the Delay Coil Fiber Optical Cable located within the DCCTs; this issue occurred with a select  
13    batch of fiber optic cables, affecting six DCCTs at the Muskrat Falls HVdc Converter Station, which have  
14    since been replaced.<sup>5</sup>

15    As noted in Hydro’s final 2024–2025 Winter Readiness Report, the OEM discovered additional DCCTs  
16    that require replacement due to cold temperature issues.<sup>6</sup> Three DCCTs were identified to be replaced

---

<sup>4</sup> Reliability and Resource Adequacy Study Review – 2024–2025 Winter Readiness Planning Report – Final Report”, Newfoundland and Labrador Hydro, December 10, 2024.

<sup>5</sup> One of these DCCTs has an operation rating to -40°C, and will be replaced with a DCCT rated to -50°C as soon as is practical.

<sup>6</sup> While none of these additional DCCTs have experienced issues associated with cold temperatures, there are indicators the issue could present itself; therefore, as a precaution, they have been identified for replacement.

1 as a precaution based on site measurements; with one replaced during December 2024. The remaining  
2 DCCTs identified to be replaced are targeted for replacement as soon as possible, depending on outage  
3 availability. Four additional DCCTs were identified as low risk for this issue, and due to lead time for  
4 manufacturing, are being targeted for replacement during scheduled outages in 2025 and 2026, with  
5 dates to be confirmed.

#### 6 ***Conductor Testing***

7 Following a bipole trip on March 30, 2024, line patrol determined that the electrode conductor was  
8 broken and damaged during an ice storm at several locations in Southern Labrador. As a result,  
9 conductor testing was completed and determined no material issues with the conductor, and found that  
10 the failure was due to overload, which is consistent with past findings. There is evidence that cyclic  
11 loading due to ice and wind on the conductor may be causing fatigue and could contribute to the failure.  
12 This was consistent with previous testing results. There will be additional conductor testing completed  
13 in 2025.

## 14 **4.2 Capital Projects**

### 15 ***Replace Turnbuckles and Install Airflow Spoilers Program***

16 With regard to the Turnbuckles Replacement and Airflow Spoiler Installation Program, Hydro continues  
17 to actively address the recommendations resulting from the localized failures experienced on the LIL  
18 over the past three winters. Hydro's capital programs to replace turnbuckles and install airflow spoilers  
19 intend to reduce galloping are ongoing, prioritizing the high-priority areas of the LIL first.

20 At the end of 2024, Hydro had completed 100% of the planned replacements of turnbuckles for that  
21 year. To date, 74% of air spoilers have been installed, with the remaining to be completed in 2025.<sup>7</sup>

### 22 ***Optimizing Clamp Designs***

23 Hydro has identified, through its preventative maintenance program and component failure  
24 investigations, multiple opportunities for clamp and conductor inspection, with refurbishment or

---

<sup>7</sup>Based on the outcome of its galloping study, Hydro is installing airflow spoilers on priority areas of the LIL to control galloping and mitigate further damage to the line. Hydro has mitigated the risk of prolonged customer outage as a result of fatigue failures due to galloping by prioritizing the most remote locations where galloping has been observed.

1 replacement of parts made according to findings. As a result, Hydro is optimizing clamp designs for the  
2 electrode conductor and optical ground wires (“OPGW”).

3 Three alternative suspension clamp designs have been installed on the electrode conductor at ten  
4 structures and will be inspected for performance on an annual basis. The contract has been awarded to  
5 a consultant for the electrode suspension assembly analysis, and the assessment will be completed in  
6 the first quarter of 2025. Hydro completed additional electrode conductor testing as a result of an  
7 incident in March 2024, with further recommendations provided within the investigation report as  
8 discussed in Section 0.

9 An alternate OPGW clamp assembly with improved slip strength was selected, ordered and received in  
10 January 2025. As the OPGW relates to communications functionality, Hydro does not anticipate that  
11 further occurrences of similar damage would result in a prolonged power interruption or customer  
12 outage.

### 13 ***Top Plate Design***

14 In December 2022 there were two incidents impacting two adjacent structures of the LIL where the  
15 connection of the top plate of the OPGW suspension detached from the tower, falling onto the cross  
16 arm. As a result Hydro is implementing a reinforcement of the top plate that secures the OPGW to A3  
17 type towers. As of the end of 2024, all sixty-one A3 tower top plates have been reinforced as planned.

18 Analysis of potential modifications to this plate for other tower types is underway and expected to be  
19 complete in the second quarter of 2025.

### 20 ***Ice Monitoring***

21 In response to icing experienced on the LIL, Hydro is undertaking capital projects in 2025 for the  
22 installation of a real-time weather station, as well as the installation of on-line ice and galloping  
23 monitoring equipment. Installation of the weather station is planned for 2025, and the contract for  
24 monitoring equipment was awarded in 2024, to be installed in 2025.

1    **4.3    High-Power Testing**

2    As reported in its first quarter of 2025 LIL Quarterly Update, Hydro postponed the 900 MW test until the  
3    late fall of 2025, when system conditions permit.<sup>8</sup>

4    Planning for the 900 MW test is underway. As previously reported, the following are prerequisite  
5    conditions for the test to occur:

- 6       • Satisfactory system conditions are present, including both those in Newfoundland and Labrador,  
7        where a high system load can be reasonably expected to occur, and neighbouring jurisdictions;
- 8       • Successful coordination with all relevant neighbouring system operators is attained; and
- 9       • Identification of risks and implementation of all necessary risk mitigation actions are in place.

10   **4.4    Software**

11   The current LIL software was commissioned in mid-October 2024. This software, as with the previous  
12   version, allows for full operation of the LIL up to 900 MW. Through dynamic commissioning, non-critical  
13   software-related issues were identified. The software to address these non-critical issues successfully  
14   passed Factory Acceptance Testing in November 2024; however, commissioning was unable to be  
15   completed in April as planned. During offline regression testing, an OEM software revision control issue  
16   was identified which necessitated postponing the online commissioning program. To ensure continued  
17   power transfer, the system was reverted to the October 2024 software version. The revision control  
18   issue is currently being addressed by the OEM, and commissioning will be rescheduled once resolved.

19   **4.5    Engineering Studies and Reports**

20   Since its commissioning in April 2023, Hydro has gained valuable insight into LIL operations. Using  
21   Hydro’s operating experience and recommendations from its investigations, supplemented by the  
22   recommendations made by Haldar and Associates Inc., Hydro has identified three potential  
23   reinforcements to LIL assets to sustain reliability, address common failure modes, and mitigate risks to  
24   the Island Interconnected System. While these potential reinforcements have been identified, further

---

<sup>8</sup> “Reliability and Resource Adequacy Study Review – Labrador-Island Link Update for the Quarter Ended March 31, 2025”, Newfoundland and Labrador Hydro, April 3, 2025, p. 2.

1 engineering assessment is required to determine the benefits, costs, schedule, and feasibility of these  
2 modifications. These include:

- 3 • Review of unbalanced ice loads for the entire line length to determine appropriate design  
4 unbalanced ice loading, followed by design and cost estimates for tower design modifications to  
5 meet unbalanced design loads;
- 6 • Feasibility assessment and cost estimates for installation of mid-span structures to reduce tower  
7 loading in critical areas; and
- 8 • Engineering design and cost estimates to relocate electrode conductors from towers to wood  
9 poles in some sections, to reduce tower loading, improve access and logistics, and minimize  
10 outages to address electrode line issues in critical areas.

11 These assessments are ongoing, at which point Hydro will be in a position to evaluate these projects  
12 based on their anticipated reliability benefits and their estimated cost. The engineering design is  
13 anticipated to be complete in the second quarter of 2025 with cost estimates planned for completion in  
14 the third quarter of 2025. A detailed update on each of these assessments is provided below.

### 15 ***Ice Loading Analysis***

16 The ice loading assessment has been completed. The unbalanced ice loads causing failures have been  
17 determined and provided to a consultant for the design of tower modifications, and feasibility of mid  
18 span structures.

### 19 ***Tower Design***

20 Analysis is ongoing to determine the requirement for modifications to the tower or transmission line  
21 design to further reduce the risk of incidents. Specifically, this includes design for strengthening  
22 electrode cross arm; electrode suspension assembly assessment and design; and design for OPGW  
23 tower peak strengthening. These studies are being undertaken by a consultant and are anticipated to be  
24 complete in the second quarter of 2025.

### 25 ***Line Modifications***

26 Hydro is undertaking engineering assessments on the potential installation of mid-span structures to  
27 reduce load on towers and to remove the electrode line from the towers (in specific sections) to reduce  
28 load on towers. Work is ongoing, and initial cost estimates were completed in fourth quarter of 2024

1 and are being reviewed internally. The feasibility of mid-span structures is being assessed through the  
2 consultant contract for tower design, and the assessment on the electrode removal is being completed  
3 internally, anticipated to be complete in the second quarter of 2025.

#### 4 **4.6 Ongoing Investigations**

5 Investigations have been completed for two incidents that occurred in 2024 that did not have customer  
6 impact, and the results have been reviewed and finalized. These incidents and the outcomes of the  
7 investigations are described below, and a copy of these investigations are provided as Attachments 1  
8 and 2 to this report.

##### 9 ***OPGW Tower Peaks – Central Newfoundland***

10 There was damage to the LIL during an icing event on February 9, 2024. The issues which were similar in  
11 nature, and occurred on eight structures in three groups. In each occurrence, the top peak of the tower  
12 where the OPGW is connected sustained damage; however, the OPGW wire itself did not physically fail.  
13 There was no impact to customers as a result of the incident. This issue occurred on eight of 3,223  
14 tower peaks. While damage to the OPGW tower peaks will not cause extended power outages, for  
15 safety reasons, outages were taken to complete the repair work. These structures are all located in  
16 central Newfoundland.

17 The investigation concluded that the likely cause of the failures was unbalanced ice loads due to ice  
18 shedding. The ice accumulation was in the range of 50–75 mm, the temperatures rose to above 0°C the  
19 day before the failures, and the modeling confirmed that these unbalanced and ice shedding loads could  
20 cause failure to the OPGW peak.

21 The recommendations to prevent further failures on the line due to unbalanced ice and ice shedding  
22 include the following:

- 23 • Monitoring of ice conditions along the line; and
- 24 • Strengthening of the tower to withstand higher unbalanced ice loads.

25 Monitoring can be done in a number of ways including line patrol, test spans with ice load and weather  
26 monitoring equipment near the line route, and in-line ice load monitoring equipment. Hydro currently

1 has a test span installed near string 1225 with plans to install another test spans in 2025 to monitor the  
2 line for ice conditions. In addition, monitors will be installed on the line in 2025 to monitor ice loading in  
3 three locations along the line. Tower strengthening is being actioned as part of a 2024–2025 project that  
4 will evaluate and update the unbalanced ice loading design used for LIL. A consultant has been  
5 contracted to provide a design and cost estimate for tower modification that will be required to meet  
6 this new unbalanced ice load design, to be completed in 2025.

7 ***Electrode Cross Arm, Conductor and OPGW Tower Peak – Southern Labrador***

8 Following a bipole trip on March 30, 2024, line patrol determined that the electrode conductor was  
9 broken and damaged during an ice storm at several locations. In some locations, the electrode  
10 conductor was touching or close to the pole conductor, which would explain the line trip. There was also  
11 damage to the steel lattice towers at the electrode cross arm and OPGW tower peaks. There was  
12 damage on a total of 12 structures of 3,223 towers. There was no customer impact as a result of the  
13 incident; however, an outage was required to clear the damaged conductor from the line while repairs  
14 were being completed. These structures are all located in southern Labrador.

15 The investigation identified that the main root cause of the damage to the tower electrode crossarms,  
16 the OPGW tower peaks, and the electrode conductor was an overload failure due to ice loads exceeding  
17 the design for this section of the line. The material testing found the physical, chemical and metallurgical  
18 evidence indicates the conductor failures were consistent with ductile limit load fracture. The ductile  
19 failure was likely caused by overloading due to ice accumulation and wind loads at the time of the  
20 failure. It is also noted that galloping due to wind could have contributed to the failure by causing cyclic  
21 loading on the conductor prior to the failure.

22 Recommendations for consideration to prevent future failures and better understand the issue with the  
23 line include the following:

- 24 • Monitoring of ice conditions along the line;
- 25 • Strengthening of the tower to withstand higher unbalanced ice loads;
- 26 • Modifying the line to reduce the loads on towers;
- 27 • Look at alternative suspension assemblies and clamp designs; and,

- 1 • Investigate using radiography to evaluate conductor issues.
- 2 Monitoring can be done in a number of ways including line patrol, test spans with ice load and weather  
3 monitoring equipment near the line route, and in line ice load monitoring equipment. Hydro currently  
4 has a test span installed near string 1225 with plans to install another test spans in 2025 to monitor the  
5 line for ice conditions. In addition, monitors will be installed on the line in 2025 to monitor ice loading in  
6 three locations along the line. Tower strengthening recommendation is being actioned as part of a  
7 2024–2025 project that will evaluate and update the unbalanced ice loading design used for LIL. A  
8 consultant has been contracted to provide a design and cost estimate for tower modification that will be  
9 required to meet this new unbalanced ice load design, to be completed in 2025.
- 10 The feasibility and a cost of other options will also be evaluated which will need to meet the new design  
11 loads by reducing the loads on the towers. This will include installing mid span structures between  
12 existing tangent structures, and removing the electrode conductor from the towers and installing it on  
13 wood pole structures for sections of the line, as required.

#### 14 **4.7 Restoration Plans and Operational Strategy**

15 In addition to engineering studies to inform potential reinforcements to mitigate the risk of component  
16 failures and outages, Hydro is currently in the process of contracting a consultant to review Hydro’s  
17 restoration plans, including review and development of specific restoration plans for a variety of  
18 potential and previously experienced scenarios. It is expected that this review will include the  
19 identification of alternative restoration approaches that can be selected based on the situation for the  
20 most efficient and effective execution of the work. Restoration plans will consider geographic and  
21 weather challenges. Restoration plan reviews will include estimates of the time to effect the repairs as  
22 well as time challenges and opportunities for restoration duration and provide cost and benefit  
23 information to identify incremental investment in restoration time improvement and quantify the  
24 associated benefits.

### 25 **5.0 Conclusion**

26 Hydro recognizes the criticality of the Muskrat Falls Assets to the supply of the Island Interconnected  
27 System, which helps to limit the thermal generation required from the Holyrood TGS and impacts the

- 1 overall reliability of the grid will continue to monitor the performance of these assets address early life
- 2 incidents such as those due to manufacturing issues or defective components.

# Attachment 1

L3501/2 Failure Investigation

OPGW Tower Peaks – Central Newfoundland

ILK-EG-ED-6200-TL-H15-0006-01





## Contents

1.0	Abbreviations and Acronyms .....	1
2.0	Introduction .....	1
3.0	Background .....	2
4.0	Purpose .....	4
5.0	Failure Description .....	5
5.1	Failure Location.....	7
5.2	Engineering Recommendations for Immediate Fix.....	10
5.3	Restoration Summary .....	10
6.0	Weather Information .....	11
7.0	Construction Quality and Maintenance Review .....	16
8.0	Analysis of Loads Causing Failures .....	17
8.1	Ice Loading .....	17
8.2	Wind and Ice Combined Loading .....	18
8.3	Unbalanced Icing.....	19
9.0	Summary and Conclusions .....	20
10.0	Recommendations .....	22

## List of Appendices

Appendix A: Quality Control Forms

1 **1.0 Abbreviations and Acronyms**

2 DE – Dead End

3 HVdc – High Voltage direct current

4 L3501/2 – Line number of the 350 kV HVdc transmission line

5 L3501 – Pole 1 of the line

6 L3502 – Pole 2 of the line

7 LIL – Labrador-Island Link

8 OPGW – Optical Ground Wire

9 P1 – Pole 1

10 P2 – Pole 2

11 ROW – Right of Way

12 Str. – Structure

13 **2.0 Introduction**

14 During February of 2024, there were multiple failures on the Newfoundland and Labrador Hydro  
15 transmission line L3501/2. The failures occurred on eight structures in three groups: 2543–2545, 2596 to  
16 2599, and 2620. The failures of these structures were similar, the top peak of the tower where the  
17 OPGW is connected failed as shown in Figure 1. The OPGW wire itself did not physically fail, nor did the  
18 rest of the tower. There was internal damage to one section of OPGW near structure 2620, which  
19 affected the communications performance.

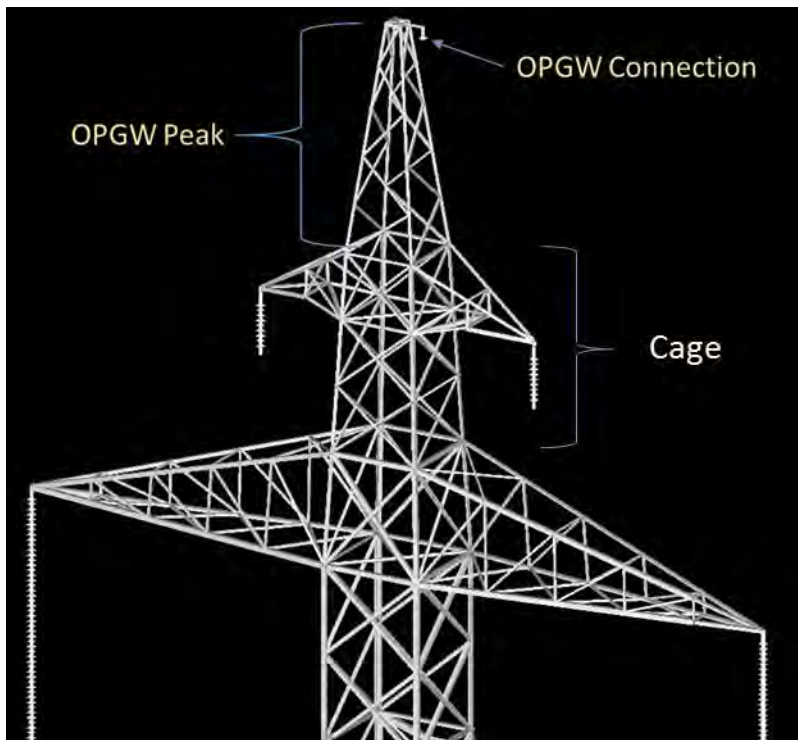


Figure 1: Tower Drawing showing OPGW Peak

### 1 3.0 Background

2 The Labrador-Island Link (“LIL”) is an important transmission line for the provincial energy grid due to its  
3 power carrying capacity that will be used to deliver a large portion of the winter peak energy and  
4 demand to the Island Interconnected System. Line L3501/2 is the 350 kV HVdc overland transmission  
5 line portion of LIL, traversing a distance of approximately 1,100 km through three major meteorological  
6 loading zones: average, alpine and eastern. The HVdc line has two pole conductors, one OPGW, and two  
7 electrode conductors for a portion of line as shown in Figure 2. The electrode conductor is attached to  
8 the lattice towers for a part of the line from Muskrat Falls to about 384 km southeast of Muskrat Falls  
9 where it diverts to a separate right of way (“ROW”) on wood poles (approximately 16 km) to an  
10 electrode site located in L’Anse-au-Diable area.

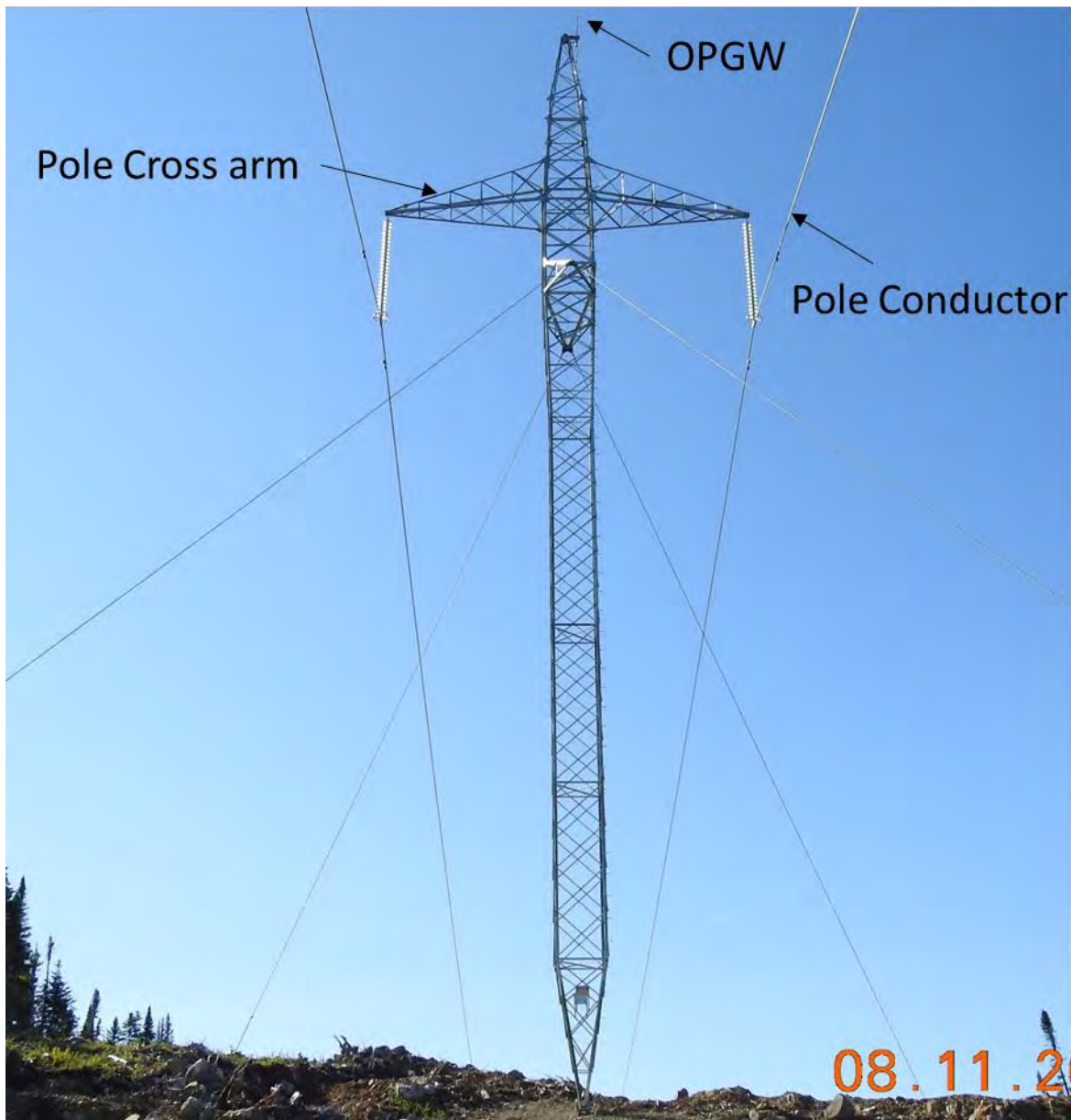


Figure 2: L3501/2 Str. Showing Wire Arrangement

- 1 The HVdc transmission line corridor has been divided into three major meteorological loading zones
- 2 referenced above in combination with 8 further subcategories related to meteorological loads, pollution
- 3 levels (inland and costal), and geographic location. The resulting combination lead to the HVdc line
- 4 consisting of 19 separate loading zones. Eleven tower types (A1, A2, A3, A4, B1, B2, C1, C2, D1, D2, and
- 5 E1) were designed to meet the loading requirements, which consist of a specified wind load, ice load,

- 1 and combination of both applied to the line. The tower types consist of both guyed towers and self-
- 2 support towers. The tower types are summarized in Table 1.

**Table 1: Tower Types**

<b>Tower Type</b>	<b>Structure Type</b>	<b>Insulator Assembly Type</b>	<b>Deflection Angle Limit (degree)</b>
A1, A2, A3, A4	Guyed	Suspension	0–1
B1	Guyed	Suspension	0–3
B2	Self-Support	Suspension	0–3
C1, C2	Self-Support	Dead End	0–30
D1, D2	Self-Support	Dead End	0–45
E1	Self-Support	Dead End	45–90

- 3 Ninety percent of all towers on the L3501/2 are suspension towers, types A1, A2, A3, A4, B1, and B2.
- 4 Figure 3 breaks down the tower distribution on the L3501/2.

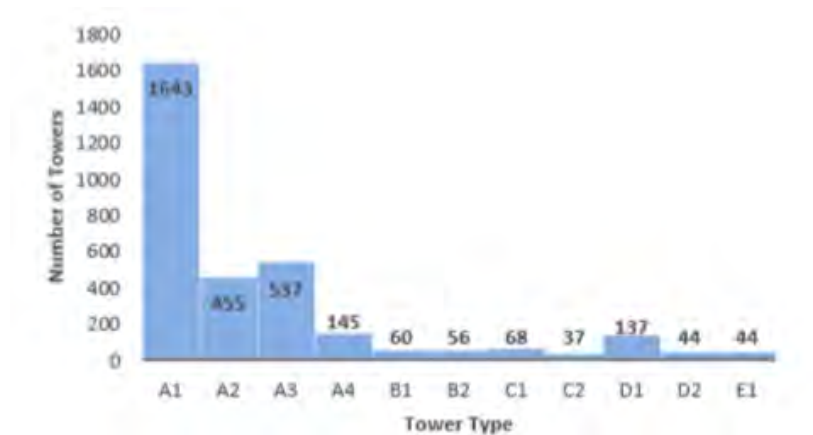


**Figure 3: Distribution of Tower Type on L3501/2**

## 5 **4.0 Purpose**

- 6 A detailed failure investigation was completed to determine the root cause of the failures and to
- 7 conclude what action can be taken in order to prevent further damage to the line.

1 The investigation will be described in detail within this report including the following components:

- 2 • Failure Description;
- 3 • Weather;
- 4 • Construction Quality Review;
- 5 • Analysis of Loads Causing Failures; and
- 6 • Galloping and Damper Issues.

## 7 **5.0 Failure Description**

8 On February 8, 2024, we received reports of significant icing on the line in the area near Clarendville  
9 (around str. 2750). On February 9<sup>th</sup> at 11:45 am there was a line trip reported in the island section of  
10 L3502 (Pole 2). L3501 (Pole 1) compensated for the loss of Pole 2. Pole 1 tripped at 11:54 am on line  
11 fault protection while reducing load. Fault Locator calculations put the location near str. 2600. A full line  
12 patrol was completed with no issue found and power was restored to the line. Due to the significant  
13 amounts of ice found on the line during patrol, it was decided to continue to monitor the line for ice  
14 accumulation and damage. On February 12<sup>th</sup> at 11:00 am, damage to the OPGW peak was found at str.  
15 2620 followed by discovery of the damage on the other structures that same day. A total of eight towers  
16 had steel damage in the section of the OPGW peak, and on three of the towers there was also steel  
17 damage to the cage section. The OPGW was still intact and connected to the towers, but the peak steel  
18 had bent significantly, as shown in Figure 4 and Figure 5. In addition to the failed OPGW tower peaks,  
19 the OPGW pulled through the suspension clamp at various locations in the surrounding structures. This  
20 occurred at 38 structures from 2540–2630, as shown in Figure 6.



**Figure 4: Failed OPGW Peak**



**Figure 5: Failed OPGW Peak**



**Figure 6: OPGW Pulled through Clamp with damaged armor rods**

1 **5.1 Failure Location**

2 Structures are numbered sequentially along the line starting at Muskrat Falls. The structure numbers  
3 that sustained OPGW peak damage include structure numbers 2543, 2544, 2545, 2596, 2597, 2598,  
4 2599, and 2620. The structure are located in central Newfoundland, as shown in Figure 7. The structures  
5 are located 40–60 km from the closest highway.

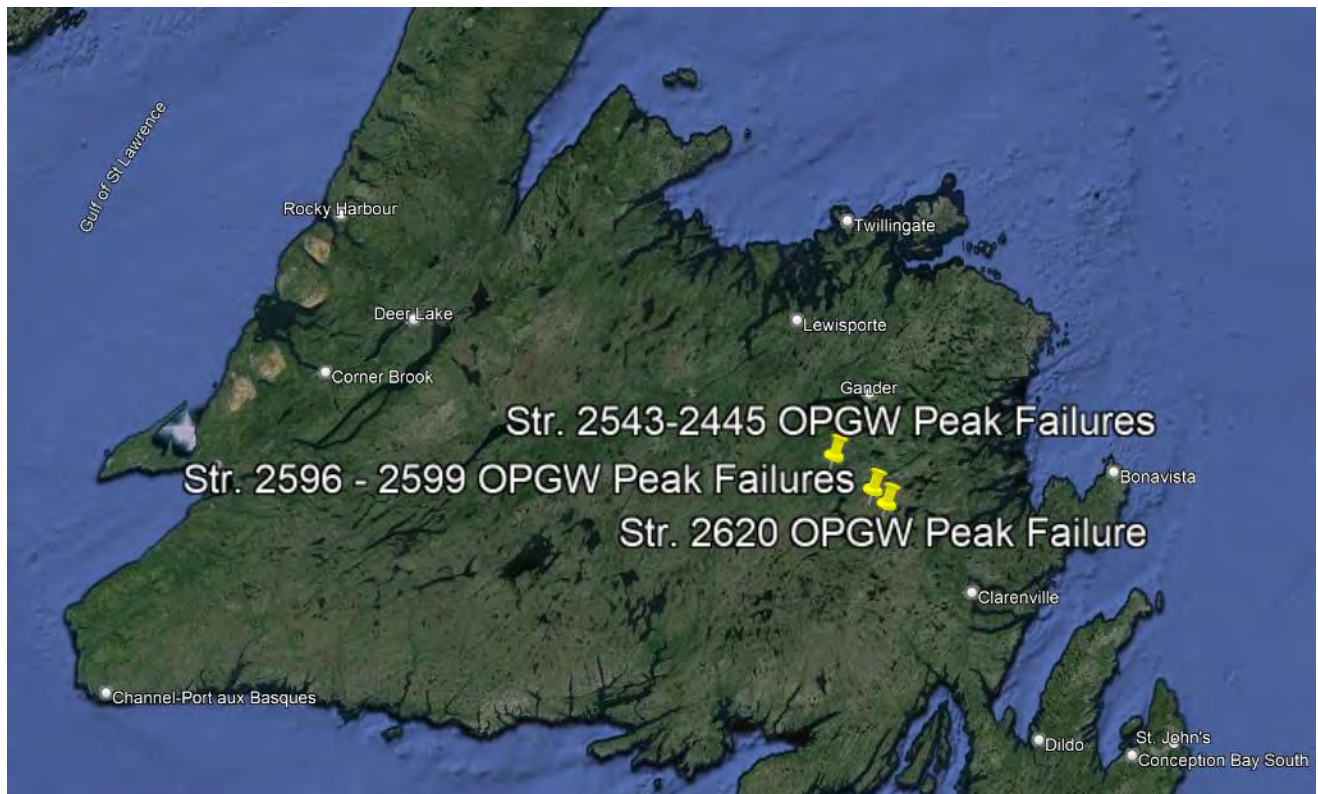


Figure 7: Map of Newfoundland Showing Location of OPGW Peak Failures

- 1 The structures are located in loading zone 10. Zone 10 is Average loading zone. The wind and ice
- 2 conditions this zone is designed for are summarized in Figure 8.

*Zone 1, 8b and 10 (see Attachment B.1)*

The following load case is to be applied in the location shown in attachment B.1. Please note that this loading is valid for the northern corridor alternative only.

Maximum Ice	50 mm radial glaze, 0.9 g/cm <sup>3</sup> density
Maximum Wind	105 km/h (10 minute average wind speed at 10 m height above ground)
Combined Ice and Wind	25 mm radial glaze, 0.9 g/cm <sup>3</sup> density 60 km/h (10 minute average wind speed at 10 m height above ground)

Figure 8: Zone 10 Wind and Ice Design Loading

**Quarterly Report on Asset Performance in Support of Resource Adequacy  
for the Twelve Months Ended March 31, 2025, Attachment 1**

---

1 The eight damaged structures are all Type A1 tangent towers. The tower body extension, and OPGW  
2 attachment heights are summarized in Table 2 below. All towers had a suspension attachment. The  
3 tower failures are contained to three separate deadend to deadend sections. The section with towers  
4 2543, 2544, and 2545 is deadended at structures 2535 and 2546. The section with towers 2596, 2597,  
5 2598, and 2599 is deadended at structures 2589 and 2600. The section with tower 2620 is deadended at  
6 2616 and 2625. The line orientation is generally southeast. Figure 9 shows the location of OPGW peak  
7 failures.

**Table 2: Damaged Structure Information Summary**

<b>Structure Number</b>	<b>Structure Type</b>	<b>Structure Height</b>	<b>Height to OPGW Attachment (m)</b>
2543	A1	A1+18.0	53.05
2544	A1	A1+18.0	53.05
2545	A1	A1+12.0	47.05
2596	A1	A1+15.0	50.05
2597	A1	A1+18.0	53.05
2598	A1	A1+18.0	53.05
2599	A1	A1+18.0	53.05
2620	A1	A1+15.0	50.05

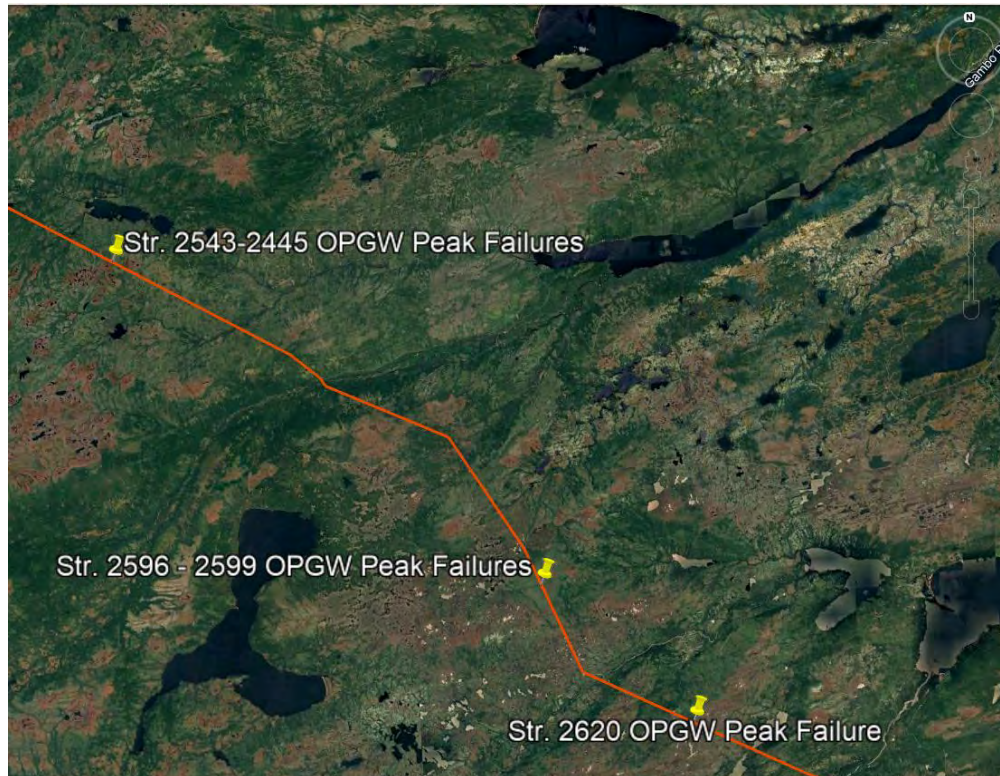


Figure 9: Location of OPGW Peak Failures

1 **5.2 Engineering Recommendations for Immediate Fix**

2 Engineering recommendation for the immediate fix were to replace the tower steel with identical  
3 spares.

4 **5.3 Restoration Summary**

5 Restoration efforts began on February 16<sup>th</sup> with snow clearing to the structures and continued until  
6 demobilization on March 28<sup>th</sup>. The peak of eight structures were replaced (like-for-like) over this time  
7 and the OPGW was replaced between certain spans and re-strung. The timeframe for the replacement  
8 of structure peaks and OPGW is shown in Table 3 below.

**Table 3: Restoration Work Timeline**

Structure Number	Work Performed	Date of Completion
2619–2621	Replaced OPGW	Feb 26th
2620	Replaced structure peak	Feb 26th
2545	Replaced structure peak	Mar 4th
2544	Replaced structure peak	Mar 6th
2543	Replaced structure peak	Mar 6th
2599	Replaced structure peak and cage	Mar 10th
2598	Replaced structure peak and cage	Mar 10th
2597	Replaced structure peak and cage	Mar 10th
2596	Replaced structure peak	Mar 15th

1 After the poles tripping on February 9<sup>th</sup>, helicopter patrols and ground snowmobile patrols were  
 2 conducted to confirm the location of damage. The poles were successfully de-blocked on February 9<sup>th</sup>  
 3 and remained in operation. On February 12<sup>th</sup>, damage to the peaks of eight structures were confirmed.  
 4 Required permits were obtained in the next few days and the OPGW was secured to all towers. The  
 5 contractor, Locke’s Electrical, was brought on to perform the repairs.

6 Snow clearing efforts reached the first structure (str. 2620) on February 17<sup>th</sup>. At the same time of snow  
 7 clearing, peaks and cages for the structures were being assembled in Shoal Harbor. All peaks were  
 8 constructed by February 21<sup>st</sup>. Snow was cleared to the last towers on February 27<sup>th</sup>. The peaks on all  
 9 eight structures were replaced by March 15<sup>th</sup>. Restrunging and splicing of OPGW was completed on  
 10 March 27<sup>th</sup>. Final demobilization occurred on March 28<sup>th</sup>.

11 There were a few delays during the repair work. Weather was one of the factors that affected the  
 12 timeline. A snowstorm on February 14<sup>th</sup> and 15<sup>th</sup> delayed snow clearing efforts due to heavy snow and  
 13 winds approaching 90km/h. During the repair process, snow clearing equipment had to back track to  
 14 clear newly fallen snow. Another snowstorm occurred on March 7<sup>th</sup> to March 8<sup>th</sup>, which delayed repair  
 15 work. Poor weather on March 12<sup>th</sup> to March 14<sup>th</sup> also affected the final tasks left for the repair.

## 16 **6.0 Weather Information**

17 On February 8<sup>th</sup>, 2024, there were reports of heavy icing on the transmission line. On February 9<sup>th</sup> at  
 18 11:45am, Pole 2 tripped, followed by Pole 1. On February 12<sup>th</sup> at 11:00am, structure 2620 was found

- 1 damaged. Figure 10 shows buildup of ice on the line on February 9<sup>th</sup> and on the chair lifts of the nearby
- 2 ski resort in White Hills.



**Figure 10: Ice Buildup on Lines and White Hills Chair lift (9-Feb-24)**

- 3 Visual reports from line patrols estimated the ice thickness to range from 50 mm–75 mm of radial ice.
- 4 The weather station at the Gander International Airport recorded the temperature, precipitation and
- 5 wind speed during the icing event. Figure 11 shows the location of the weather station (about 38 km
- 6 from the nearest failed tower peak).

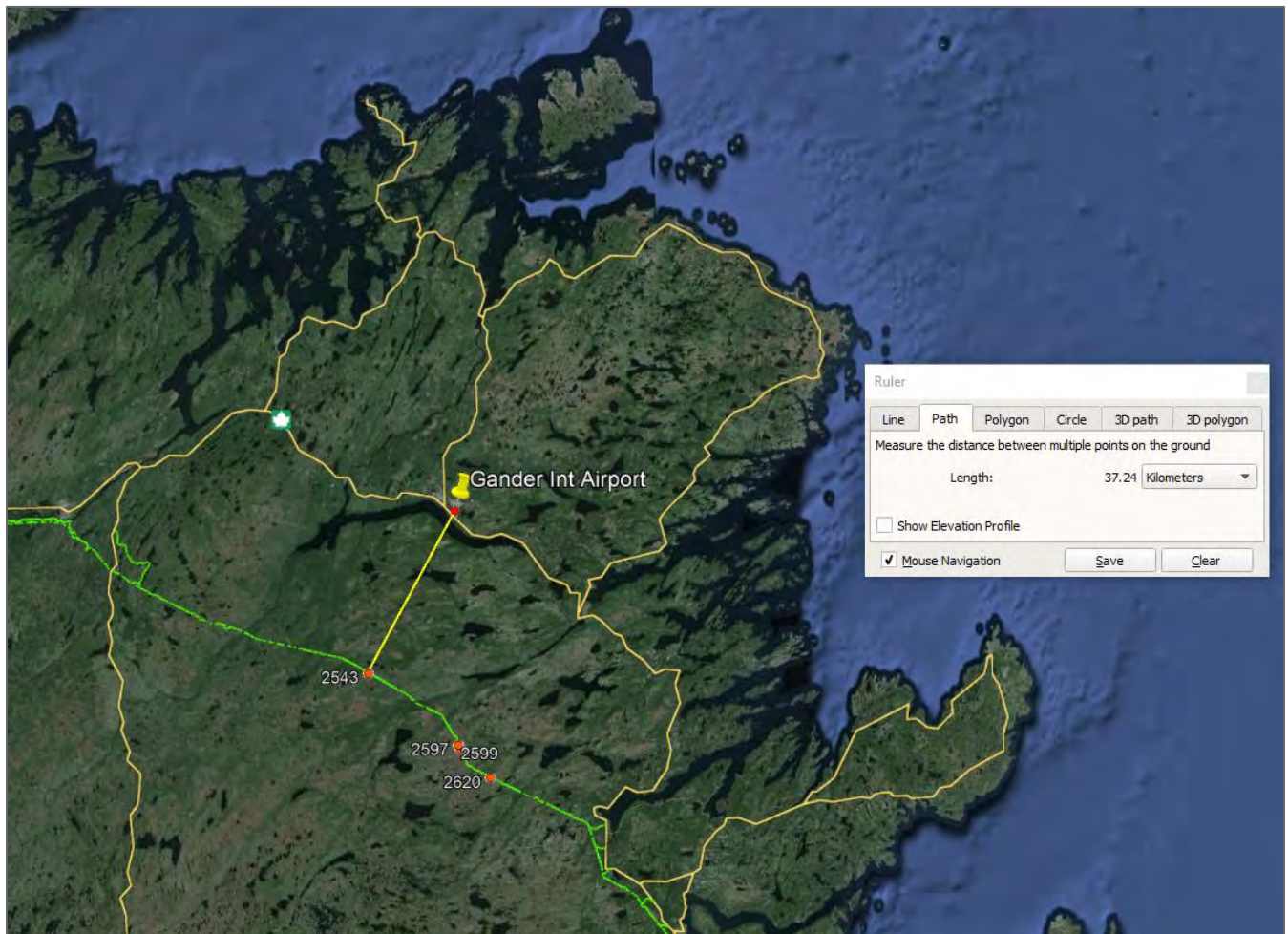


**Figure 11: The Gander International Airport Weather Station**

- 1 The station picked up freezing precipitation that occurred in the afternoon of February 5<sup>th</sup> and
- 2 continued until 5:30 pm on February 6<sup>th</sup>. It then changed to snow and lasted until the morning of
- 3 February 8<sup>th</sup>. Heavy icing was noted on the line on the 8<sup>th</sup>. The weather station is situated at a lower
- 4 elevation than the towers. Therefore, it is possible that lower temperatures and higher wind speeds
- 5 occurred at the elevation of the towers. The snow that was present in Gander from February 6<sup>th</sup> to
- 6 February 8<sup>th</sup> may have been freezing precipitation at the tower elevation.
  
- 7 Pole 1 tripped at 11:45 am on February 9<sup>th</sup> after a possible 3 day icing/snow event. Figure 12 shows the
- 8 ice on the line on February 10<sup>th</sup>.



**Figure 12: Ice at Str. 2561**

- 1 Figure 13 below is a graph of the temperature and precipitation captured at the Gander International
- 2 Airport weather station from February 5<sup>th</sup> to February 13<sup>th</sup>. A mixture of freezing rain and snow was
- 3 captured by the weather station for 4 days prior to the Poles tripping. The temperature also remained
- 4 below zero and reached a low of approximately -7°C before the trip. The towers are at a higher
- 5 elevation than the weather station. Therefore, they could have seen more freezing rain than snow
- 6 during those days prior to the trip.

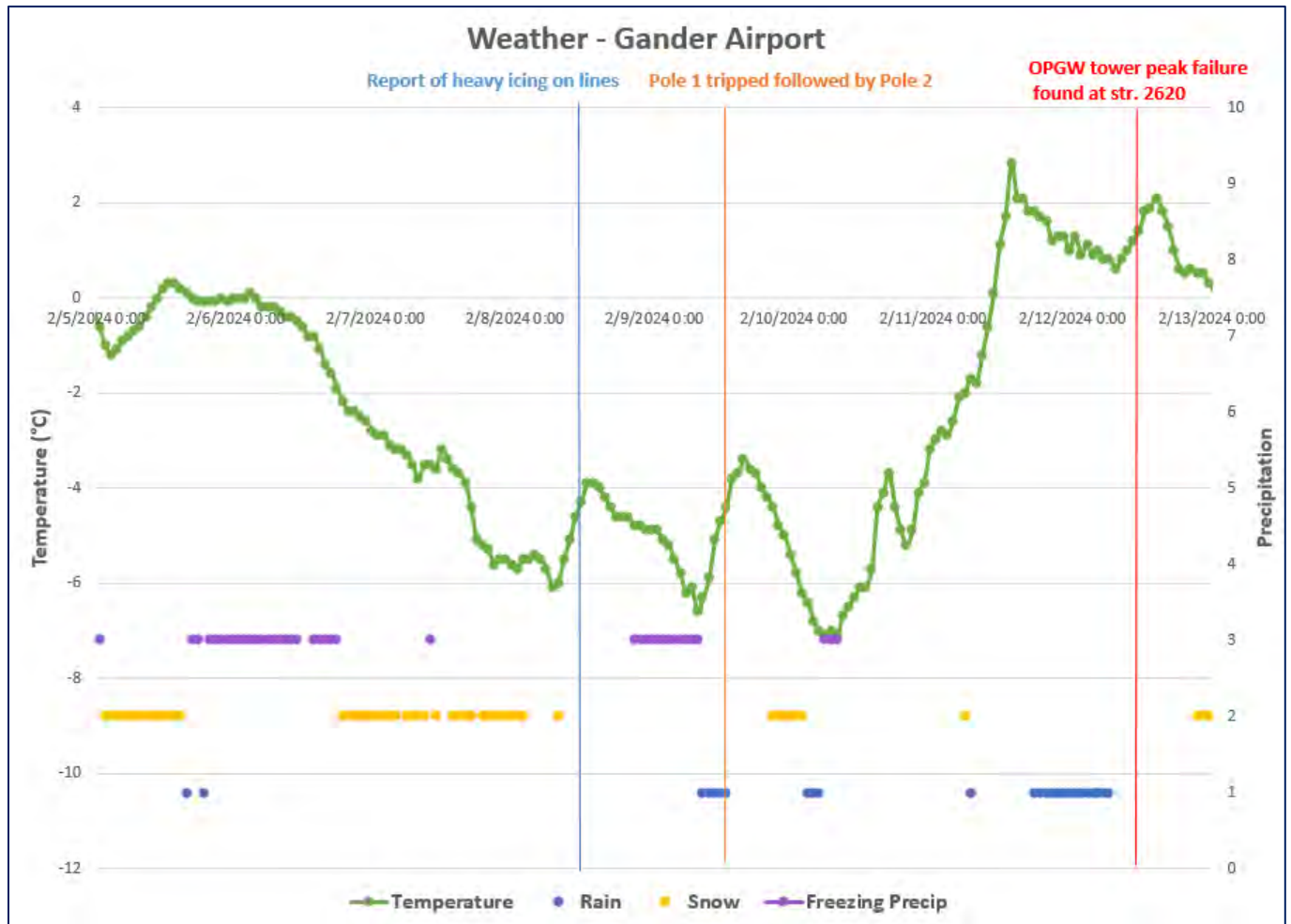
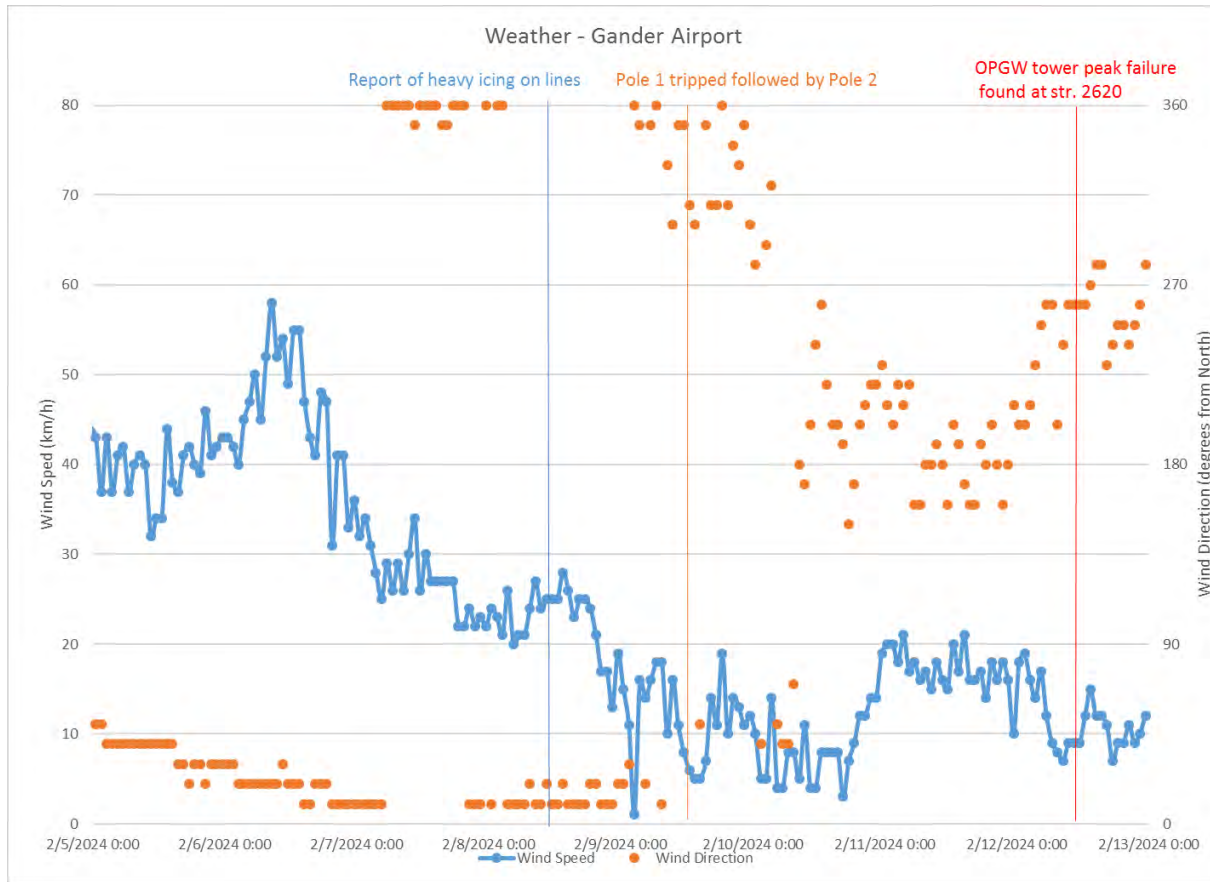


Figure 13: Temperature and Precipitation Recorded from 5-Feb-2024 to 13-Feb-2024

- 1 Wind speed and wind direction was also captured by the Gander weather station between February 5<sup>th</sup>
- 2 and February 13<sup>th</sup>, as shown in Figure 14. The wind peaked at 68 km/h 3 days before the trip and
- 3 dropped to around 10–25 km/h a day before the trip, and under 20 km/h the day the damage was
- 4 found. Reports from the site during the repairs indicated that the winds at the site of the failure were
- 5 consistently higher than the wind in nearby towns. Note that the Gander weather station is at an
- 6 elevation of 151 m above sea level, and the failed structures elevations range from 275–302 m.



**Figure 14: Wind Speed (km/h) and Wind Direction (Degrees from North) from 5-Feb-2024 to 13-Feb-2024**

1 **7.0 Construction Quality and Maintenance Review**

2 The Final Construction Packages contained all the relevant quality control sheets for the construction of  
 3 the line. The form VC-F0113 is the Lattice Tower Assembly Check, and VC-F0112 is the Lattice Tower  
 4 Inspection. Form VC-F0113 and VC-F0112 are complete for all 8 structures. Deficiencies were noted and  
 5 the correction were completed in 2017. See Appendix A for details.

6 There were no Non-Conformance Reports (“NCRs”) submitted on the tower steel for str. 2620, 2545,  
 7 2544, 2543, 2599, 2598, 2597, 2596 during construction. In addition, there are no work orders  
 8 submitted on the structures since installation.

## 1 **8.0 Analysis of Loads Causing Failures**

2 A complete as-built model of L3501/2 includes the existing terrain, as-built tower locations and heights,  
3 with complete finite element tower models. PLS-CADD is a transmission line design program that allows  
4 the user to enter different loading conditions to analyze how they will affect the line and structures  
5 under the as-built conditions. The program allows the user to complete detailed analysis of how  
6 increasing loads will affect the towers performance and ultimately how the towers will fail under  
7 extreme loading conditions.

### 8 **8.1 Ice Loading**

9 As discussed in Section 6.0, reports and pictures from site show the ice thickness at the location of the  
10 failures was approximately 50–75 mm of radial glaze ice at or exceeding the design ice load of 50 mm of  
11 radial glaze ice.

12 Modeling of the line with 55, 60, 65, 70, and 75 mm of ice shows that failure would occur on the  
13 structures in question (str. 2620, 2545, 2544, 2543, 2599, 2598, 2597, 2596) with ice only starting at 65  
14 mm. However, the model also shows that if failures were to occur due to ice alone, these failures would  
15 be contained to the cage of the structure and not match the failures experienced in the field. See Figure  
16 15 for a comparison of the actual failure experienced in the field compared to the modeling of a tower  
17 failure under ice loading of 65 mm. Note that in the modeled tower, the red members represent the  
18 members that are above 100% of their capacity.

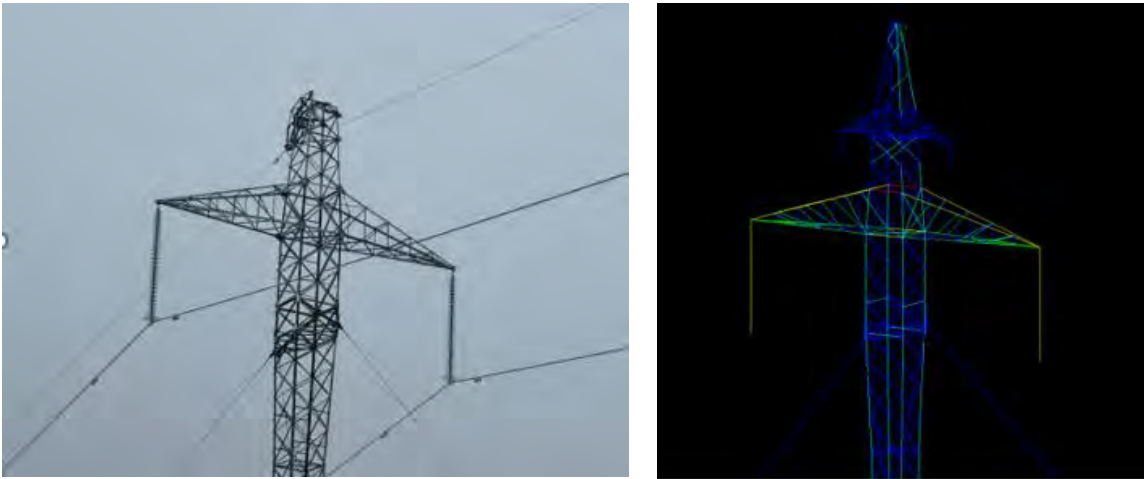


Figure 15: Failure in the Field Compared to Modeling of Tower Failure Under Ice Loading

## 1 8.2 Wind and Ice Combined Loading

2 As noted in Section 5.1, the combined wind and ice design load case uses 25 mm of radial glaze ice and  
3 60 km/h 10 min average wind speed. The failed structures may have seen loading condition around  
4 these values on the day of the failures. The maximum wind speed on that day of the trip and the day the  
5 damage was found was 20 km/h<sup>1</sup> at the nearest weather station at Gander Airport, and the maximum  
6 ice load was estimated between 50 to 75 mm of radial glaze ice. As noted in Section 6.0, it is likely the  
7 wind speed at the location of the failure was higher than reported at the nearest weather station.

8 Modeling of the line with 60 km/h of wind combined with 55, 60, 65, 70, and 75 mm of ice shows that  
9 failure would occur on the structures in question (str. 2620, 2545, 2544, 2543, 2599, 2598, 2597, 2596)  
10 starting at ice thicknesses of 65 mm. However, the model also shows, that if failures were to occur due  
11 to combined wind and ice, these failures would be contained to the cage of the structure and not match  
12 the failures experienced in the field. See Figure 16 for a comparison of the actual failure experienced in

---

<sup>1</sup> Note that the weather data was taken from the Government of Canada Climate website that states the data at a station could be averaged at 1, 2, or 10 minute periods. Therefore, equivalent 10 minute average wind speed could range from 17 to 18 km/h.

- 1 the field compared to the modeling of a tower failure under combined wind/ice loading of 60 km/h wind
- 2 and 65 mm of radial glaze ice.



**Figure 16: Failure in the Field Compared to Modeling of Tower Failure Under Wind and Ice Combined Loading**

### 3 **8.3 Unbalanced Icing**

4 Unbalanced icing is a loading case that considers the loads on a structure when there are different  
5 amount of ice on the front span and back span of the structure, as well on the different wires: Pole 1,  
6 Pole 2, OPGW. The unbalanced icing can occur due to variation in the ice accretion, or due to ice  
7 shedding. The design load cases for unbalanced ice for tangent towers is 100% of the maximum design  
8 ice thickness at one side and 70% of ice on the other side, one conductor at a time. For loading Zone 10  
9 this 100% max ice is 50 mm and 70% of max ice is 35 mm. The three design load cases for unbalanced  
10 ice are:

- 11 • Pole 1 100/70% of 50 mm max ice
- 12 • Pole 2 100/70% of 50 mm max ice
- 13 • OPGW 100/70% of 50 mm max ice mm

1 To evaluate the possible conditions that caused the failures in this event, the unbalance load  
2 combinations of 100/70%, 100/50%, and 100/30 % were analyzed for 55, 60, 65, 70, and 75 mm of radial  
3 glaze ice on the OPGW. This results in 20 load case combinations (when considering each combination  
4 on the str. both front/back and back/front). All load cases resulted in failure of the towers. The lowest  
5 load case of 100/50% of 55 mm of ice resulted in damaged contained to the OPGW peak, as seen in the  
6 field. See Figure 17 comparison of the actual failure experienced in the field compared to the modeling  
7 of a tower failure under unbalanced ice load of 100/50% of 55 mm of radial glaze ice.



**Figure 17: Failure in the Field Compared to Modeling of Tower Failure Under Unbalanced Ice Loading**

## 8 **9.0 Summary and Conclusions**

9 There are several conclusions to draw from the failure analysis of the structures:

- 10 • Failure at all structures was mostly contained to the OPGW peak, with some damaged members  
11 in the cage below.
- 12 • Ice loads in the area ranged in radial thickness from 50 to 75 mm

- 1       • Temperatures rose to above freezing on the day before the failures.
  - 2       • Modeling of the line with the wind and ice loads observed at site alone, does not cause the
  - 3           modeled towers to fail at the OPGW peak.
  - 4       • Modeling of the line with unbalanced ice load will cause the modeled towers to fail at the
  - 5           OPGW peak.
- 6 Failures at all eight structures were mostly contained to the OPGW peak, with three structures also
- 7 sustaining damaged members in the cage, just below the peak. The OPGW cable did not break, but one
- 8 section did have internal damage. There was no damage to the pole cross arm or the body of the tower.
- 9 Ice loads in the area of the failures ranged in radial thickness from 50–75 mm. The maximum design ice
- 10 load for this zone is 50 mm of radial ice. The assumed ice loads of 50–75 mm alone would not cause
- 11 failure to the OPGW peaks.
- 12 The design load case for combined wind and ice is 60 km/h and 25 mm of radial glaze ice. Although the
- 13 ice loads on the towers were higher than the design loads for this load combination, modeling
- 14 confirmed the towers would not fail at the OPGW peak under these loads.
- 15 Temperatures rose above 0°C the day before the failures. This could cause ice to shed from the lines.
- 16 Unbalanced ice loads can result from ice shedding, if the ice sheds unevenly from the front and back
- 17 spans of a tower. Modeling confirmed that unbalanced ice loads could cause failures to the OPGW peak
- 18 under the icing conditions observed at site.
- 19 As highlighted above, the modeling confirmed that the wind and ice loads observed at site alone do not
- 20 cause the towers to fail, but the unbalanced ice will cause the tower peaks to fail.
- 21 Based on the information summarized, the likely cause of the failures was unbalanced ice loads due to
- 22 ice shedding. The ice accumulation was in the range of 50 to 75 mm, the temperatures rose to above
- 23 0°C the day before the failures, and the modeling confirmed that these unbalanced and ice shedding
- 24 loads could cause failure to the OPGW peak. The towers are designed for specific unbalanced ice loads
- 25 of 100/70% of 50 mm of radial glaze ice. However, ice with a higher differential in the unbalanced loads
- 26 could cause failure.

## 10.0 Recommendations

The recommendations to prevent further failures on the line due to unbalanced ice and ice shedding include the following:

- Monitoring of ice conditions along the line
- Strengthening of the tower to withstand higher unbalanced ice loads

Monitoring can be done in a number of ways including line patrol, test spans with ice load and weather monitoring equipment near the line route, and in line ice load monitoring equipment. While monitoring itself will not prevent failures it is sometime possible to remove ice from the lines if accumulation occurs slowly. Monitoring can also help find, and prepare for failures, and it can be used to better understand the amount of ice on the lines for future upgrades.

Monitoring of ice can be accomplished by line patrol. From past recommendation, the line crews has increased the helicopter patrols to 4 times a winter, with additional patrols as needed. The amount of ice on the lines can be estimated from pictures. Ice that has fallen from the lines can be weighed and measured. Check sheets and forms have been created and shared with Engineering and Operations to ensure all the necessary information is being collect when possible. There is an email address to send this information to a centralized location that is monitored by Engineering.

To gain a better understanding of the ice loads experienced by the line, monitoring of the line is required. We currently have a test span installed near str. 1225 with plans to install another test spans in 2025. The test span consists of one span of conductor between two wood poles, with a load cell to monitor ice load, and equipment to monitor wind, and temperature. Unfortunately, the icing in the area of str. 1225 at the time of the failures also caused damage to the solar panel power at the test span, so at this time we have no data from that site. Replacement parts have been received and installed, and the repairs are scheduled be completed in 2025.

In addition, monitors will be installed on the line in 2025 to monitor ice loading in three locations along the line.

The tangent towers on the line are designed for unbalance ice loads of 70% maximum design ice thickness on one wire, on one side of the tower and 100% on one wire the other side of the tower. If the

1 differential in ice thickness is higher, there is a chance the tower will fail. It is recommended that the  
2 towers be analyzed for more conservative unbalanced ice loads. Any recommended changes to the  
3 towers would have to consider the slip strength of the clamps, the redistribution of loads within the  
4 towers, and the constructability of the reinforcements considering the line is built and in service. This  
5 recommendation is being actioned as part of a 2024-2025 project that will evaluate and update the  
6 unbalanced ice loading design used for LIL. This will consist of evaluating all available data (Haldar  
7 reports, failures investigation, operational experience to date, CSA 22.3 60826 standard, best industry  
8 practices) to determine an updated unbalanced ice load design for LIL. This evaluation was completed in  
9 2024. A consultant has been contracted to provide a design and cost estimate for tower modification  
10 that will be required to meet this new unbalanced ice load design, to be completed in 2025. The  
11 feasibility and a cost of other options will also be evaluated which will to meet the new design loads by  
12 reducing the loads on the towers. This will include installing mid span structures between existing  
13 tangent structures, as required.

14 Currently, the OPGW peak is designed for a longitudinal force of 32 kN, and the slip strength of the  
15 OPGW clamps is 35 kN. Note that a successful full scale test of the Type A1 towers was complete during  
16 the design, included the load case with 32 kN of longitudinal on the tower peak. If the towers were  
17 modified to increase the longitudinal capacity, it would make sense to also increase the slip capacity of  
18 the clamps. This can be accomplished by using a double clamp assembly design. This modified design  
19 was ordered and is scheduled to be delivered in the first quarter of 2025. See Figure 18 below.

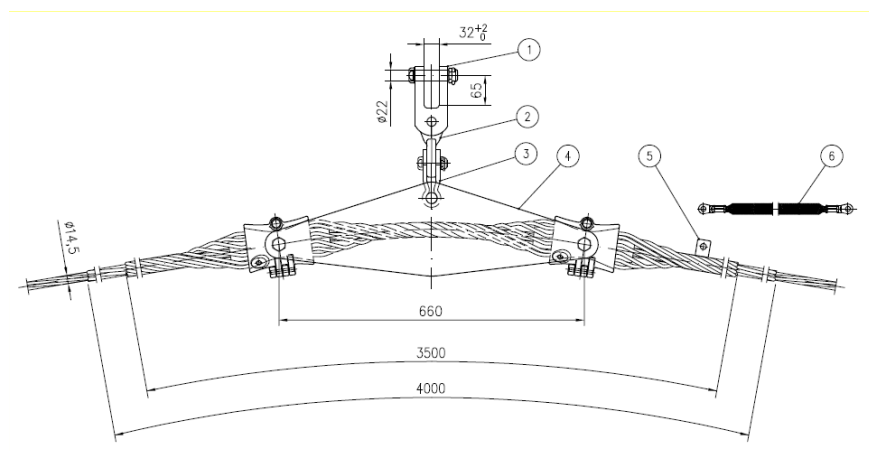


**Figure 18: Modified Double Clamp Design**

- 1 The OPGW peaks failing is preferable to the failure occurring lower in the tower body, as that could
- 2 cause a prolonged power outage or a complete tower failure. A complete tower failure would take more
- 3 time to repair and could also trigger a cascade failure on the line. If reinforcement of the tower peak is
- 4 implemented, consideration must be given to minimize the level of effort and outage time required to
- 5 complete the work on existing in-service towers.

# Appendix A

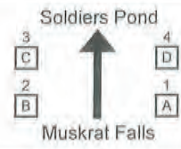
## Quality Control Forms



VC-F0113 : R009

	Document Description			<b>Lattice Tower Assembly Check</b>		
	Created By: Eric Winter		Doc. Number	<b>VC-F0113</b>	Revision	<b>R009</b>
	Date: 01/Jan/2013		VC Number:	VC7343	Contract no.:	CT0327-001
	Revised By: Michael Grieve		Client:	Nalcor Energy	Project no.:	505573
	Rev Date: 08/Aug/2016		Crew:	Floyd Schonauer	Supervisor:	Michael Grieve
	Tower Number:	<b>576</b>	Line Number:	<b>4</b>	Date:	<b>22/Jun/2017</b>
Area of Tower Checked:		Tower Type: <input type="text" value="A1"/>				
Crossarm/peaks	<input checked="" type="checkbox"/> Complete	Body Extension:	<input type="text" value="9.0"/> + <input type="text" value="9.0"/>	Leg Extension:	<input type="text"/> <input type="text"/> <input type="text"/> <input type="text"/>	
Cage	<input checked="" type="checkbox"/> Complete	<i>Capture all Defects on F0047 Deficiency Form and all Missing steel on F0140 Missing Steel Form</i>				
Body	<input checked="" type="checkbox"/> Complete					
Extensions	<input checked="" type="checkbox"/> Complete					
*Check torque 10% for guy towers and 20% for self support towers unless otherwise directed*						
<b>Item Description</b>					<b>Check</b>	
1. Review the line data to verify structure type						
2. Correct Tower and extension are assembled (see staking list)						
3. Inspect all steel for quantities and damage						
4. Report any shortages or damage to the Material Coordinator						
5. Refer to structure layout drawing for steel placement						
6. Install correct bolts as per Manufacturers drawings						
7. Install lock washers as per Manufacturers drawings						
8. All Installed bolts torqued to Manufacturers specifications						
9. All Torqued bolt heads to be identified with RED marker						
10. All verified torqued bolts indicated with BLACK marker						
11. OPGW support installed to inside of line angle						
12. All step bolts installed as per design (refer to tower drawing for each tower type)						
13. Tower checked for any loose bolts, nuts & washers or debris						
14. Any deficiencies identified? (If yes, attach deficiency list) <span style="float: right;"><input type="radio"/> Yes <input checked="" type="radio"/> No</span>						
Torque Wrench S/N: 79118333152, 79118333155, 79118333156						
Notes:						
	Name (Print)	DATE	Signature			
QC Crew	F. Schonauer	22/Jun/2017	F. Schonauer			
Valard QA Review	Alicia Follett	26/Jun/2017	Alicia Follett <i>AF</i>			
Nalcor QA Inspector	<i>Fair</i>	<i>REVIEW ONLY</i>	<i>Andrews</i>			

**Quarterly Report on Asset Performance in Support of Resource Adequacy  
for the Twelve Months Ended March 31, 2025, Attachment 1, Appendix A, Page 2 of 30**

	Document Description			<b>Lattice Tower Inspection</b>		
	Created By: Eric Winter		Doc. Number	<b>VC-F0112</b>	Revision	<b>R010</b>
	Date: 01/Jan/2013		VC Number:	VC7343	Contract no.:	CT0327-001
	Revised By: Drew Williams		Client:	Nalcor Energy	Project no.:	505573
	Rev Date: 06/Aug/2016		Crew:	Charles Calder	Supervisor:	Michael Grieve
Tower Number:	<b>576</b>	Line Number:	<b>4</b>	Date:	<b>21/Jul/2017</b>	
Inspection Type <input type="radio"/> Climbing <input checked="" type="radio"/> Visual <input type="radio"/> Helicopter Patrol					Check	
Body Extension: <input type="text" value="9"/> + <input type="text" value="9"/>	Leg Extension: <input type="text"/> <input type="text"/> <input type="text"/> <input type="text"/>	Tower Type:	A1			
1. Review the line data to verify structure type					<input checked="" type="checkbox"/>	
2. Ensure that erected tower on site is correct (str type & extensions)					<input checked="" type="checkbox"/>	
3. Inspect all steel for debris and damage					<input checked="" type="checkbox"/>	
4. Report any shortages or damage to the Material Coordinator					<input checked="" type="checkbox"/>	
5. Refer to structure layout drawing for steel placement and orientation					<input checked="" type="checkbox"/>	
6. Erected Steel as per Manufacturers drawings (no missing parts or damaged members)					<input checked="" type="checkbox"/>	
7. Climbing inspection of all crossarm connections-torque check all bolts					<input checked="" type="checkbox"/>	
8. Climbing inspection of all splice locations-torque check all splice bolts					<input checked="" type="checkbox"/>	
9. Climbing inspection of all body extension connections-torque check all bolts					<input checked="" type="checkbox"/>	
10. Torque check on all stub leg bolts					N/A <input type="checkbox"/>	
11. Torque check on all floors not checked during assembly stage-torque check all bolts					<input checked="" type="checkbox"/>	
12. All step bolts installed on step bolt legs					<input checked="" type="checkbox"/>	
13. Tower Checked for any loose bolts, nuts & washers during climbing inspection					<input checked="" type="checkbox"/>	
14. All erection materials removed from tower (sling, tag lines, etc.)					<input checked="" type="checkbox"/>	
15. Danger & number signs installed per design on both transverse faces					<input checked="" type="checkbox"/>	
16. Aerial marker signs installed per design on both transverse faces					<input type="radio"/> Yes <input checked="" type="radio"/> N/A	
17. Visual inspection of tower using binoculars completed					<input checked="" type="checkbox"/>	
18. Any deficiencies identified? (If yes, attach deficiency list)					<input checked="" type="radio"/> Yes <input type="radio"/> No	
Notes: <del>Structure number not installed (2543)</del> DM						
For Review Only						
	Name (Print)	DATE	Signature			
Crew	Charles Calder	21/Jul/2017	Charles Calder			
Valard QA Review	A. Medgyesi	24/Jul/2017	A. Medgyesi    A.M.			
Nalcor QC Inspector	A. Corcoran	31-Aug-17	A. Corcoran			



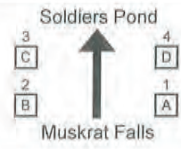
VC-F0113 : R009

	Document Description			<b>Lattice Tower Assembly Check</b>		
	Created By: Eric Winter		Doc. Number	<b>VC-F0113</b>	Revision	<b>R009</b>
	Date: 01/Jan/2013		VC Number:	VC7343	Contract no.:	CT0327-001
	Revised By: Michael Grieve		Client:	Nalcor Energy	Project no.:	505573
	Rev Date: 08/Aug/2016		Crew:	Floyd Schonauer	Supervisor:	Michael Grieve
	Tower Number:	<b>577</b>	Line Number:	<b>4</b>	Date:	<b>22/Jun/2017</b>
Area of Tower Checked:		Tower Type: <input type="text" value="A1"/>				
Crossarm/peaks	<input checked="" type="checkbox"/> Complete	Body Extension: <input type="text" value="9.0"/> + <input type="text" value="9.0"/>		Leg Extension: <input type="text"/> <input type="text"/> <input type="text"/> <input type="text"/>		
Cage	<input checked="" type="checkbox"/> Complete	<i>Capture all Defects on F0047 Deficiency Form and all Missing steel on F0140 Missing Steel Form</i>				
Body	<input checked="" type="checkbox"/> Complete					
Extensions	<input checked="" type="checkbox"/> Complete					
*Check torque 10% for guy towers and 20% for self support towers unless otherwise directed*						
<b>Item Description</b>					<b>Check</b>	
1. Review the line data to verify structure type					<input checked="" type="checkbox"/>	
2. Correct Tower and extension are assembled (see staking list)					<input checked="" type="checkbox"/>	
3. Inspect all steel for quantities and damage					<input checked="" type="checkbox"/>	
4. Report any shortages or damage to the Material Coordinator					<input checked="" type="checkbox"/>	
5. Refer to structure layout drawing for steel placement					<input checked="" type="checkbox"/>	
6. Install correct bolts as per Manufacturers drawings					<input checked="" type="checkbox"/>	
7. Install lock washers as per Manufacturers drawings					<input checked="" type="checkbox"/>	
8. All Installed bolts torqued to Manufacturers specifications					<input checked="" type="checkbox"/>	
9. All Torqued bolt heads to be identified with RED marker					<input checked="" type="checkbox"/>	
10. All verified torqued bolts indicated with BLACK marker					<input checked="" type="checkbox"/>	
11. OPGW support installed to inside of line angle					<input checked="" type="checkbox"/>	
12. All step bolts installed as per design (refer to tower drawing for each tower type)					<input checked="" type="checkbox"/>	
13. Tower checked for any loose bolts, nuts & washers or debris					<input checked="" type="checkbox"/>	
14. Any deficiencies identified? (If yes, attach deficiency list)					<input checked="" type="radio"/> Yes <input type="radio"/> No	
Torque Wrench S/N: 79118333152, 79118333155, 79118333156						
Notes:						
	Name (Print)	DATE	Signature			
QC Crew	F. Schonauer	22/Jun/2017	F. Schonauer			
Valard QA Review	Alicia Follett	26/Jun/2017	Alicia Follett <i>AF</i>			
Nalcor QA Inspector	<i>Fack A</i>	<i>30 Jun 2017</i>	<i>F. Schonauer</i>			

FOR REVIEW ONLY



**Quarterly Report on Asset Performance in Support of Resource Adequacy  
for the Twelve Months Ended March 31, 2025, Attachment 1, Appendix A, Page 6 of 30**

	Document Description			<b>Lattice Tower Inspection</b>		
	Created By: Eric Winter		Doc. Number	<b>VC-F0112</b>	Revision	<b>R010</b>
	Date: 01/Jan/2013		VC Number:	VC7343	Contract no.:	CT0327-001
	Revised By: Drew Williams		Client:	Nalcor Energy	Project no.:	505573
	Rev Date: 06/Aug/2016		Crew:	Charles Calder	Supervisor:	Michael Grieve
Tower Number:	<b>577</b>	Line Number:	<b>4</b>	Date:	<b>21/Jul/2017</b>	
Inspection Type <input type="radio"/> Climbing <input checked="" type="radio"/> Visual <input type="radio"/> Helicopter Patrol					Check	
Body Extension: <input type="text" value="9"/> + <input type="text" value="9"/>	Leg Extension: <input type="text"/> <input type="text"/> <input type="text"/> <input type="text"/>	Tower Type:	A1			
1. Review the line data to verify structure type					<input checked="" type="checkbox"/>	
2. Ensure that erected tower on site is correct (str type & extensions)					<input checked="" type="checkbox"/>	
3. Inspect all steel for debris and damage					<input checked="" type="checkbox"/>	
4. Report any shortages or damage to the Material Coordinator					N/A <input type="checkbox"/>	
5. Refer to structure layout drawing for steel placement and orientation					<input checked="" type="checkbox"/>	
6. Erected Steel as per Manufacturers drawings (no missing parts or damaged members)					<input checked="" type="checkbox"/>	
7. Climbing inspection of all crossarm connections-torque check all bolts					<input checked="" type="checkbox"/>	
8. Climbing inspection of all splice locations-torque check all splice bolts					<input checked="" type="checkbox"/>	
9. Climbing inspection of all body extension connections-torque check all bolts					<input checked="" type="checkbox"/>	
10. Torque check on all stub leg bolts					N/A <input type="checkbox"/>	
11. Torque check on all floors not checked during assembly stage-torque check all bolts					<input checked="" type="checkbox"/>	
12. All step bolts installed on step bolt legs					<input checked="" type="checkbox"/>	
13. Tower Checked for any loose bolts, nuts & washers during climbing inspection					<input checked="" type="checkbox"/>	
14. All erection materials removed from tower (sling, tag lines, etc.)					<input checked="" type="checkbox"/>	
15. Danger & number signs installed per design on both transverse faces					<input checked="" type="checkbox"/>	
16. Aerial marker signs installed per design on both transverse faces					<input type="radio"/> Yes <input checked="" type="radio"/> N/A	
17. Visual inspection of tower using binoculars completed					<input checked="" type="checkbox"/>	
18. Any deficiencies identified? (If yes, attach deficiency list)					<input checked="" type="radio"/> Yes <input type="radio"/> No	
Notes: <del>Structure number not installed (2544)</del> DM						
For Review Only						
		Name (Print)	DATE	Signature		
Crew	Charles Calder	21/Jul/2017	Charles Calder			
Valard QA Review	A. Medgyesi	24/Jul/2017	A. Medgyesi    A.M.			
Nalcor QC Inspector	A. Concoran	31-Aug-17	A. Concoran			



**Quarterly Report on Asset Performance in Support of Resource Adequacy  
for the Twelve Months Ended March 31, 2025, Attachment 1, Appendix A, Page 8 of 30**

	Document Description			Deficiency List	
	Created By: Eric Winter		Doc. Number		VC-F0047-A
	Date: 01/Jan/13	Revision R002	VC Number: VC7343	Contract no.:	CT0327-001
	Revised By: Evan McKinnon		Client: Nalcor Energy	Project no.:	505573
	Date: 01/Aug/14		Crew: Charles Calder	Supervisor: Michael Grieve	
	Tower Number:	577	Line Number:	4	Date: 21/Jul/2017

**Deficiency List Classification**

I = Important Punch List Item  
M = Minor Punch List Item

H = Housekeeping  
MS = Missing Steel

R = Reclamation

**Deficiency List Scope**

Assembly Erection

Item	Class	Description	Responsibility	Date Initiated	Deficiency Sign-Off	Date Completed	Correction Completion
1	M	Step Bolt Peak Face In	Valard	21/Jul/2017	CC		

<b>Comments</b>
For Review Only

QC Crew:  
Valard QA:  
Nalcor QC Inspector:

Deficiencies Identified			Correction Completed		
Print Name	Signature	Date	Print Name	Signature	Date
Charles Calder	Charles Calder	21/Jul/2017			
A. Medgyesi	A. Medgyesi	24/Jul/2017			
A. Concoran	A. Concoran	31-Aug-17			

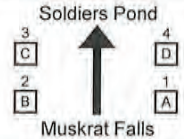
VC-F0113 : R009

	Document Description			<b>Lattice Tower Assembly Check</b>			
	Created By: Eric Winter		Doc. Number	<b>VC-F0113</b>		Revision	<b>R009</b>
	Date: 01/Jan/2013		VC Number:	VC7343	Contract no.:	CT0327-001	
	Revised By: Michael Grieve		Client: Nalcor Energy		Project no.: 505573		
	Rev Date: 08/Aug/2016		Crew: QAQC		Supervisor: Michael Grieve		
	Tower Number:	<b>578</b>	Line Number:	<b>4</b>	Date: 23/Jun/2017		
Area of Tower Checked:		Tower Type: <input type="text" value="A1"/>					
Crossarm/peaks	<input checked="" type="checkbox"/> Complete	Body Extension:	<input type="text" value="6.0"/> + <input type="text" value="6.0"/>	Leg Extension:	<input type="text"/> <input type="text"/> <input type="text"/> <input type="text"/>		
Cage	<input checked="" type="checkbox"/> Complete	<i>Capture all Defects on F0047 Deficiency Form and all Missing steel on F0140 Missing Steel Form</i>					
Body	<input checked="" type="checkbox"/> Complete						
Extensions	<input checked="" type="checkbox"/> Complete						
*Check torque 10% for guy towers and 20% for self support towers unless otherwise directed*						<b>Check</b>	
<b>Item Description</b>							
1. Review the line data to verify structure type		<input checked="" type="checkbox"/>					
2. Correct Tower and extension are assembled (see staking list)		<input checked="" type="checkbox"/>					
3. Inspect all steel for quantities and damage		<input checked="" type="checkbox"/>					
4. Report any shortages or damage to the Material Coordinator		<input checked="" type="checkbox"/>					
5. Refer to structure layout drawing for steel placement		<input checked="" type="checkbox"/>					
6. Install correct bolts as per Manufacturers drawings		<input checked="" type="checkbox"/>					
7. Install lock washers as per Manufacturers drawings		<input checked="" type="checkbox"/>					
8. All Installed bolts torqued to Manufacturers specifications		<input checked="" type="checkbox"/>					
9. All Torqued bolt heads to be identified with RED marker		<input checked="" type="checkbox"/>					
10. All verified torqued bolts indicated with BLACK marker		<input checked="" type="checkbox"/>					
11. OPGW support installed to inside of line angle		<input checked="" type="checkbox"/>					
12. All step bolts installed as per design (refer to tower drawing for each tower type)		<input checked="" type="checkbox"/>					
13. Tower checked for any loose bolts, nuts & washers or debris		<input checked="" type="checkbox"/>					
14. Any deficiencies identified? (If yes, attach deficiency list)		<input checked="" type="radio"/> Yes <input type="radio"/> No					
Torque Wrench S/N: 79118333152, 79118333155, 79118333156							
Notes:							
	Name (Print)	DATE	Signature				
QC Crew	Floyd S	23/Jun/2017	Floyd S				
Valard QA Review	Kaitlyn O'Reilly	25/Jun/2017	Kaitlyn O'Reilly <i>KG</i>				
Nalcor QA Inspector	<i>Zack A. ...</i>	<i>...</i>	<i>Zack A. ...</i>				

FOR REVIEW ONLY



**Quarterly Report on Asset Performance in Support of Resource Adequacy  
for the Twelve Months Ended March 31, 2025, Attachment 1, Appendix A, Page 11 of 30**

	Document Description			<b>Lattice Tower Inspection</b>		
	Created By: Eric Winter		Doc. Number	<b>VC-F0112</b>	Revision	<b>R010</b>
	Date: 01/Jan/2013		VC Number:	VC7343	Contract no.:	CT0327-001
	Revised By: Drew Williams		Client:	Nalcor Energy	Project no.:	505573
	Rev Date: 06/Aug/2016		Crew:	Charles Calder	Supervisor:	Michael Grieve
	Tower Number:	<b>578</b>	Line Number:	<b>4</b>	Date:	<b>21/Jul/2017</b>
Inspection Type <input type="radio"/> Climbing <input checked="" type="radio"/> Visual <input type="radio"/> Helicopter Patrol					Check	
Body Extension: <input type="text" value="6"/> + <input type="text" value="6"/>	Leg Extension: <input type="text"/> <input type="text"/> <input type="text"/> <input type="text"/>	Tower Type:	A1			
1. Review the line data to verify structure type					<input checked="" type="checkbox"/>	
2. Ensure that erected tower on site is correct (str type & extensions)					<input checked="" type="checkbox"/>	
3. Inspect all steel for debris and damage					<input checked="" type="checkbox"/>	
4. Report any shortages or damage to the Material Coordinator					N/A <input type="checkbox"/>	
5. Refer to structure layout drawing for steel placement and orientation					<input checked="" type="checkbox"/>	
6. Erected Steel as per Manufacturers drawings (no missing parts or damaged members)					<input checked="" type="checkbox"/>	
7. Climbing inspection of all crossarm connections-torque check all bolts					<input checked="" type="checkbox"/>	
8. Climbing inspection of all splice locations-torque check all splice bolts					<input checked="" type="checkbox"/>	
9. Climbing inspection of all body extension connections-torque check all bolts					<input checked="" type="checkbox"/>	
10. Torque check on all stub leg bolts					N/A <input type="checkbox"/>	
11. Torque check on all floors not checked during assembly stage-torque check all bolts					<input checked="" type="checkbox"/>	
12. All step bolts installed on step bolt legs					<input checked="" type="checkbox"/>	
13. Tower Checked for any loose bolts, nuts & washers during climbing inspection					<input checked="" type="checkbox"/>	
14. All erection materials removed from tower (sling, tag lines, etc.)					<input checked="" type="checkbox"/>	
15. Danger & number signs installed per design on both transverse faces					<input checked="" type="checkbox"/>	
16. Aerial marker signs installed per design on both transverse faces					<input type="radio"/> Yes <input checked="" type="radio"/> N/A	
17. Visual inspection of tower using binoculars completed					<input checked="" type="checkbox"/>	
18. Any deficiencies identified? (If yes, attach deficiency list)					<input checked="" type="radio"/> Yes <input type="radio"/> No	
Notes: <del>Structure number not installed (2545)</del> DM						
For Review Only						
	Name (Print)	DATE	Signature			
Crew	Charles Calder	21/Jul/2017	Charles Calder			
Valard QA Review	A. Medgyesi	24/Jul/2017	A. Medgyesi <i>A.M.</i>			
Nalcor QC Inspector	<i>A. Concor AW</i>	<i>04-Sept-17</i>	<i>A. Concor</i>			

**Quarterly Report on Asset Performance in Support of Resource Adequacy  
for the Twelve Months Ended March 31, 2025, Attachment 1, Appendix A, Page 12 of 30**

	Document Description			<b>Deficiency List</b>	
	Created By: Eric Winter		Doc. Number		<b>VC-F0047-E</b>
	Date: 01/Jan/13	Revision R002	VC Number: VC7343	Contract no.: CT0327-001	
	Revised By: Evan McKinnon		Client: Nalcor Energy	Project no.: 505573	
	Date: 01/Aug/14		Crew: Charles Calder	Supervisor: Michael Grieve	
	Tower Number:	<b>578</b>	Line Number:	<b>4</b>	Date: <b>21/Jul/2017</b>

**Deficiency List Classification**  
 I = Important Punch List Item    H = Housekeeping    R = Reclamation  
 M = Minor Punch List Item        MS = Missing Steel

**Deficiency List Scope**  
 Erection

Item	Class	Description	Responsibility	Date Initiated	Deficiency Sign-Off	Date Completed	Correction Completion
1	M	Step Bolt Peak Face In	Valard	21/Jul/2017	CC	24/Sep/2017	FS

**Comments**

---



---



---



---



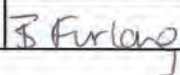
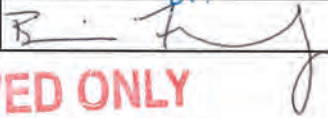
---

QC Crew:  
 Valard QA:  
 Nalcor QC Inspector:

Deficiencies Identified			Correction Completed		
Print Name	Signature	Date	Print Name	Signature	Date
Charles Calder	Charles Calder	21/Jul/2017	Floyd Schonauer	Floyd Schonauer	24/Sep/2017
A. Medgyesi	A. Medgyesi	24/Jul/2017	Kaitlyn O'Reilly	Kaitlyn O'Reilly	26/Sep/2017
Angela Corcoran	Angela Corcoran	04/Sep/2017	B. Pawling	[Signature]	7 Oct 17

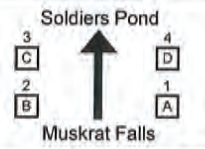
**REVIEWED ONLY**

**VC-F0113 : R009**

	Document Description			<b>Lattice Tower Assembly Check</b>		
	Created By: Eric Winter		Doc. Number	<b>VC-F0113</b>	Revision <b>R009</b>	
	Date: 01/Jan/2013		VC Number:	VC7343	Contract no.:	CT0327-001
	Revised By: Michael Grieve		Client:	Nalcor Energy	Project no.:	505573
	Rev Date: 08/Aug/2016		Crew:	Floyd Schonauer	Supervisor:	Michael Grieve
	Tower Number:	<b>629</b>	Line Number:	<b>4</b>	Date: <b>02/Jul/2017</b>	
Area of Tower Checked:		Tower Type: <input type="text" value="A1"/>				
Crossarm/peaks	<input checked="" type="checkbox"/> Complete	Body Extension:	<input type="text" value="7.5"/> + <input type="text" value="7.5"/>	Leg Extension: <input type="text"/> <input type="text"/> <input type="text"/> <input type="text"/>		
Cage	<input checked="" type="checkbox"/> Complete	<i>Capture all Defects on F0047 Deficiency Form and all Missing steel on F0140 Missing Steel Form</i>			Soldiers Pond  Muskrat Falls	
Body	<input checked="" type="checkbox"/> Complete					
Extensions	<input checked="" type="checkbox"/> Complete					
*Check torque 10% for guy towers and 20% for self support towers unless otherwise directed*						<b>Check</b>
<b>Item Description</b>						
1. Review the line data to verify structure type						
2. Correct Tower and extension are assembled (see staking list)						
3. Inspect all steel for quantities and damage						
4. Report any shortages or damage to the Material Coordinator						
5. Refer to structure layout drawing for steel placement						
6. Install correct bolts as per Manufacturers drawings						
7. Install lock washers as per Manufacturers drawings						
8. All Installed bolts torqued to Manufacturers specifications						
9. All Torqued bolt heads to be identified with RED marker						
10. All verified torqued bolts indicated with BLACK marker						
11. OPGW support installed to inside of line angle						
12. All step bolts installed as per design (refer to tower drawing for each tower type)						
13. Tower checked for any loose bolts, nuts & washers or debris						
14. Any deficiencies identified? (If yes, attach deficiency list) <span style="float: right;"><input checked="" type="radio"/> Yes <input type="radio"/> No</span>						
Torque Wrench S/N: 79118333152 , 79118333156						
Notes:						
	Name (Print)	DATE	Signature			
QC Crew	F. Schonauer	02/Jul/2017	F. Schonauer			
Valard QA Review	Alicia Follett	03/Jul/2017	Alicia Follett 			
Nalcor QA Inspector		4 Jul 17				

REVIEWED ONLY



	Document Description			<b>Lattice Tower Inspection</b>			
	Created By: Eric Winter		Doc. Number	<b>VC-F0112</b>	Revision <b>R010</b>		
	Date: 01/Jan/2013		VC Number: VC7343	Contract no.: CT0327-001			
	Revised By: Drew Williams		Client: Nalcor Energy	Project no.: 505573			
	Rev Date: 06/Aug/2016		Crew: QAQC	Supervisor: Michael Grieve			
	Tower Number:	<b>629</b>	Line Number:	<b>4</b>	Date: <b>25/Jul/2017</b>		
Inspection Type <input type="radio"/> Climbing <input type="radio"/> Visual <input type="radio"/> Helicopter Patrol					<b>Check</b>		
Body Extension: <input type="text" value="7.5"/> + <input type="text" value="7.5"/>	Leg Extension: <input type="text"/> <input type="text"/> <input type="text"/> <input type="text"/>	Tower Type: <b>A1</b>					
1. Review the line data to verify structure type					<input checked="" type="checkbox"/>		
2. Ensure that erected tower on site is correct (str type & extensions)					<input checked="" type="checkbox"/>		
3. Inspect all steel for debris and damage					<input checked="" type="checkbox"/>		
4. Report any shortages or damage to the Material Coordinator					<input checked="" type="checkbox"/>		
5. Refer to structure layout drawing for steel placement and orientation					<input checked="" type="checkbox"/>		
6. Erected Steel as per Manufacturers drawings (no missing parts or damaged members)					<input checked="" type="checkbox"/>		
7. Climbing inspection of all crossarm connections-torque check all bolts					<input checked="" type="checkbox"/>		
8. Climbing inspection of all splice locations-torque check all splice bolts					<input checked="" type="checkbox"/>		
9. Climbing inspection of all body extension connections-torque check all bolts					<input checked="" type="checkbox"/>		
10. Torque check on all stub leg bolts					N/A <input type="checkbox"/>		
11. Torque check on all floors not checked during assembly stage-torque check all bolts					<input checked="" type="checkbox"/>		
12. All step bolts installed on step bolt legs					<input checked="" type="checkbox"/>		
13. Tower Checked for any loose bolts, nuts & washers during climbing inspection					<input checked="" type="checkbox"/>		
14. All erection materials removed from tower (sling, tag lines, etc.)					<input type="checkbox"/>		
15. Danger & number signs installed per design on both transverse faces					<input type="checkbox"/>		
16. Aerial marker signs installed per design on both transverse faces					<input type="radio"/> Yes <input checked="" type="radio"/> N/A		
17. Visual inspection of tower using binoculars completed					<input checked="" type="checkbox"/>		
18. Any deficiencies identified? (If yes, attach deficiency list)					<input checked="" type="radio"/> Yes <input type="radio"/> No		
Notes: Structure Number Not Installed (2596)							
FOR REVIEW ONLY							
	Name (Print)	DATE	Signature				
Crew	Charles Calder	25/Jul/2017	Charles Calder				
Valard QA Review	Kaitlyn O'Reilly	02/Aug/2017	Kaitlyn O'Reilly <i>KO</i>				
Nalcor QC Inspector	<i>A. Concoran</i>	<i>07-Aug-17</i>	<i>A Concoran</i>				

**Quarterly Report on Asset Performance in Support of Resource Adequacy  
for the Twelve Months Ended March 31, 2025, Attachment 1, Appendix A, Page 16 of 30**

	Document Description			<b>Deficiency List</b>	
	Created By: Eric Winter		Doc. Number		VC-F0047-E
	Date: 01/Jan/13	Revision R002	VC Number: VC7343	Contract no.: CT0327-001	
	Revised By: Evan McKinnon		Client: Nalcor Energy	Project no.: 505573	
	Date: 01/Aug/14		Crew: QAQC	Supervisor: Michael Grieve	
	Tower Number:	629	Line Number:	4	Date:

**Deficiency List Classification**

I = Important Punch List Item  
M = Minor Punch List Item

H = Housekeeping  
MS = Missing Steel

R = Reclamation

**Deficiency List Scope**

Erection

Item	Class	Description	Responsibility	Date Initiated	Deficiency Sign-Off	Date Completed	Correction Completion
1	M	Step Bolts Face In	Valard	25/Jul/2017	CC	Aug 31, 17	CC
2	M	B509 X1 - Damaged	QAQC	25/Jul/2017	CC	Aug 31, 17	CC
3	M	B510 X1 - Damaged	QAQC	25/Jul/2017	CC	Aug 31, 17	CC

**Comments**

---



---

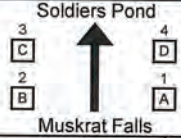
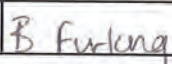
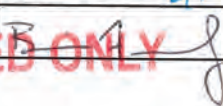


---

**FOR REVIEW ONLY**

Deficiencies Identified			Correction Completed		
Print Name	Signature	Date	Print Name	Signature	Date
QC Crew: Charles Calder	Charles Calder	25/Jul/2017	Charles Calder	Charles Calder	Aug 31, 17
Valard QA: Kaitlyn O'Reilly	Kaitlyn O'Reilly	02/Aug/2017	B Gardiner	B Gardiner	01-SEP-17
Nalcor QC Inspector: A. CONCORAN	A. CONCORAN	02-AUG-17	Zack A	Zack A	8 sep 2017

**VC-F0113 : R009**

	Document Description			<b>Lattice Tower Assembly Check</b>			
	Created By: Eric Winter		Doc. Number	<b>VC-F0113</b>			
	Date: 01/Jan/2013		VC Number: VC7343	Revision	<b>R009</b>		
	Revised By: Michael Grieve		Contract no.:	CT0327-001			
	Rev Date: 08/Aug/2016		Client: Nalcor Energy	Project no.:	505573		
	Tower Number: <b>630</b>		Crew: Tom Wright	Supervisor: Michael Grieve			
Line Number: <b>4</b>		Date: <b>02/Jul/2017</b>					
Area of Tower Checked:		Tower Type: <input type="text" value="A1"/>					
Crossarm/peaks	<input checked="" type="checkbox"/> Complete	Body Extension: <input type="text" value="9.0"/> + <input type="text" value="9.0"/>	Leg Extension: <input type="text"/> <input type="text"/> <input type="text"/> <input type="text"/>				
Cage	<input checked="" type="checkbox"/> Complete	<i>Capture all Defects on F0047 Deficiency Form and all Missing steel on F0140 Missing Steel Form</i>					
Body	<input checked="" type="checkbox"/> Complete						
Extensions	<input checked="" type="checkbox"/> Complete						
*Check torque 10% for guy towers and 20% for self support towers unless otherwise directed*						<b>Check</b>	
<b>Item Description</b>							
1. Review the line data to verify structure type						<input checked="" type="checkbox"/>	
2. Correct Tower and extension are assembled (see staking list)						<input checked="" type="checkbox"/>	
3. Inspect all steel for quantities and damage						<input checked="" type="checkbox"/>	
4. Report any shortages or damage to the Material Coordinator						<input checked="" type="checkbox"/>	
5. Refer to structure layout drawing for steel placement						<input checked="" type="checkbox"/>	
6. Install correct bolts as per Manufacturers drawings						<input checked="" type="checkbox"/>	
7. Install lock washers as per Manufacturers drawings						<input checked="" type="checkbox"/>	
8. All Installed bolts torqued to Manufacturers specifications						<input checked="" type="checkbox"/>	
9. All Torqued bolt heads to be identified with RED marker						<input checked="" type="checkbox"/>	
10. All verified torqued bolts indicated with BLACK marker						<input checked="" type="checkbox"/>	
11. OPGW support installed to inside of line angle						<input checked="" type="checkbox"/>	
12. All step bolts installed as per design (refer to tower drawing for each tower type)						<input checked="" type="checkbox"/>	
13. Tower checked for any loose bolts, nuts & washers or debris						<input checked="" type="checkbox"/>	
14. Any deficiencies identified? (If yes, attach deficiency list)						<input checked="" type="radio"/> Yes <input type="radio"/> No	
Torque Wrench S/N: 79118333105							
Notes:							
	Name (Print)	DATE	Signature				
QC Crew	Tom Wright	02/Jul/2017	Tom Wright				
Valard QA Review	Alicia Follett	03/Jul/2017	Alicia Follett 				
Nalcor QA Inspector		4 Jul 17					

REVIEWED ONLY

**Quarterly Report on Asset Performance in Support of Resource Adequacy  
for the Twelve Months Ended March 31, 2025, Attachment 1, Appendix A, Page 18 of 30**

	Document Description			<b>Deficiency List</b>	
	Created By: Eric Winter		Doc. Number		<b>VC-F0047-A</b>
	Date: 01/Jan/13	Revision R002	VC Number: VC7343	Contract no.: CT0327-001	
	Revised By: Evan McKinnon		Client: Nalcor Energy	Project no.: 505573	
	Date: 01/Aug/14		Crew: Tom Wright	Supervisor: Michael Grieve	
	Tower Number:	<b>630</b>	Line Number:	<b>4</b>	Date: <b>02/Jul/2017</b>

**Deficiency List Classification**

I = Important Punch List Item  
M = Minor Punch List Item

H = Housekeeping  
MS = Missing Steel

R = Reclamation

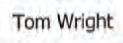
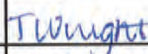
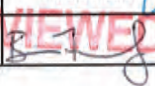
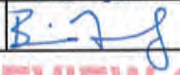
**Deficiency List Scope**

Assembly

Item	Class	Description	Responsibility	Date Initiated	Deficiency Sign-Off	Date Completed	Correction Completion
1	MS	9M04 x 1	Nalcor	02/Jul/2017	TW	06-JULY-17	TW
2	MS	BB23 x 1	Valard	02/Jul/2017	TW	06-JULY-17	TW
3	MS	CG108 x 1	Valard	02/Jul/2017	TW	06-JULY-17	TW

<b>Comments</b>

QC Crew: Tom Wright  
Valard QA: Alicia Follett  
Nalcor QC Inspector: B. Furlong

Deficiencies Identified			Correction Completed		
Print Name	Signature	Date	Print Name	Signature	Date
Tom Wright		02/Jul/2017	Tom Wright		06-JULY-17
Alicia Follett		03/Jul/2017	B. Gardiner		03-AUG-17
B. Furlong		4 Jul 17	B. Furlong		15 Aug 17

**REVIEWED ONLY**

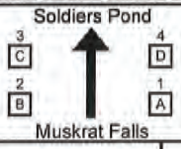
**FOR REVIEW ONLY**

**Quarterly Report on Asset Performance in Support of Resource Adequacy  
for the Twelve Months Ended March 31, 2025, Attachment 1, Appendix A, Page 19 of 30**

	Document Description			<b>Lattice Tower Inspection</b>		
	Created By: Eric Winter		Doc. Number	<b>VC-F0112</b>	Revision	<b>R010</b>
	Date: 01/Jan/2013		VC Number:	VC7343	Contract no.:	CT0327-001
	Revised By: Drew Williams		Client:	Nalcor Energy	Project no.:	505573
	Rev Date: 06/Aug/2016		Crew:	QAQC	Supervisor:	Michael Grieve
	Tower Number:	<b>630</b>	Line Number:	<b>4</b>	Date:	<b>25/Jul/2017</b>
Inspection Type <input type="radio"/> Climbing <input checked="" type="radio"/> Visual <input type="radio"/> Helicopter Patrol					Check	
Body Extension: <input type="text" value="9"/> + <input type="text" value="9"/>	Leg Extension: <input type="text"/> <input type="text"/> <input type="text"/> <input type="text"/>	Tower Type: <b>A1</b>				
1. Review the line data to verify structure type					<input checked="" type="checkbox"/>	
2. Ensure that erected tower on site is correct (str type & extensions)					<input checked="" type="checkbox"/>	
3. Inspect all steel for debris and damage					<input checked="" type="checkbox"/>	
4. Report any shortages or damage to the Material Coordinator					<input type="checkbox"/> <i>N/A</i>	
5. Refer to structure layout drawing for steel placement and orientation					<input checked="" type="checkbox"/>	
6. Erected Steel as per Manufacturers drawings (no missing parts or damaged members)					<input checked="" type="checkbox"/>	
7. Climbing inspection of all crossarm connections-torque check all bolts					<input checked="" type="checkbox"/>	
8. Climbing inspection of all splice locations-torque check all splice bolts					<input checked="" type="checkbox"/>	
9. Climbing inspection of all body extension connections-torque check all bolts					<input checked="" type="checkbox"/>	
10. Torque check on all stub leg bolts					<input type="checkbox"/> <i>N/A</i>	
11. Torque check on all floors not checked during assembly stage-torque check all bolts					<input checked="" type="checkbox"/>	
12. All step bolts installed on step bolt legs					<input checked="" type="checkbox"/>	
13. Tower Checked for any loose bolts, nuts & washers during climbing inspection					<input checked="" type="checkbox"/>	
14. All erection materials removed from tower (sling, tag lines, etc.)					<input checked="" type="checkbox"/>	
15. Danger & number signs installed per design on both transverse faces					<input checked="" type="checkbox"/>	
16. Aerial marker signs installed per design on both transverse faces					<input type="radio"/> Yes <input checked="" type="radio"/> N/A	
17. Visual inspection of tower using binoculars completed					<input checked="" type="checkbox"/>	
18. Any deficiencies identified? (If yes, attach deficiency list)					<input checked="" type="radio"/> Yes <input type="radio"/> No	
Notes: <del>Structure Numbers Not Installed (2597)</del> <i>DM</i>						
<b>FOR REVIEW ONLY</b>						
	Name (Print)	DATE	Signature			
Crew	Charles Calder	25/Jul/2017	Charles Calder			
Valard QA Review	Kaitlyn O'Reilly	02/Aug/2017	Kaitlyn O'Reilly <i>KO</i>			
Nalcor QC Inspector	<i>A. CONCORAN</i>	<i>07-Aug-17</i>	<i>A. Concoran</i>			



**VC-F0113 : R009**

	Document Description			<b>Lattice Tower Assembly Check</b>		
	Created By: Eric Winter		Doc. Number	<b>VC-F0113</b>		Revision <b>R009</b>
	Date: 01/Jan/2013		VC Number: VC7343	Contract no.:		CT0327-001
	Revised By: Michael Grieve		Client: Nalcor Energy	Project no.:		505573
	Rev Date: 08/Aug/2016		Crew: Floyd Schonauer	Supervisor:		Michael Grieve
Tower Number: <b>631</b>		Line Number: <b>4</b>	Date: <b>04/Jul/2017</b>			
<b>Area of Tower Checked:</b>		Tower Type: <input type="text" value="A1"/>				
Crossarm/peaks	<input checked="" type="checkbox"/> Complete	Body Extension: <input type="text" value="9.0"/> + <input type="text" value="9.0"/>	Leg Extension: <input type="text"/> <input type="text"/> <input type="text"/> <input type="text"/>			
Cage	<input checked="" type="checkbox"/> Complete	<b>Capture all Defects on F0047 Deficiency Form and all Missing steel on F0140 Missing Steel Form</b>				
Body	<input checked="" type="checkbox"/> Complete					
Extensions	<input checked="" type="checkbox"/> Complete					
*Check torque 10% for guy towers and 20% for self support towers unless otherwise directed*						
<b>Item Description</b>						
1. Review the line data to verify structure type		<input checked="" type="checkbox"/>				
2. Correct Tower and extension are assembled (see staking list)		<input checked="" type="checkbox"/>				
3. Inspect all steel for quantities and damage		<input checked="" type="checkbox"/>				
4. Report any shortages or damage to the Material Coordinator		<input checked="" type="checkbox"/>				
5. Refer to structure layout drawing for steel placement		<input checked="" type="checkbox"/>				
6. Install correct bolts as per Manufacturers drawings		<input checked="" type="checkbox"/>				
7. Install lock washers as per Manufacturers drawings		<input checked="" type="checkbox"/>				
8. All Installed bolts torqued to Manufacturers specifications		<input checked="" type="checkbox"/>				
9. All Torqued bolt heads to be identified with RED marker		<input checked="" type="checkbox"/>				
10. All verified torqued bolts indicated with BLACK marker		<input checked="" type="checkbox"/>				
11. OPGW support installed to inside of line angle		<input checked="" type="checkbox"/>				
12. All step bolts installed as per design (refer to tower drawing for each tower type)		<input checked="" type="checkbox"/>				
13. Tower checked for any loose bolts, nuts & washers or debris		<input checked="" type="checkbox"/>				
14. Any deficiencies identified? (If yes, attach deficiency list)		<input checked="" type="radio"/> Yes <input type="radio"/> No				
Torque Wrench S/N: 79118333152, 79118333156						
<b>FOR REVIEW ONLY</b>						
<b>Notes:</b>						
	Name (Print)	DATE	Signature			
QC Crew	F. Schonauer	04/Jul/2017	F. Schonauer			
Valard QA Review	B. Gardiner	04/Aug/2017	B. Gardiner <i>BG</i>			
Nalcor QA Inspector	<i>A. Concoran</i>	<i>07-Aug-17</i>	<i>A. Concoran</i>			



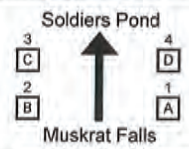




VC-F0113 : R009

	Document Description			<b>Lattice Tower Assembly Check</b>		
	Created By: Eric Winter		Doc. Number	<b>VC-F0113</b>	Revision <b>R009</b>	
	Date: 01/Jan/2013		VC Number:	VC7343	Contract no.: CT0327-001	
	Revised By: Michael Grieve		Client:	Nalcor Energy	Project no.: 505573	
	Rev Date: 08/Aug/2016		Crew:	QAQC	Supervisor: Michael Grieve	
	Tower Number:	<b>632</b>	Line Number:	<b>4</b>	Date: <b>03/Jul/2017</b>	
Area of Tower Checked:		Tower Type: <input type="text" value="A1"/>				
Crossarm/peaks	<input checked="" type="checkbox"/> Complete	Body Extension: <input type="text" value="9.0"/> + <input type="text" value="9.0"/>		Leg Extension: <input type="text"/> <input type="text"/> <input type="text"/> <input type="text"/>		
Cage	<input checked="" type="checkbox"/> Complete	<i>Capture all Defects on F0047 Deficiency Form and all Missing steel on F0140 Missing Steel Form</i>				
Body	<input checked="" type="checkbox"/> Complete					
Extensions	<input checked="" type="checkbox"/> Complete					
*Check torque 10% for guy towers and 20% for self support towers unless otherwise directed*						
<b>Item Description</b>					<b>Check</b>	
1. Review the line data to verify structure type						
2. Correct Tower and extension are assembled (see staking list)						
3. Inspect all steel for quantities and damage						
4. Report any shortages or damage to the Material Coordinator						
5. Refer to structure layout drawing for steel placement						
6. Install correct bolts as per Manufacturers drawings						
7. Install lock washers as per Manufacturers drawings						
8. All Installed bolts torqued to Manufacturers specifications						
9. All Torqued bolt heads to be identified with RED marker						
10. All verified torqued bolts indicated with BLACK marker						
11. OPGW support installed to inside of line angle						
12. All step bolts installed as per design (refer to tower drawing for each tower type)						
13. Tower checked for any loose bolts, nuts & washers or debris						
14. Any deficiencies identified? (If yes, attach deficiency list) <span style="float: right;"><input type="radio"/> Yes <input checked="" type="radio"/> No</span>						
Torque Wrench S/N: 79118333152						
Notes:						
	Name (Print)	DATE	Signature			
QC Crew	Floyd S	03/Jul/2017	Floyd S			
Valard QA Review	Kaitlyn O'Reilly	06/Jul/2017	Kaitlyn O'Reilly <i>KO</i>			
Nalcor QA Inspector	<i>B Furlong</i>	<i>8 Jul 17</i>	<i>B Furlong</i>			

REVIEWED ONLY

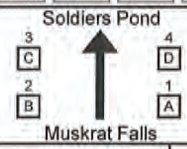
	Document Description			<b>Lattice Tower Inspection</b>			
	Created By: Eric Winter		Doc. Number	<b>VC-F0112</b>		Revision	<b>R010</b>
	Date: 01/Jan/2013		VC Number:	VC7343	Contract no.:	CT0327-001	
	Revised By: Drew Williams		Client:	Nalcor Energy	Project no.:	505573	
	Rev Date: 06/Aug/2016		Crew:	QAQC	Supervisor:	Michael Grieve	
	Tower Number:	632	Line Number:	4	Date:	25/Jul/2017	
Inspection Type			<input type="radio"/> Climbing <input checked="" type="radio"/> Visual <input type="radio"/> Helicopter Patrol				Check
Body Extension:	9 + 9	Leg Extension:	<input type="checkbox"/> <input type="checkbox"/> <input type="checkbox"/> <input type="checkbox"/>	Tower Type:	A1		
1. Review the line data to verify structure type						<input checked="" type="checkbox"/>	
2. Ensure that erected tower on site is correct (str type & extensions)						<input checked="" type="checkbox"/>	
3. Inspect all steel for debris and damage						<input checked="" type="checkbox"/>	
4. Report any shortages or damage to the Material Coordinator						N/A <input type="checkbox"/>	
5. Refer to structure layout drawing for steel placement and orientation						<input checked="" type="checkbox"/>	
6. Erected Steel as per Manufacturers drawings (no missing parts or damaged members)						<input checked="" type="checkbox"/>	
7. Climbing inspection of all crossarm connections-torque check all bolts						<input checked="" type="checkbox"/>	
8. Climbing inspection of all splice locations-torque check all splice bolts						<input checked="" type="checkbox"/>	
9. Climbing inspection of all body extension connections-torque check all bolts						<input checked="" type="checkbox"/>	
10. Torque check on all stub leg bolts						<input checked="" type="checkbox"/>	
11. Torque check on all floors not checked during assembly stage-torque check all bolts						<input checked="" type="checkbox"/>	
12. All step bolts installed on step bolt legs						<input checked="" type="checkbox"/>	
13. Tower Checked for any loose bolts, nuts & washers during climbing inspection						<input checked="" type="checkbox"/>	
14. All erection materials removed from tower (sling, tag lines, etc.)						<input checked="" type="checkbox"/>	
15. Danger & number signs installed per design on both transverse faces						<input checked="" type="checkbox"/>	
16. Aerial marker signs installed per design on both transverse faces						<input type="radio"/> Yes <input checked="" type="radio"/> N/A	
17. Visual inspection of tower using binoculars completed						<input checked="" type="checkbox"/>	
18. Any deficiencies identified? (If yes, attach deficiency list)						<input checked="" type="radio"/> Yes <input type="radio"/> No	
Notes: <del>Structure Numbers Not Installed (2599)</del> DM							
FOR REVIEW ONLY							
	Name (Print)	DATE	Signature				
Crew	Charles Calder	25/Jul/2017	Charles Calder				
Valard QA Review	Kaitlyn O'Reilly	02/Aug/2017	Kaitlyn O'Reilly <i>KO</i>				
Nalcor QC Inspector	<i>A. CORCORAN</i>	<i>07-Aug-17</i>	<i>A. Corcoran</i>				



**VC-F0113 : R009**

	Document Description			<b>Lattice Tower Assembly Check</b>		
	Created By: Eric Winter	Doc. Number	<b>VC-F0113</b>	Revision	<b>R009</b>	
	Date: 01/Jan/2013	VC Number:	VC7343	Contract no.:	CT0327-001	
	Revised By: Michael Grieve	Client: Nalcor Energy	Project no.: 505573			
	Rev Date: 08/Aug/2016	Crew: QAQC	Supervisor: Michael Grieve			
	Tower Number:	<b>653</b>	Line Number:	<b>4</b>	Date: 11/Jul/2017	

Area of Tower Checked:		Tower Type: <input type="text" value="A1"/>	
Crossarm/peaks	<input checked="" type="checkbox"/> Complete	Body Extension: <input type="text" value="7.5"/> + <input type="text" value="7.5"/>	Leg Extension: <input type="text"/> <input type="text"/> <input type="text"/> <input type="text"/>
Cage	<input checked="" type="checkbox"/> Complete	<i>Capture all Defects on F0047 Deficiency Form and all Missing steel on F0140 Missing Steel Form</i>	
Body	<input checked="" type="checkbox"/> Complete		
Extensions	<input checked="" type="checkbox"/> Complete		



*Check torque 10% for guy towers and 20% for self support towers unless otherwise directed*		<b>Check</b>
<b>Item Description</b>		
1. Review the line data to verify structure type		<input checked="" type="checkbox"/>
2. Correct Tower and extension are assembled (see staking list)		<input checked="" type="checkbox"/>
3. Inspect all steel for quantities and damage		<input checked="" type="checkbox"/>
4. Report any shortages or damage to the Material Coordinator		<input checked="" type="checkbox"/>
5. Refer to structure layout drawing for steel placement		<input checked="" type="checkbox"/>
6. Install correct bolts as per Manufacturers drawings		<input checked="" type="checkbox"/>
7. Install lock washers as per Manufacturers drawings		<input checked="" type="checkbox"/>
8. All Installed bolts torqued to Manufacturers specifications		<input checked="" type="checkbox"/>
9. All Torqued bolt heads to be identified with RED marker		<input checked="" type="checkbox"/>
10. All verified torqued bolts indicated with BLACK marker		<input checked="" type="checkbox"/>
11. OPGW support installed to inside of line angle		<input checked="" type="checkbox"/>
12. All step bolts installed as per design (refer to tower drawing for each tower type)		<input checked="" type="checkbox"/>
13. Tower checked for any loose bolts, nuts & washers or debris		<input checked="" type="checkbox"/>
14. Any deficiencies identified? (If yes, attach deficiency list)	<input type="radio"/> Yes <input checked="" type="radio"/> No	

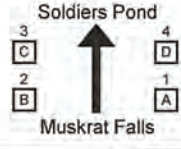
Torque Wrench S/N: 79118333152

Notes:

	Name (Print)	DATE	Signature
QC Crew	Floyd	11/Jul/2017	Floyd Schonauer
Valard QA Review	Kaitlyn O'Reilly	12/Jul/2017	Kaitlyn O'Reilly <i>KO</i>
Nalcor QA Inspector	<i>B Furlong</i>	<i>14 Jul 17</i>	<i>B. Furlong</i>

FOR REVIEW ONLY

**Quarterly Report on Asset Performance in Support of Resource Adequacy  
for the Twelve Months Ended March 31, 2025, Attachment 1, Appendix A, Page 29 of 30**

	Document Description			<b>Lattice Tower Inspection</b>			
	Created By: Eric Winter		Doc. Number	<b>VC-F0112</b>	Revision <b>R010</b>		
	Date: 01/Jan/2013		VC Number: VC7343	Contract no.: CT0327-001			
	Revised By: Drew Williams		Client: Nalcor Energy	Project no.: 505573			
	Rev Date: 06/Aug/2016		Crew: QAQC	Supervisor: Michael Grieve			
	Tower Number:	<b>653</b>	Line Number:	<b>4</b>	Date: <b>08/Aug/2017</b>		
Inspection Type <input type="radio"/> Climbing <input checked="" type="radio"/> Visual <input type="radio"/> Helicopter Patrol					Check		
Body Extension: <input type="text" value="7.5"/> + <input type="text" value="7.5"/>	Leg Extension: <input type="text"/> <input type="text"/> <input type="text"/> <input type="text"/>	Tower Type: <b>A1</b>					
1. Review the line data to verify structure type					<input checked="" type="checkbox"/>		
2. Ensure that erected tower on site is correct (str type & extensions)					<input checked="" type="checkbox"/>		
3. Inspect all steel for debris and damage					<input checked="" type="checkbox"/>		
4. Report any shortages or damage to the Material Coordinator					<input checked="" type="checkbox"/>		
5. Refer to structure layout drawing for steel placement and orientation					<input checked="" type="checkbox"/>		
6. Erected Steel as per Manufacturers drawings (no missing parts or damaged members)					<input checked="" type="checkbox"/>		
7. Climbing inspection of all crossarm connections-torque check all bolts					<input checked="" type="checkbox"/>		
8. Climbing inspection of all splice locations-torque check all splice bolts					<input checked="" type="checkbox"/>		
9. Climbing inspection of all body extension connections-torque check all bolts					<input checked="" type="checkbox"/>		
10. Torque check on all stub leg bolts					N/A <input type="checkbox"/>		
11. Torque check on all floors not checked during assembly stage-torque check all bolts					<input checked="" type="checkbox"/>		
12. All step bolts installed on step bolt legs					<input checked="" type="checkbox"/>		
13. Tower Checked for any loose bolts, nuts & washers during climbing inspection					<input checked="" type="checkbox"/>		
14. All erection materials removed from tower (sling, tag lines, etc.)					<input checked="" type="checkbox"/>		
15. Danger & number signs installed per design on both transverse faces					<input checked="" type="checkbox"/>		
16. Aerial marker signs installed per design on both transverse faces					<input checked="" type="radio"/> Yes <input type="radio"/> N/A		
17. Visual inspection of tower using binoculars completed					<input checked="" type="checkbox"/>		
18. Any deficiencies identified? (If yes, attach deficiency list)					<input checked="" type="radio"/> Yes <input type="radio"/> No		
Notes: <del>Structure Number Not Installed (2620)</del> DM							
Name (Print)		DATE	Signature				
Crew	Charles Calder	08/Aug/2017	Charles Calder				
Valard QA Review	Kaitlyn O'Reilly	10/Aug/2017	Kaitlyn O'Reilly KO				
Nalcor QC Inspector	Faek	<b>REVIEWED ONLY</b>		M. Andrews			



# Attachment 2

L3501/2 Failure Investigation  
Ice Storm Southern Labrador

ILK-EG-ED-6200-TL-H15-0007-01

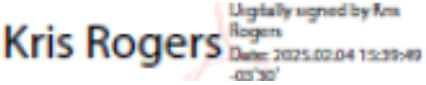


## L3501/2 Failure Investigation – Ice Storm Southern Labrador

Revision						Remarks
No	By	Rev.	Chk.	Appr.	Date	
1	MV	00	RM	KR	3-Feb-2025	
2						
3						

Prepared By: *Maria Veitch*  
Maria Vetich

Checked By: *Rebecca Manuel*  
Rebecca Manuel

Approved By:   
Kris Rogers

## Contents

1.0	Abbreviations and Acronyms .....	1
2.0	Introduction .....	1
3.0	Background .....	2
4.0	Purpose .....	4
5.0	Failure Description .....	4
5.1	Failure Location .....	8
5.2	Engineering Recommendations for Repairs .....	9
5.3	Restoration Summary .....	10
6.0	Weather Information .....	10
7.0	Construction Quality, and Maintenance Review .....	13
8.0	Material Testing .....	14
9.0	Analysis of Loads Causing Failures .....	14
9.1	Ice Loading .....	15
9.2	Ice Shedding .....	18
10.0	Summary and Conclusions .....	19
11.0	Recommendations .....	20

## List of Appendices

Appendix A: NL Hydro Transmission Line Failure (Conductor EL-1 and EL-2 at Suspension Tower 1225)  
report by Wayland Engineering Ltd.

## 1.0 Abbreviations and Acronyms

- DE – Deadend
- HVdc – High Voltage direct current
- L3501/2 – Line number of the 350 kV HVdc transmission line
- L3501 – Pole 1 of the line
- L3502 – Pole 2 of the line
- LIL – Labrador-Island Link
- OPGW – Optical Ground Wire
- P1 – Pole 1
- P2 – Pole 2
- ROW – Right of Way
- Str. – Structure

## 2.0 Introduction

On Saturday March 30, 2024, Pole 2 tripped at 06:45. Pole 1 tripped at 06:52 on electrode line fault protection. From a patrol of the line it was discovered that the electrode conductor was broken and damaged at several locations between str. 1218–1228. In some locations, the electrode conductor was touching or close to the pole conductor which would explain the line trip. There was also damage to the steel lattice towers at the electrode crossarm and OPGW tower peaks as shown in Figure 1. There were a few strands of pole conductor damaged in one location. The line patrol noted there was significant ice on the lines before failures (and remaining in some locations).

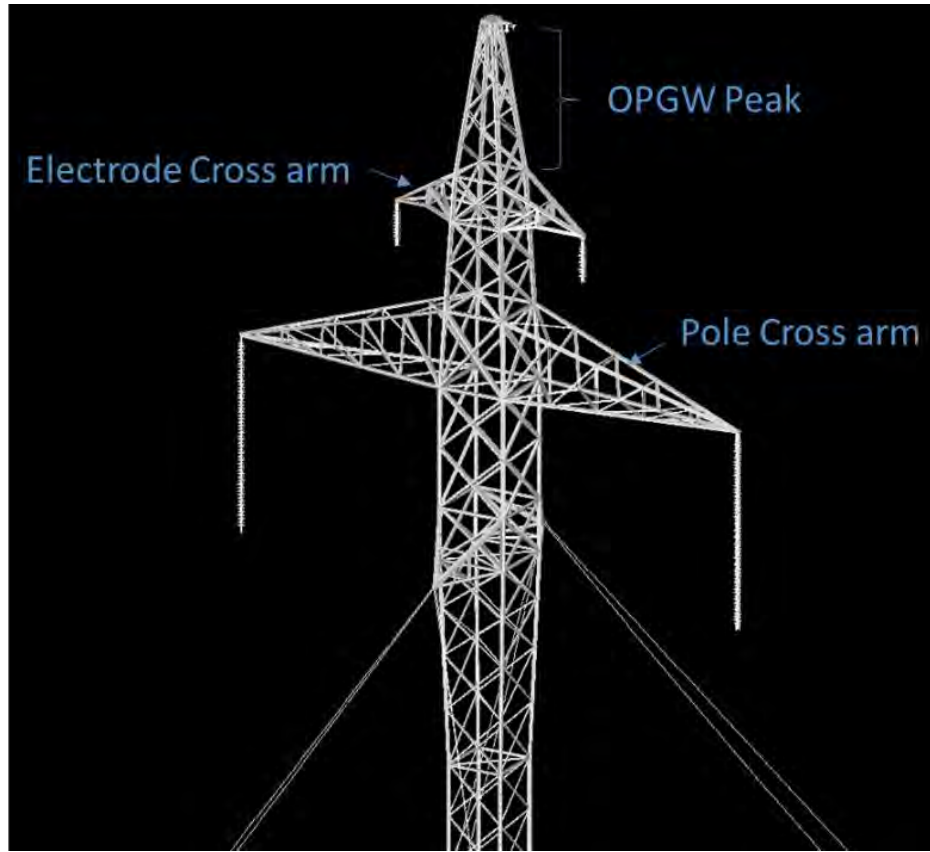
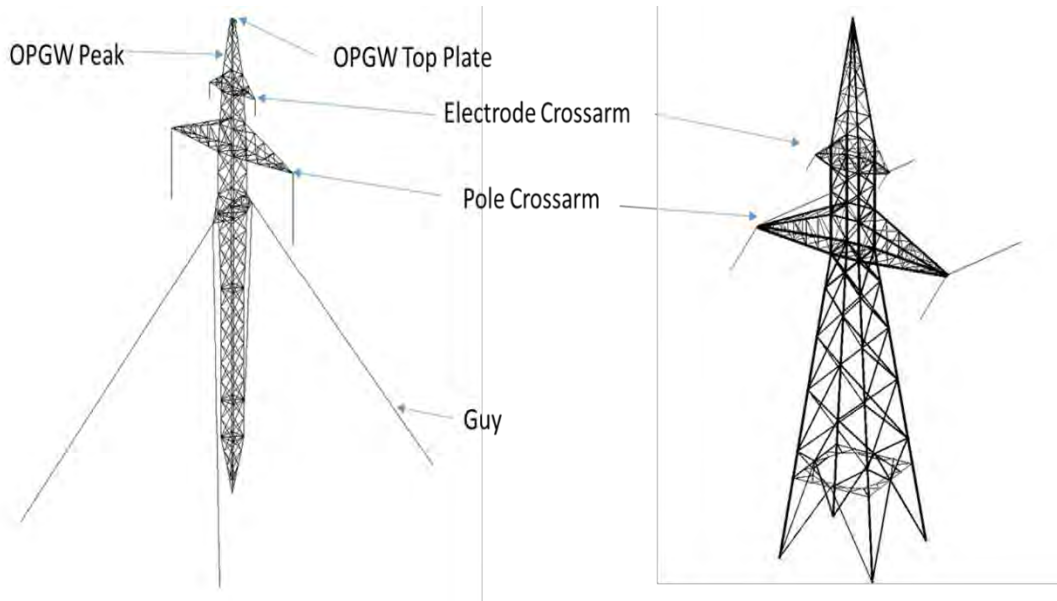


Figure 1: Tower Drawing Showing Sections

### 1 3.0 Background

2 The Labrador-Island Link (“LIL”) is an important transmission line for the provincial energy grid due to its  
3 power carrying capacity that is used to deliver a large portion of the winter peak energy and demand to  
4 the Island Interconnected System. Line L3501/2 is the 350 kV HVdc overland transmission line portion of  
5 LIL traversing a distance of approximately 1,100 km through three major meteorological loading zones:  
6 average, alpine and eastern. The HVdc line has two poles, one OPGW, and two electrode conductors for  
7 a portion of line, as shown in Figure 2. The electrode conductor is attached to the lattice towers for a  
8 part of the line from Muskrat Falls to about 384 km southeast of Muskrat Falls where it diverts to a  
9 separate right of way (“ROW”) on wood poles to an electrode site approximately 16 km away, located in  
10 the L’Anse-au-Diable area. Note that sections of L3501/2 without the electrode on the towers do not  
11 have electrode cross arms.



**Figure 2: Suspension and Deadend Tower Diagram**

1 The HVdc transmission line corridor has been divided into three major meteorological loading zones  
 2 referenced above in combination with 8 further subcategories related to meteoroidal loads, pollution  
 3 levels (inland and costal), and geographic location. The resulting combination lead to the HVdc line  
 4 consisting of 19 separate loading zones. Eleven tower types (A1, A2, A3, A4, B1, B2, C1, C2, D1, D2, and  
 5 E1) were designed to meet the loading requirements, which consist of a specified wind load, ice load,  
 6 and combination of both applied to the line. The tower type consists of both guyed towers and self-  
 7 support towers. The tower types are summarized in Table 1.

**Table 1: Tower Types**

Tower Type	Structure Type	Insulator Assembly Type	Deflection Angle Limit (degree)
A1, A2, A3, A4	Guyed	Suspension	0–1
B1	Guyed	Suspension	0–3
B2	Self-Support	Suspension	0–3
C1, C2	Self-Support	Dead End	0–30
D1, D2	Self-Support	Dead End	0–45
E1	Self-Support	Dead End	45–90

8 Ninety percent of all towers on the L3501/2 are suspension towers, types A1, A2, A3, A4, B1, and B2.  
 9 Figure 3 breaks down the tower distribution on the L3501/2.

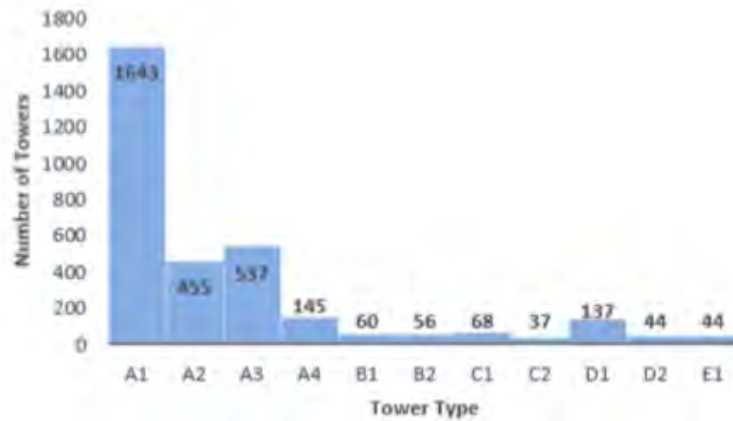


Figure 3: Distribution of Tower Type on L3501/2

## 1 4.0 Purpose

2 Considering the importance of L3501/2 to the provincial energy grid and the need to understand the  
3 line's performance, a detailed failure investigation was completed to determine the root cause of the  
4 failures and to conclude what action can be taken in order to prevent further damage to the line.

5 The investigation will be described in detail within this report and includes the following components:

- 6 • Failure Description;
- 7 • Weather;
- 8 • Construction Quality and Maintenance Review;
- 9 • Material Testing;
- 10 • Analysis of Loads Causing Failures.

## 11 5.0 Failure Description

12 During a line patrol on March 30, 2024, damage was discovered between structure 1218 and 1228. A  
13 helicopter patrol the next day identified additional damage at structure 1232, and was able to detail the  
14 damage on all structures. The damage included bent and failed steel members in the electrode cross  
15 arms and in the OPGW peak, conductor damage included bird caging, broken strands and fully broken  
16 conductor, and minor damage to the pole conductor of just a few strands. A summary of the damage is  
17 shown in Table 2.

**Table 2: Summary of Structure and Conductor Damage**

Tower	Crossarm Damage		Conductor Damage		Pole Conductor	OPGW Tower Peak
	EL1	EL2	EL1	EL2		
1216	no	no	no	no	no	no
1217	no	no	no	no	no	no
1218	no	yes	no	yes	no	no
1219	no	yes	no	yes	no	no
1220	no	no	no	yes	no	no
1221	no	yes	no	yes	no	yes
1222	yes	yes	yes	yes	no	no
1223	yes	yes	yes	yes	no	no
1224	yes	yes	yes	yes	no	no
1225	yes	yes	yes	yes	no	yes
1226	yes	yes	yes	yes	no	no
1227	yes	yes	yes	yes	yes	no
1228	yes	no	yes	no	no	yes
1229	no	no	no	no	no	no
1232	no	no	no	no	no	yes

1 Figure 4 to Figure 7 show pictures of the various failures.



**Figure 4: Str. 1228 Electrode Cross Arm Failure**



**Figure 5: Str. 1224 Electrode Cross Arm Failures**



**Figure 6: OPGW Peak Failure**



**Figure 7: Str. 1221 Minor OPGW Peak Damage, Bird Caging of Electrode Conductor, Electrode Conductor on Ground**

## 5.1 Failure Location

- 1 Structures are numbered sequentially along the line starting at Muskrat Falls. Structure numbers that
- 2 sustained damage are str. 1218–1228 and 1232. These structures are located on the south coast of
- 3 Labrador as shown in Figure 8. The structures are located 11–16 km from the closest highway.

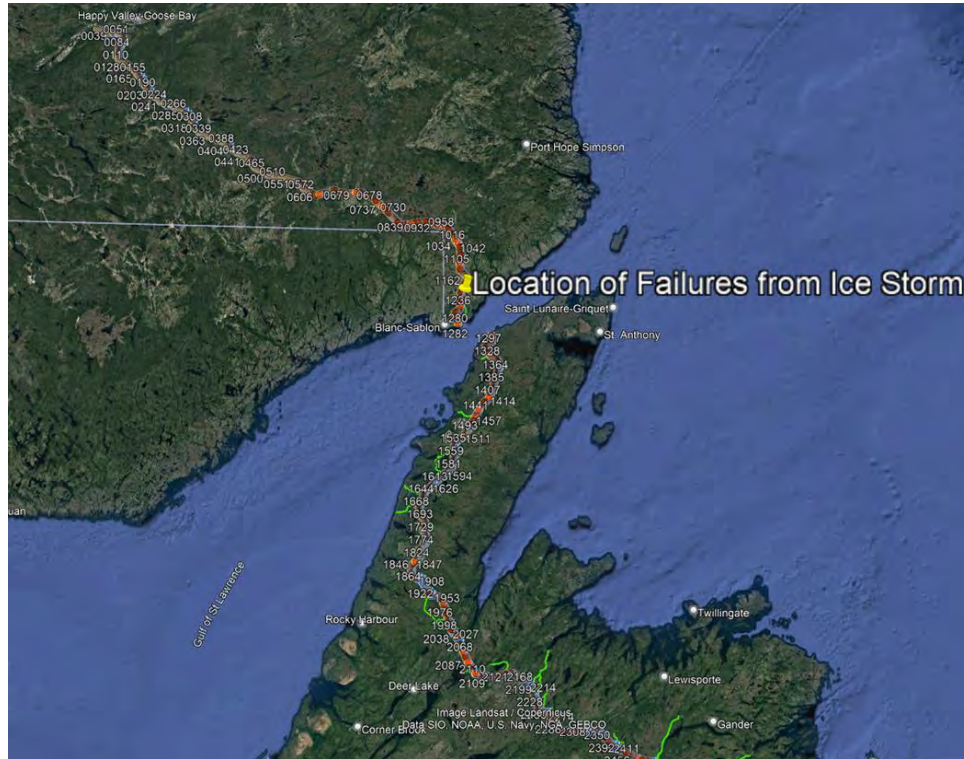


Figure 8: Map of Newfoundland and Labrador showing Location of Failures

- 5 The structures are located in loading zone 3a. Zone 3a is an Average loading zone. The wind and ice
- 6 conditions this zone is designed for are summarized in Figure 9.

### Zone 3, 4, 6 and 8a

<b>Maximum Ice</b>	<b>50 mm radial glaze, 0.9 g/cm<sup>3</sup> density</b>
<b>Maximum Wind</b>	<b>120 km/h (10 minute average wind speed at 10 m height about ground)</b>
<b>Combined Ice and Wind</b>	<b>25 mm radial glaze, 0.9 g/cm<sup>3</sup> density</b>
	<b>60 km/h ((10 minute average wind speed at 10 m height about ground)</b>

**Maximum wind and combined wind values assume Terrain Type C as per CSA C22.3 NO 60826-10.**

Figure 9: Zone 3a Wind and Ice Design Loading

1 The twelve structures with steel or conductor damage are all Type A1 tangent towers. The tower body  
2 extension, and electrode and OPGW attachment heights are summarized in Table 3. All towers had a  
3 suspension attachment. Structures 1218–1228 are within the same deadend to deadend section, with  
4 structure 1232 in a separate section.

**Table 3: Damaged Structure Information Summary**

Structure Number	Structure Type	Structure Height	Height to Electrode Attachment (m)	Height to OPGW Attachment (m)
1218	A1	A1+6.0	33.968	41.05
1219	A1	A1+12.0	39.966	47.05
1220	A1	A1+6.0	33.969	41.05
1221	A1	A1+7.5	35.469	42.55
1222	A1	A1+12.0	39.966	47.05
1223	A1	A1+9.0	36.962	44.05
1224	A1	A1+6.0	33.965	41.05
1225	A1	A1+4.5	32.462	39.55
1226	A1	A1+12.0	39.969	47.05
1228	A1	A1+9.0	36.964	44.05
1232	A1	A1+10.5	NA	45.55

## 5.2 Engineering Recommendations for Repairs

6 There were two options considered for repair of the failed section of line. The first option was to install  
7 the failed electrode conductor on wood poles in parallel with the existing steel line. The second option  
8 was to replace the failed conductor and structural steel as-built with identical spares.

9 Installation of electrode conductor on wood poles would include moving the OPGW to the intact  
10 electrode crossarms. With this option, less than half of the electrode crossarms would need to be  
11 repaired immediately, and none of the tower peaks. The tower peaks could be fixed later during a  
12 scheduled outage, and the electrode conductor could remain on the wood poles. This would have the  
13 added advantage of reducing the risk of failure to the electrode crossarms and conductor in future icing  
14 events. A disadvantage of this option would be the OPGW would not provide optimal lightning  
15 protection when on the electrode crossarm.

1 The second option would restore everything to the as-built state, requiring no additional work at a later  
2 date, and providing appropriate lightening protection.

3 Both options were evaluated for cost and schedule, and it was determined that the second option of  
4 restoring to the as-built condition would present less risk of cost and schedule delays.

### 5 **5.3 Restoration Summary**

6 Crews and equipment mobilized to site on April 3<sup>rd</sup> with work beginning on April 4<sup>th</sup>. The work began  
7 with cleanup of the failed electrode conductor and securing the OPGW to allow for tower repairs. The  
8 contractor started repair work on April 10<sup>th</sup>. Tower steel was replaced and electrode conductor was  
9 replaced, with all work being completed by April 19<sup>th</sup>.

### 10 **6.0 Weather Information**

11 There were observations of significant icing on the lines on March 30<sup>th</sup>, as shown in Figure 10.  
12 Observations at site estimated the ice thickness on the conductor to be approximately 120–140 mm of  
13 radial ice. An ice sample that fell from the OPGW (see Figure 11) was collected, measured, and weighed.  
14 From this sample, the equivalent radial thickness was estimated to be 100–125 mm at a density of 0.6  
15 g/cm<sup>3</sup>.



**Figure 10: Ice on OGPW at Time of Failure**



Figure 11: Ice Sample from OPGW

1 Weather from the nearest weather station at Blanc Sablon is shown in Figure 12 and Figure 13. The  
2 Blanc Sablon weather station is located approximately 25 km southwest of the damage location. The  
3 elevation of the weather station is 37.2 m, and the elevation of the damaged structures ranges from  
4 235.6 to 299.7 m. The higher elevation would likely mean higher winds and colder temperature at the  
5 structures than reported at the weather station.

6 Before the failures occurred the weather conditions consisted of a mix of rain and fog and the  
7 temperature at Blanc Sablon was recorded near zero. Data from the weather station indicated the  
8 temperature started to rise right before the pole tripped. It is assumed that at the locations of the tower  
9 and conductor damage, the temperatures were slightly colder and the precipitation types therefore  
10 were freezing rain and freezing fog. Figure 14 shows the total precipitation in the 36 h period around the  
11 time of the failure from 12:00 h on March 29<sup>th</sup> to 0:00 h on March 31<sup>st</sup>. A yellow star on Figure 14  
12 displays the approximate location of the failures. The figure shows that the area received 55 – 60 mm of  
13 precipitation during this time. It also indicates that the area of the failures received significantly more  
14 precipitation than Blanc Sablon, which recorded 16 mm of rain on March 29<sup>th</sup> and 14 mm of rain on  
15 March 30<sup>th</sup>.

**Quarterly Report on Asset Performance in Support of Resource Adequacy  
for the Twelve Months Ended March 31, 2025, Attachment 2**



**Figure 12: Temperatures and Precipitation Type at Blanc Sablon Weather Station**

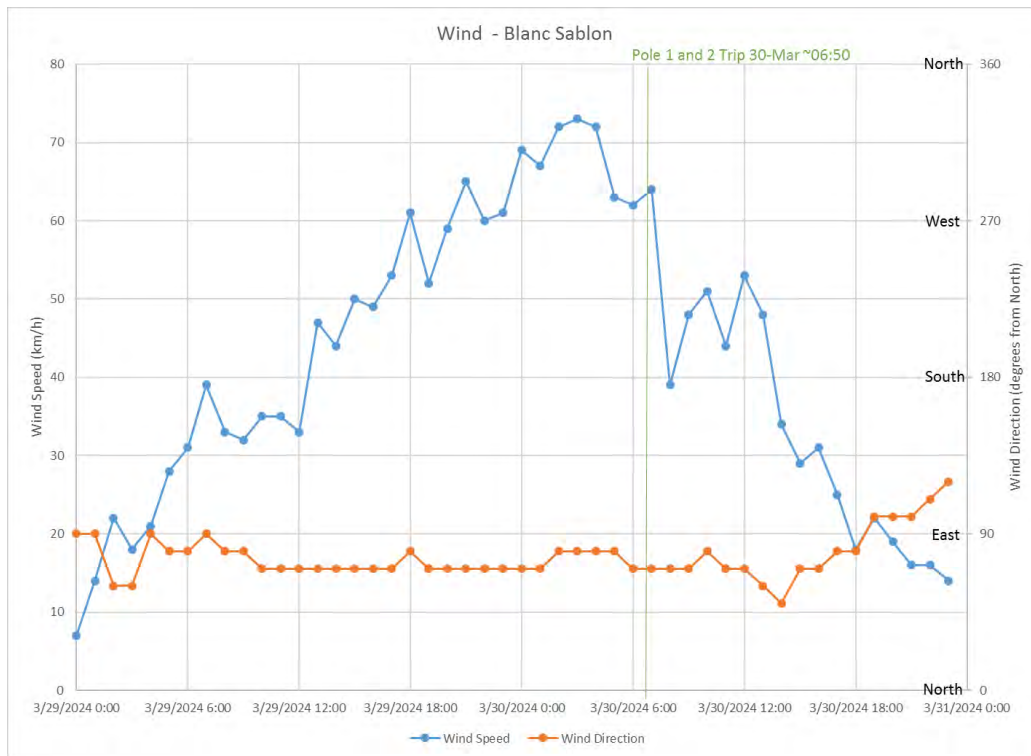


**Figure 13: Wind Speed and Direction at Blanc Sablon Weather Station**

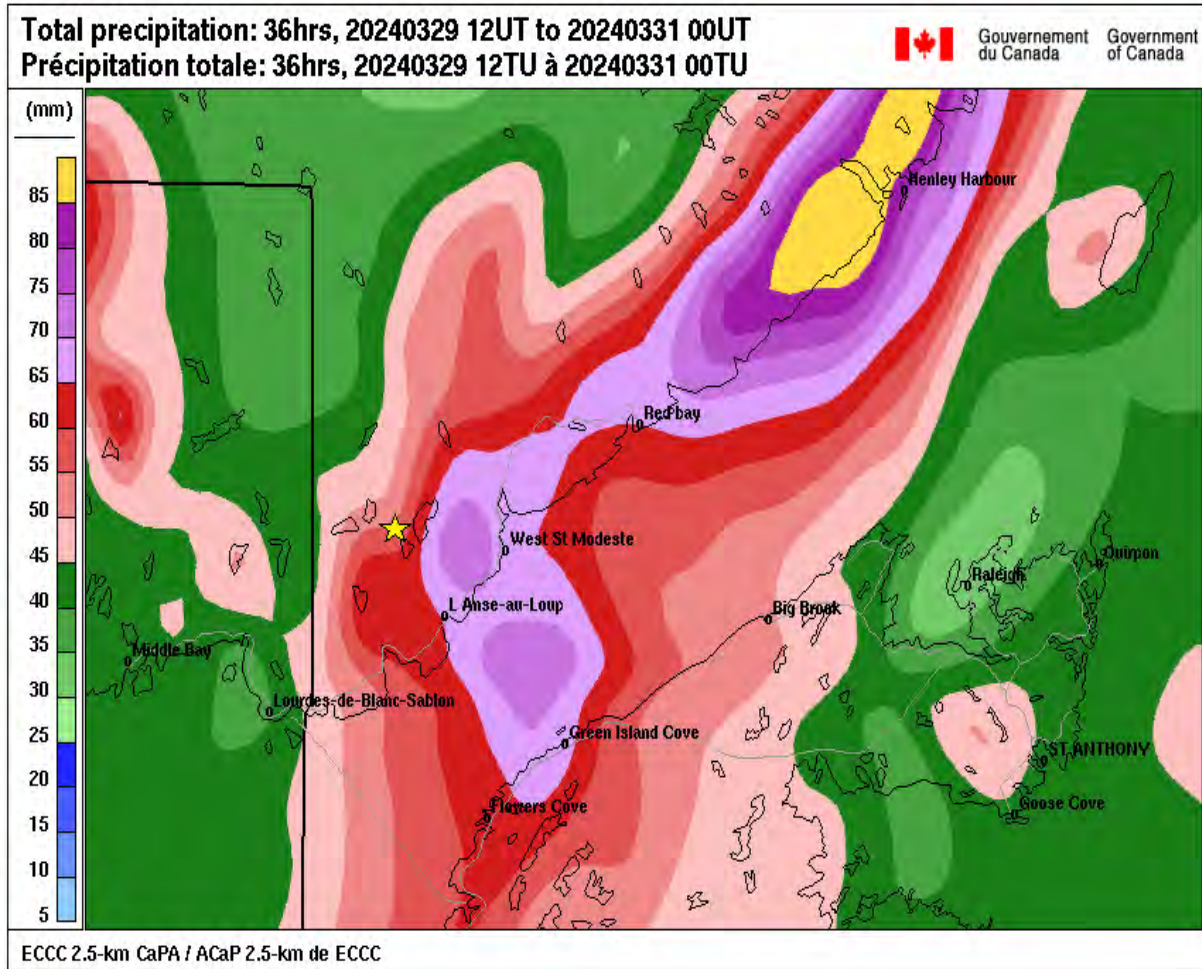


Figure 14: Total Precipitation on Labrador South Coast from 12:00 h 29-Mar-2024 to 0:00 31-Mar-2024

## 1 7.0 Construction Quality, and Maintenance Review

2 The final construction quality control inspection of the structures from 1218–1228, and 1232 was  
3 completed in May of 2016, and showed no issue with the tower steel. There were no non-conformance  
4 reports on the tower steel for these towers. The electrode conductor of this section of line was strung  
5 on March 29, 2016. There were no quantity control issues noted at that time.

6 On the 12 structures that had conductor or tower damage there were 99 previous corrective work  
7 orders. The types of work orders include broken dampers (OPGW, pole, and electrode), broken corona  
8 rings, and the OPGW pulled through the suspension assembly. The damper damage could be caused by  
9 Aeolian vibration or galloping of the lines. The corona ring damage could be caused by galloping or ice  
10 accumulation. The OPGW pull through is likely caused by unbalanced ice load from ice shedding.

## 1 **8.0 Material Testing**

2 Material testing of the electrode conductor was completed by Wayland Engineering Ltd. (“Wayland”) to  
3 determine the cause of failure and if there were any issues with the conductor. The summary of  
4 conclusions and recommendations is included in this section and the complete report can be found in  
5 Appendix A.

6 Wayland concluded that the physical, chemical and metallurgical evidence indicates that the failure of  
7 conductors is consistent with ductile limit load fracture of the aluminum conductor strands. The force  
8 required to cause the failure was attributed to the combination of ice accumulation and sustained wind  
9 velocities. Wayland also suggests it was probable that wind induced galloping was present in the lines  
10 prior to the failures, which generated an additional cyclic force. Cyclic force could cause fatigue on the  
11 conductor reducing the strength, making it more susceptible to ductile failure.

12 Wayland notes that the evidence suggests that the steel reinforcing core migrated towards, and was in  
13 contact with, the lower surface of the insulator wire clamp. The downward bearing force responsible for  
14 the migration was sufficient to distort and cold pressure weld (fuse) adjacent aluminum wires together  
15 in the lower circumferential half of the conductor. It is reasonable to assume that the distortion and  
16 fusing of the aluminum strands would result in a decrease in the overall breaking strength of the  
17 conductor where it enters the wire clamp.

18 Wayland recommended that radiographing imaging could be used as a non-destructive method to  
19 detect if the steel core migration is happening in other sections of the line. They recommended  
20 consulting with experts in the field of radiography to investigate the feasibility of this testing.

## 21 **9.0 Analysis of Loads Causing Failures**

22 A complete as-built model of L3501/2 includes the existing terrain, as-built tower locations and heights,  
23 with complete finite element tower models. PLS-CADD is a transmission line design program that allows  
24 the user to enter different loading conditions to analyze how they will affect the line and structures  
25 under the as-built conditions. The program allows the user to complete detailed analysis of how  
26 increasing loads will affect the towers performance and ultimately how the towers will fail under  
27 extreme loading conditions.

1 Tower failure is defined in the analysis as any component of the tower exceeding its maximum damage  
2 limit. The reaction of the tower to the load cases can be quantified by the maximum utilization, which is  
3 the ratio of the force applied to any member from the specified loads divided by the damage limit  
4 capacity, expressed as a percentage. Any value greater than 100% is considered a tower failure.

$$\text{Maximum Utilization} = \frac{\text{Force}}{\text{Damage Limit Capacity}} \times 100\%$$

## 5 **9.1 Ice Loading**

6 As discussed in Section 6.0, reports from site estimate the ice thickness at the location of the failures at  
7 approximately 120–140 mm of radial thickness. The sample of ice that fell from the OPGW was  
8 measured and was estimated to range from 100–125 mm of radial glaze ice with a density of 0.6 g/cm<sup>3</sup>.  
9 Both estimates exceeding the design ice load of 50 mm of radial glaze ice with a density of 0.9 g/cm<sup>3</sup>.

10 Modeling of the section of line was completed with 70, 80, 90, 100, 125, and 140 mm of radial ice with a  
11 density 0.6 g/cm<sup>3</sup>. The modeling of the ice was also done with the thickness of the pole conductor ice  
12 reduced by 70%. This was because ice accretion modeling, and in-field experience have proven there is  
13 less ice accretion on the larger diameter conductor.

14 The modeling showed failures in the tower at the electrode cross arm only at 90, 100, and 125 mm of  
15 radial ice. Under 140 mm of radial ice some towers show failure lower in the tower, at the pole crossarm  
16 level. Table 4 shows the comparison of the structure damaged in the field to the structures above 100%  
17 utilization in the model. The results suggest that the electrode crossarm failure could be caused by radial  
18 ice ranging from 90–100 mm.

19 Figure 15 and Figure 16 show the in-field damage to structure 1224, and the model of str. 1224 under  
20 100 mm of radial ice. The model shows that only the members in the electrode crossarm would exceed  
21 the capacity and failure under these conditions, similar to what was observed in the field at this  
22 structure.

**Table 4: Comparison of Field Damage and Modeling Results for Ice Loading**

Tower	Field Damage			Modeling 90 mm		Modeling 100 mm	
	Crossarm Damage		OPGW Tower	EL Crossarm Damage	OPGW	EL Crossarm Damage	OPGW
	EL1	EL2	Peak	(% Utilization)	Tower Peak	(% Utilization)	Tower Peak
1210	no	no	no	79	no	92	no
1211	no	no	no	44	no	50	no
1212	no	no	no	97	no	114	no
1213	no	no	no	97	no	114	no
1214	no	no	no	86	no	102	no
1215	no	no	no	87	no	103	no
1216	no	no	no	109	no	128	no
1217	no	no	no	92	no	109	no
1218	no	yes	no	105	no	124	no
1219	no	yes	no	114	no	133	no
1220	no	no	no	102	no	119	no
1221	no	yes	yes	101	no	119	no
1222	yes	yes	no	95	no	113	no
1223	yes	yes	no	116	no	135	no
1224	yes	yes	no	107	no	125	no
1225	yes	yes	yes	108	no	126	no
1226	yes	yes	no	98	no	115	no
1227	yes	yes	no	106	no	125	no
1228	yes	no	yes	111	no	130	no
1229	no	no	no	62	no	68	no



Figure 15: Str. 1224 with Damaged Electrode Crossarm

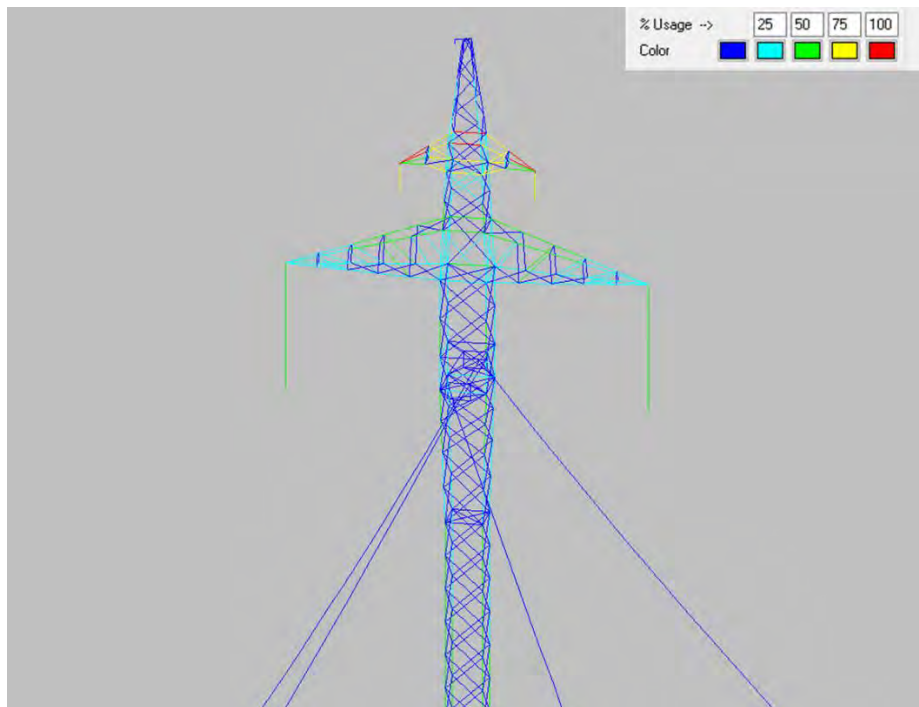


Figure 16: Model of Str. 1224 showing Members in the Electrode Crossarm Exceeding Capacity

1 The modeling of the electrode conductor shows that the utilization at 90 mm of radial ice is 98% of the  
2 ultimate tension and when increased to 100 mm of ice is 109% of the ultimate tension. Therefore, ice  
3 accumulation between 90–100 mm of radial ice could cause the conductor to fail. The line was also  
4 modeled for a combination of wind and ice. The modeling suggested 60 mm of radial ice with a 60 km/h  
5 10 minute average wind could also cause the conductor to fail.

## 6 **9.2 Ice Shedding**

7 Modeling of the line was completed with 70, 80, 90, 100, 125, and 140 mm of radial ice with a density of  
8  $0.6 \text{ g/cm}^3$ , and an unbalanced combination of 100% ice on the back span, and 70%, 80% on the ahead  
9 span (or vice-versa). From these modeling runs, it was determined that ice of 95 mm radial thickness  
10 with an unbalanced of 70/100% and 80/100% on the OPGW can produce similar failures to those seen  
11 on str. 1221 and 1228 respectively with damage to both the electrode crossarms and OPGW peak. See  
12 Figure 17 and Figure 18 for comparison of structure 1221 damage and model.



**Figure 17: Str. 1221 with OPGW Peak and Electrode Crossarm Damage**

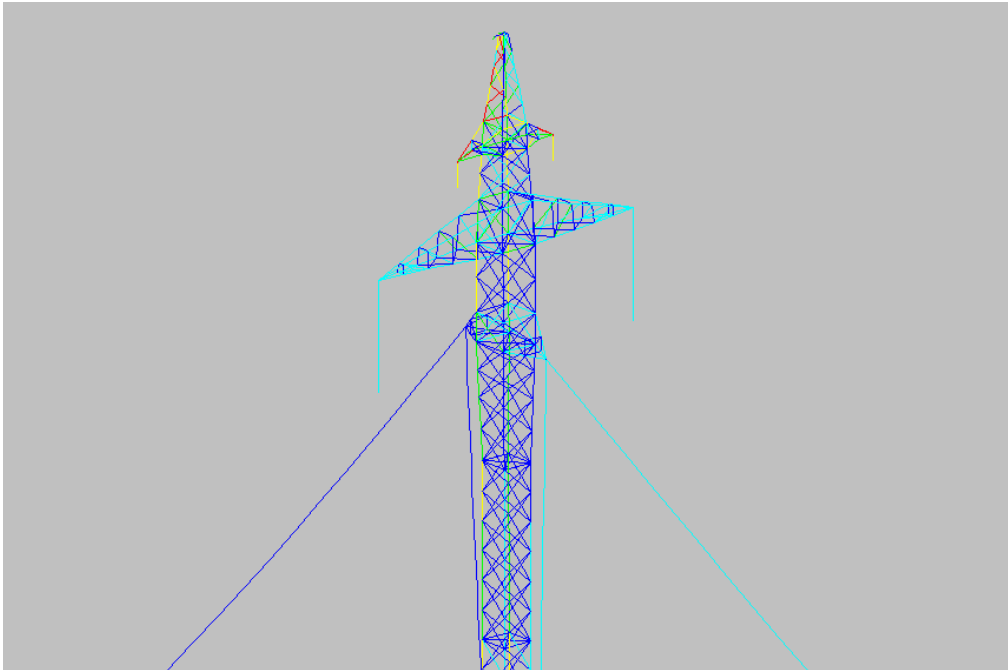


**Figure 18: Model of Str. 1221 on Unbalanced Ice Load Case showing Members in the OPGW Peak and Electrode Crossarm Exceeding Capacity**

## 10.0 Summary and Conclusions

The main root cause of the damage to the tower electrode crossarms, the OPGW tower peaks, and the electrode conductor was an overload failure due to ice loads exceeding the design for this section of the line.

Ice loads in the area at the time of the failure were estimated to range from 100–125 mm of radial glaze ice with a density of  $0.6 \text{ g/cm}^3$ . This far exceeds to the design loads of this section of the line which is 50 mm of radial glaze ice with a density of  $0.9 \text{ g/cm}^3$ . It is worth noting that the area of damage ranges from str. 1218–1232, and the design loads for the line change from “alpine” to “average” loading at str. 1209. The ice load design of the alpine zone is 115 mm of radial ice with a density of  $0.5 \text{ g/cm}^3$ .

Temperatures at the nearby weather station at Blanc Sablon were near zero during the time when ice was accumulating on the lines, and rose to  $3^\circ\text{C}$  the day of the failures, suggesting that ice shedding causing unbalanced ice loads on the structures could have contributed to the damage of the towers.

The modeling shows the damage to the electrode crossarms could be caused by ice loading range from 90–100 mm of radial ice with a density of  $0.6 \text{ g/cm}^3$ , and the damage to the OPGW peak could be cause by an 70/100% or 80/100% unbalanced ice load of 95 mm of radial ice with a density of  $0.6 \text{ g/cm}^3$ . The

1 modeling also shows the electrode conductor damage could be caused by 100 mm of radial ice with a  
2 density of 0.6 g/cm<sup>3</sup>.

3 The material testing found that the physical, chemical and metallurgical evidence indicates the  
4 conductor failures were consistent with ductile limit load fracture. The ductile failure was likely caused  
5 by overloading due to ice accumulation and wind loads at the time of the failure. It is also noted that  
6 galloping due to wind could have contributed to the failure by causing cyclic loading on the conductor  
7 prior to the failure.

## 8 **11.0 Recommendations**

9 Recommendations for consideration to prevent future failures and better understand the issue with the  
10 line include the following:

- 11 • Monitoring of ice conditions along the line;
- 12 • Strengthening of the tower to withstand higher unbalanced ice loads;
- 13 • Modifying the line to reduce the loads on towers;
- 14 • Look at alternative suspension assemblies and clamp designs; and
- 15 • Investigate using radiography to evaluate conductor issues.

16 Monitoring can be done in a number of ways including line patrol, test spans with ice load and weather  
17 monitoring equipment near the line route, and in line ice load monitoring equipment. While monitoring  
18 itself will not prevent failures it is sometimes possible to remove ice from the lines if accumulation  
19 occurs slowly. Monitoring can also help find, and prepare for failures, and it can be used to better  
20 understand the amount of ice on the lines for future upgrades.

21 Monitoring of ice can be accomplished by line patrol. From a past recommendation, the line crews have  
22 increased the helicopter patrols to four times a winter, with additional patrols as needed. The amount of  
23 ice on the lines can be estimated from pictures. Ice that has fallen from the lines can be weighed and  
24 measured. Check sheets and forms have been created and shared with Engineering and Operations to  
25 ensure all the necessary information is being collected when possible. There is an email address to send  
26 this information to a centralized location that is monitored by Engineering.

1 To gain a better understanding of the ice loads experienced by the line, monitoring of the line is  
2 required. We currently have a test span installed near str. 1225 with plans to install another test span in  
3 2025. The test span consists of one span of conductor between two wood poles, with a load cell to  
4 monitor ice load, and equipment to monitor wind, and temperature. Unfortunately, the icing in the area  
5 of str. 1225 at the time of the failures also caused damage to the solar panel power at the test span, so  
6 at this time we have no data from that site. Replacement parts have been ordered, delivered and  
7 installed, and the repairs are scheduled be completed in 2025.

8 In addition, monitors will be installed on the line in 2025 to monitor ice loading in three locations along  
9 the line.

10 The tangent towers on the line are designed for unbalanced ice loads of 70% maximum design ice  
11 thickness on one wire, on one side of the tower and 100% on one wire the other side of the tower. If the  
12 differential in ice thickness is higher, there is a chance the tower will fail. It is recommended that the  
13 towers be analyzed for more conservative unbalanced ice loads. Any recommended changes to the  
14 towers would have to consider the slip strength of the clamps, the redistribution of loads within the  
15 towers, and the constructability of the reinforcements considering the line is built and in service. This  
16 recommendation is being actioned as part of a 2024–2025 project that will evaluate and update the  
17 unbalanced ice loading design used for L3501/2. This will consist of evaluating all available data (Haldar  
18 reports, failures investigation, operational experience to date, CSA 22.3 60826 standard, industry best  
19 practices) to determine an updated unbalanced ice load design for L3501/2. This assessment was  
20 completed in 2024. A consultant will be contracted to provide a design and cost estimate for tower  
21 modification that will be required to meet this new unbalanced ice load design, to be completed in  
22 2025. The feasibility and cost of other options will also be evaluated which will need to meet the new  
23 design loads by reducing the loads on the towers. This will include installing mid span structures  
24 between existing tangent structures, and removing the electrode conductor from the towers and  
25 installing it on wood pole structures for sections of the line, as required.

26 The failures of the conductor occurred at the suspension clamp. As part of the tower analysis project  
27 (initiated in 2024), the electrode suspension assembly will be analyzed to determine if modification can  
28 be made to transfer less load to the conductor during unbalanced icing. There is also an ongoing analysis  
29 where three different electrode suspension clamps have been installed at 10 structures (20 clamps in  
30 total) to determine if they perform better than the existing clamp under unbalanced ice loading

1 conditions. The conductor at these clamp location will be examined on an annual basis to look for signs  
2 of wear or damage.

3 The material testing found that the steel core of the conductor had migrated down through the  
4 aluminum layers, and caused deformation and cold fusing of the aluminum strands. This may have  
5 occurred during the high ice accumulation on the lines or during galloping of the lines. To determine if  
6 this process of steel core migration has started in other locations of the line, it is recommended that the  
7 possibility of using radiography to assess the conductor condition be investigated.

# Appendix A

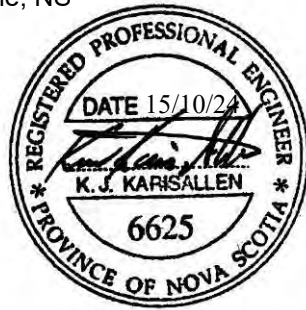
NL Hydro Transmission Line Failure (Conductor EL-1 and EL-2 at Suspension Tower 1225) report by Wayland Engineering Ltd.



# NL HYDRO TRANSMISSION LINE FAILURE

*(Conductor EL-1 and EL-2 at Suspension Tower 1225)*

Prepared By:  
K.J. KarisAllen, P.Eng.  
Wayland Engineering Ltd.  
Unit 9B, 2 Beechville Park Drive  
Beechville, NS  
B3T 1L7



Prepared For:  
Maria Veitch, P.Eng.  
Newfoundland and Labrador Hydro  
500 Columbus Drive  
St. John's, NL  
A1E 0A1

## Wayland Engineering Ltd.

Wayland Engineering Ltd – Report No. J2413A  
October 2024

## **Executive summary**

---

Wayland Engineering Ltd. was asked by Newfoundland and Labrador Hydro (NL Hydro) to conduct an investigation for two electrical conductors (EL-1 and EL-2) removed from suspension Tower #1225. The conductors routed electrical power along the approximately 1090 km long transmission corridor between Muskrat Falls and Soldiers Pond. On March 30, 2024, Pole #2 tripped at approximately 6:45 am. It was also reported that Pole #1 tripped at approximately 6:52 am owing to an electrode line fault protection event. A subsequent field inspection conducted on the lines detected various forms of damage between Tower #1218 and Tower #1228. NL Hydro requested that Wayland Engineering provide an opinion on the mechanism(s) responsible for the failures sustained by conductor EL-1 and EL-2 from Tower #1225.

A summary of the conclusions and recommendations generated by the investigation conducted includes:

- The physical, chemical and metallurgical evidence indicates that the mechanism responsible for the failure of conductors EL-1 and EL-2 at Tower #1225 is consistent with ductile limit load fracture of the aluminum conductor strands.
- The force required to precipitate a ductile limit load fracture mechanism of the aluminum conductor strands was attributed to the combination of ice accumulation and sustained wind velocities on the day prior to and during the day of the failures. It is also probable that wind induced galloping was present in the lines prior to the failures, which generated an additional cyclic force.
- The evidence suggests that the steel reinforcing core migrated towards, and was in contact with, the lower surface of the insulator wire clamp. The downward bearing force responsible for the migration was sufficient to distort and cold pressure weld (fuse) adjacent aluminum wires together in the lower circumferential half of the conductor. It is reasonable to assume that the distortion and fusing of the aluminum strands would result in a decrease in the overall breaking strength of the conductor where it enters the wire clamp.
- It has been postulated that one in situ, non-destructive method of detecting steel core migration is radiographic imaging. It should be noted that if radiographic imaging is utilized, it should include a reference marker on the bottom surface of the wire clamp. It is recommended that in consultation with experts in the field of radiography, that NL Hydro consider investigating the feasibility of radiographic imaging to detect the presence of incipient damage in the conductors.

## Table of contents

---

Executive summary .....	ii
Table of contents .....	iii
List of figures .....	iv
List of tables .....	viii
1 BACKGROUND .....	1
2 PRELIMINARY EXAMINATION.....	4
2.1 Preliminary Examination of Failed Conductor EL-1.....	4
2.2 Preliminary Examination of Failed Conductor EL-2.....	10
3 EVALUATION OF THE CONDUCTOR DIMENSIONAL AND MECHANICAL PROPERTIES.....	17
3.1 Dimensional Characterization of Failed Conductor EL-1 Wire Strands .....	18
3.2 Dimensional Characterization of Failed Conductor EL-2 Wire Strands .....	19
3.3 Dimensional Characterization of an Intact Service Exposed (Used) Conductor Wire Strands .....	20
3.4 Uniaxial Tension Testing of an Intact Service Exposed (Used) Conductor .....	21
4 METALLURGICAL CHARACTERIZATION OF THE FAILED CONDUCTOR DAMAGE (EL-1 AND EL-2) .....	25
4.1 Metallurgical Characterization of Failed Conductor EL-1 .....	25
4.2 Metallurgical Characterization of Failed Conductor EL-2 .....	30
5 SUMMARY AND DISCUSSION OF THE PHYSICAL EVIDENCE .....	35
5.1 Summary of the Physical Evidence .....	35
5.2 General Discussion.....	36
6 CONCLUSIONS AND RECOMMENDATIONS .....	37
References .....	38
Annex A ..Data Sheet for the ACSR Grackle (Zinc Coated) Conductor .....	39
Annex B...Dimensional Characterization of the Failed Section of ACSR Grackle (Zinc Coated) Conductor EL-1.....	41
Annex C...Dimensional Characterization of the Failed Section of ACSR Grackle (Zinc Coated) Conductor EL-2.....	43
Annex D ..Dimensional Characterization of the Intact Service Exposed Section of ACSR Grackle (Zinc Coated) Conductor.....	45

## List of figures

---

Figure 1-1: Google map provided by NL Hydro [1] showing the general compass directions of the segments of the transmission lines between Tower #1200 and Tower #1229. The map also shows the reported direction of the reported wind (easterly) on the day prior to and during the day of the failures [1].....	2
Figure 1-2: General view of suspension Tower #1225 subsequent to the line failures on March 30, 2024 [1]. The image shows the locations of conductor EL-1 and EL-2 (ellipse), which were attached to the crossarms of the tower via suspension insulators. ....	3
Figure 1-3: Schematic showing the general configuration of an ACSR Grackle 54/19 conductor specification. ....	3
Figure 2-1: Top-down view of the wire clamp and failed section of the EL-1 conductor as received for analysis.....	5
Figure 2-2: Side view of the wire clamp and failed section of the EL-1 conductor as received for analysis. ....	5
Figure 2-3: Photograph of the upper vertical external circumferential surface of conductor EL-1 as installed in the field. The image shows the fracture ends of the wire strands observed on the upper circumferential surface of the conductor (ellipse). ....	6
Figure 2-4: Photograph of the lower vertical external circumferential surface of conductor EL-1 as installed in the field. The image shows the significant aluminum strand to strand fusing observed on the lower circumferential surface. ....	6
Figure 2-5: Close-up view of a representative example of the fracture failure morphologies observed for conductor EL-1 (subsequent to conductor disassembly). The first morphology was characterized by a tapered (necked) interval immediately adjacent to the strand fracture surface. ....	7
Figure 2-6: Close-up view of a representative example of the fracture failure morphologies observed for conductor EL-1 (subsequent to conductor disassembly). The second morphology was characterized by an oblique fracture plane extending across the diameter of the strand. ....	7
Figure 2-7: Close-up view of a representative example of the aluminum strand fusing observed (subsequent to conductor disassembly). ....	8
Figure 2-8: Close-up view of a second representative example of the aluminum strand fusing observed (subsequent to conductor disassembly). ....	8
Figure 2-9: Top-down view of the lower circumferential surface of the wire clamp associated with conductor EL-1. The image shows the localized brinelling (ellipse) observed adjacent to the outboard axial end (on the conductor failure side) of the clamp. The image also shows the approximate outline associated with the cross-sectional view of the brinelling in Figure 2-10. ....	9
Figure 2-10: Close-up sectional view through the localized brinelling (arrow) shown in Figure 2-9. The image shows the approximate semi-circular morphology of the damage observed at the site (ellipse). ....	9
Figure 2-11: Top-down view of the wire clamp and failed section of the EL-2 conductor as received for analysis.....	11
Figure 2-12: Side view of the wire clamp and failed section of the EL-2 conductor as received for analysis. ....	11

Figure 2-13: Photograph showing a view of the failed section of the EL-2 conductor with an attached Stockbridge damper as received for analysis. .... 11

Figure 2-14: Photograph showing a second view of the failed section of the EL-2 conductor with an attached Stockbridge damper as received for analysis. .... 12

Figure 2-15: Photograph of the upper vertical external circumferential surface of conductor EL-2 as installed in the field. The image shows the fracture ends of the wire strands observed on the upper circumferential surface of the conductor. .... 12

Figure 2-16: Photograph of the lower vertical external circumferential surface of conductor EL-2 as installed in the field. The image shows the significant aluminum strand to strand fusing observed on the lower circumferential surface. .... 13

Figure 2-17: Close-up view of a representative example of the fracture failure morphologies observed for conductor EL-2 (subsequent to conductor disassembly). The first morphology was characterized by a tapered (necked) interval immediately adjacent to the strand fracture surface. .... 13

Figure 2-18: Close-up view of a representative example of the fracture failure morphologies observed for conductor EL-2 (subsequent to conductor disassembly). The second morphology was characterized by an oblique fracture plane extending across the diameter of the strand. .... 14

Figure 2-19: Close-up view of a representative example of the aluminum strand fusing observed (subsequent to conductor disassembly). .... 14

Figure 2-20: Close-up view of a second representative example of the aluminum strand fusing observed (subsequent to conductor disassembly). .... 15

Figure 2-21: Top-down view of the lower circumferential surface of the wire clamp associated with conductor EL-2. The image shows the localized brinelling (ellipse) observed adjacent to the outboard axial end (on the conductor failure side) of the clamp. The image also shows the approximate outline associated with the cross-sectional view of the brinelling in Figure 2-22. .... 15

Figure 2-22: Close-up sectional view through the localized brinelling (arrow) shown in Figure 2-21. The image shows the approximately semi-circular morphology of the damage observed at the site. .... 16

Figure 3-1: Image showing the coiled length of the service exposed (used) conductor provided by NL Hydro as received for analysis. .... 17

Figure 3-2: SEM backscatter image of a representative example of a zinc coated steel reinforcing strand for the failed conductor EL-1. The image shows the significant variation in the thickness of the zinc coating observed around the circumference of the steel reinforcing strand. .... 18

Figure 3-3: SEM backscatter image of a representative example of a zinc coated steel reinforcing strand for the failed conductor EL-2. The image shows the significant variation in the thickness of the zinc coating observed around the circumference of the steel reinforcing strand. .... 19

Figure 3-4: SEM backscatter image of a representative example of a zinc coated steel reinforcing strand for the intact service exposed conductor. The image shows the significant variation in the thickness of the zinc coating observed around the circumference of the steel reinforcing strand. .... 20

Figure 3-5: Photograph showing the epoxy filled socket fixture (ellipse) utilized to terminate the conductor at both ends. .... 22

Figure 3-6: Photograph showing the load train utilized to test the intact service exposed conductor in uniaxial tension (the arrow indicates the conductor). .... 22

Figure 3-7: Photograph showing the service exposed conductor subsequent to failure. The axial position of the conductor failure was approximately 21 cm from the beginning of one of the epoxy filled terminations. .... 23

Figure 3-8: Close-up view of the conductor showing the relative positions of the outer aluminum and the inner steel reinforcing wire strand failures. .... 23

Figure 3-9: Close-up view of a representative example of the fracture failure morphology observed for the aluminum conductors associated with the uniaxial tension test. The morphology was characterized by a tapered (necked) interval immediately adjacent to the strand fracture surface. .... 24

Figure 3-10: SEM fractographic images of a representative example of the fracture surface associated with the failure of the outer aluminum wire strands. The image shows the cup and cone failure (A) and the void coalescence (B) typically associated with a ductile, limit load fracture mechanism. .... 24

Figure 4-1: Low magnification SEM secondary image of a representative example of the fracture surface (ellipse) associated with the tapered-end (necked) geometry observed terminating the failed aluminum wire strands during the preliminary examination of conductor EL-1 (Figure 2-5). The image shows the general cup and cone morphology of the failed end of the wire strand. .... 27

Figure 4-2: High magnification fractographic image within the proximity of the strand centroid shown in Figure 4-1. The image indicates that the strand fracture mechanism was dominated by void coalescence (i.e. ductile fracture) at the site. .... 27

Figure 4-3: Low magnification SEM secondary image of a representative example of the fracture surface associated with the oblique geometry observed terminating the failed aluminum wire strands during the preliminary examination of conductor EL-1 (Figure 2-6). .... 28

Figure 4-4: High magnification fractographic image within the proximity of the strand centroid showing the topological features associated with the strand fracture mechanism. Similar to Figure 4-2, the image suggests that the strand fracture mechanism was dominated by void coalescence (i.e. ductile fracture) at the site. .... 28

Figure 4-5: Sectional view SEM backscatter image of a representative example of the strand to strand fusing observed in conductor EL-1. The image also shows the location of the SEM EDS analyses conducted to determine the composition of the high density (light) phase observed (results are summarized in Table 4-1). .... 29

Figure 4-6: Sectional view SEM backscatter image of a representative example of the clamp material immediately adjacent to the site of localized brinelling observed. The image also shows the location of the SEM EDS analyses conducted to determine the composition of the high density (light) phase observed (results are summarized in Table 4-2). .... 29

Figure 4-7: Low magnification SEM secondary image of a representative example of the fracture surface (ellipse) associated with the tapered-end (necked) geometry observed terminating the failed aluminum wire strands during the preliminary examination of conductor EL-2 (Figure 2-17). The image shows the general cup and cone morphology of the failed end of the wire strand. .... 32

Figure 4-8: High magnification fractographic image within the proximity of the strand centroid shown in Figure 4-1. The image indicates that the strand fracture mechanism was dominated by void coalescence (i.e. ductile fracture) at the site. .... 32

Figure 4-9: Low magnification SEM secondary image of a representative example of the fracture surface associated with the oblique geometry observed terminating the failed aluminum wire strands during the preliminary examination of conductor EL-2 (Figure 2-18). .... 33

Figure 4-10: High magnification fractographic image within the proximity of the strand centroid showing the topological features associated with the strand fracture mechanism. Similar to Figure 4-8, the image suggests that the strand fracture mechanism was dominated by void coalescence (i.e. ductile fracture) at the site. .... 33

Figure 4-11: Sectional view SEM backscatter image of a representative example of the strand to strand fusing observed in conductor EL-2. The image also shows the location of the SEM EDS analyses conducted to determine the composition of the high density (light) phase observed (results are summarized in Table 4-3)..... 34

Figure 4-12: Sectional view SEM backscatter images of a representative example of the clamp material immediately adjacent to the site of localized brinelling observed. The image also shows the location of the SEM EDS analyses conducted to determine the composition of the high density (light) phase observed (results are summarized in Table 4-4). .... 34

Figure B-1: SEM backscatter image of a representative example of a zinc coated steel reinforcing strand for failed conductor EL-1. The image shows the significant variation in the thickness of the zinc coating observed around the circumference of the steel reinforcing strand..... 42

Figure B-2: SEM backscatter image of a representative example of a zinc coated steel reinforcing strand for failed conductor EL-1. The image shows the significant variation in the thickness of the zinc coating observed around the circumference of the steel reinforcing strand..... 42

Figure B-3: SEM backscatter image of a representative example of a zinc coated steel reinforcing strand for failed conductor EL-1. The image shows the significant variation in the thickness of the zinc coating observed around the circumference of the steel reinforcing strand..... 42

Figure C-1: SEM backscatter image of a representative example of a zinc coated steel reinforcing strand for failed conductor EL-2. The image shows the significant variation in the thickness of the zinc coating observed around the circumference of the steel reinforcing strand..... 44

Figure C-2: SEM backscatter image of a representative example of a zinc coated steel reinforcing strand for failed conductor EL-2. The image shows the significant variation in the thickness of the zinc coating observed around the circumference of the steel reinforcing strand..... 44

Figure C-3: SEM backscatter image of a representative example of a zinc coated steel reinforcing strand for failed conductor EL-2. The image shows the significant variation in the thickness of the zinc coating observed around the circumference of the steel reinforcing strand..... 44

Figure D-1: SEM backscatter image of a representative example of a zinc coated steel reinforcing strand for the intact conductor. The image shows the significant variation in the thickness of the zinc coating observed around the circumference of the steel reinforcing strand..... 46

Figure D-2: SEM backscatter image of a representative example of a zinc coated steel reinforcing strand for the intact conductor. The image shows the significant variation in the thickness of the zinc coating observed around the circumference of the steel reinforcing strand..... 46

Figure D-3: SEM backscatter image of a representative example of a zinc coated steel reinforcing strand for the intact conductor. The image shows the significant variation in the thickness of the zinc coating observed around the circumference of the steel reinforcing strand..... 46

## List of tables

---

Table 1-1: Summary of the damage detected by the field inspection between Tower #1222 and Tower #1228 subsequent to the failure events on March 30, 2024 [1]. .....	2
Table 3-1: Summary of wire strand diameter ranges for the 6 layers associated with the failed conductor EL-1. The detailed measurement results have been provided in Annex B. ....	18
Table 3-2: Summary of wire strand diameter ranges for the 6 layers associated with the failed conductor EL-2. The detailed measurement results have been provided in Annex C. ....	19
Table 3-3: Summary of wire strand diameter ranges for the 6 layers associated with the intact service exposed conductor. The detailed measurement results have been provided in Annex D. ....	20
Table 4-1: Semi-quantitative SEM EDS analysis results for the strand to strand fusing observed in conductor EL-1. Figure 4-5 shows the locations of the EDS analyses. ...	26
Table 4-2: Semi-quantitative SEM EDS analysis results for the clamp material immediately adjacent to the site of localized brinelling in conductor EL-1. Figure 4-6 shows the locations of the EDS analyses. ....	26
Table 4-3: Semi-quantitative SEM EDS analysis results for the strand to strand fusing observed in conductor EL-2. Figure 4-11 shows the locations of the EDS analyses. .	31
Table 4-4: Semi-quantitative SEM EDS analysis results for the clamp material immediately adjacent to the site of localized brinelling in conductor EL-2. Figure 4-12 shows the locations of the EDS analyses. ....	31
Table A-1: Manufactures' data sheet for the ACSR Grackle conductor (zinc coated steel reinforcing core). ....	39
Table B-1: Summary of the outer aluminum conductor and inner steel reinforcing wire strand diameter measurements for the failed section of conductor EL-1. ....	41
Table C-1: Summary of the outer aluminum conductor and inner steel reinforcing wire strand diameter measurements for the failed section of conductor EL-2. ....	43
Table D-1: Summary of the outer aluminum conductor and inner steel reinforcing wire strand diameter measurements for the used intact service exposed conductor provided for uniaxial tension testing. ....	45

# 1 BACKGROUND

---

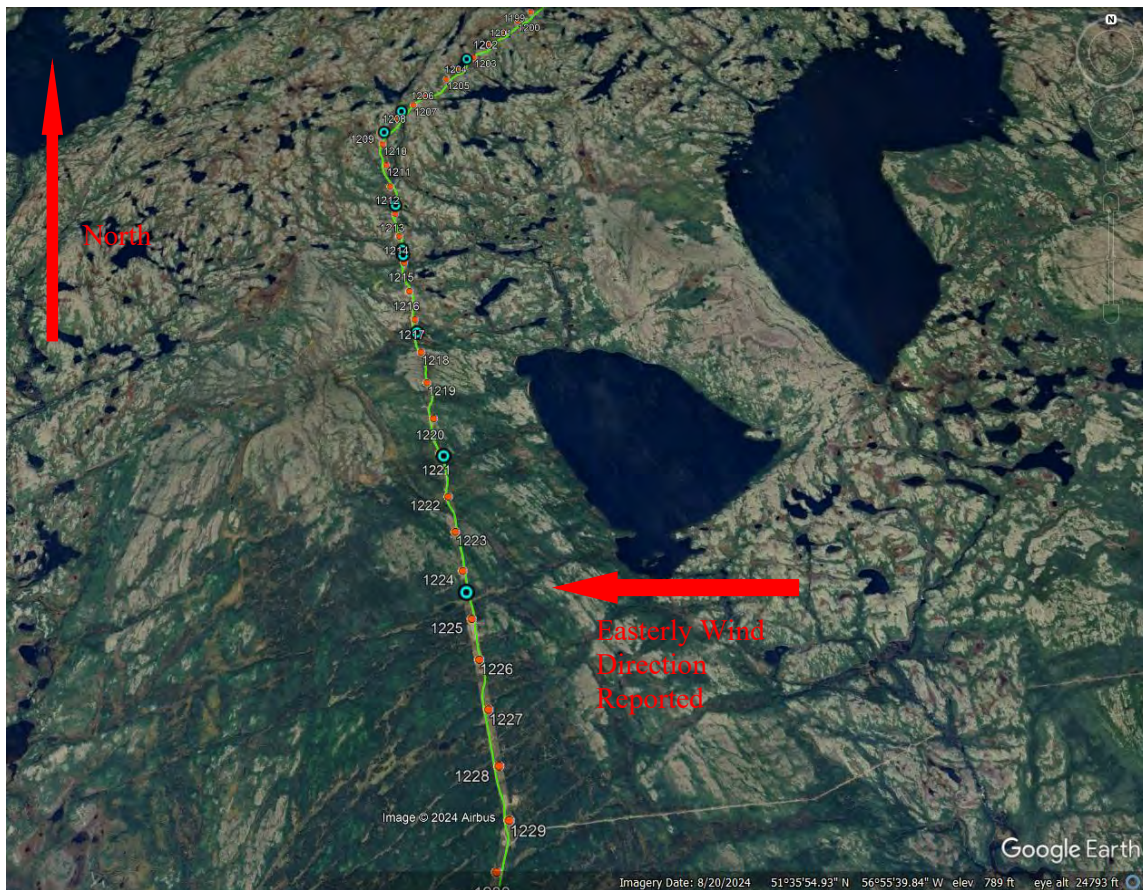
Wayland Engineering Ltd. was asked by Newfoundland and Labrador Hydro (NL Hydro) to conduct an investigation for two electrical conductors (EL-1 and EL-2) removed from suspension Tower #1225. The conductors routed electrical power along the approximately 1090 km long transmission corridor between Muskrat Falls and Soldiers Pond [1]. On March 30, 2024, Pole #2 tripped at approximately 6:45 am [1]. It was also reported that Pole #1 tripped at approximately 6:52 am owing to an electrode line fault protection event [1]. A subsequent field inspection conducted on the lines detected various forms of damage between Tower #1218 and Tower #1228 (Table 1-1 [1]). It has been indicated that there was significant ice accumulation on the line prior to failure (estimated radial thickness of the ice was in the range between 100 – 125 mm) [1]. It was also assumed that based on the failures and observation of icing conditions after the failures, there were unbalanced ice loads on the line due to ice shedding prior to the failures on March 30 [1]. It was reported that on the day prior to the failures, the wind velocity was approximately 70 km/h from an easterly direction [1]. During the day of the conductor failures, an easterly wind velocity of approximately 60 km/h was reported [1]. It has been indicated that the line was designed for a maximum wind velocity of 120 km/h in the absence of accumulated ice [1]. For a radial ice accumulation of approximately 25 mm, the design criterion for the maximum wind velocity reduces to 60 km/h [1]. The combination of the ice accumulation and wind velocities reported suggests that the line was operating in excess of the design criteria both on the day prior to and during the day of the failures sustained by conductors EL-1 and EL-2.

Figure 1-1 is a map showing the general compass directions of the line segments between suspension Tower #1200 and Tower #1229. It was also reported that the distances from Tower #1224 to Tower #1225 and Tower #1225 to Tower #1226 were approximately 378 m and 303 m, respectively [1]. It has been indicated that conductors EL-1 and EL-2 between Tower 1209 and Tower #1228 were installed in 2017 and had been subjected to approximately 7 years of service prior to the failures in 2024 [1]. Figure 1-1 also shows the direction of the easterly wind velocities reported on the day prior to and during the day of the conductor failure events. Of relevance to the current investigation was the approximate orthogonal angle of the wind direction with respect to the axis of the conductors, which may induce large amplitude vibrations (i.e. galloping) in the lines (particularly for conditions of asymmetric ice accumulation on the conductors). It has been noted that galloping of the conductors has been observed by NL Hydro on multiple occasions in the vicinity of Tower #1225 since the installation of the lines in 2017 [1].

Figure 1-2 is a field photograph of Tower #1225 subsequent to the failure of the conductors. The image shows the locations of conductor EL-1 and EL-2, which were attached to the crossarms of the tower via suspension insulators. It was reported that both conductor EL-1 and EL-2 conformed to an ACSR Grackle conductor specification. The Grackle 54/19 conductor specification with a 1192.5 kcmil size is a concentric-lay-stranded configuration with 54 outer aluminum conductors and 19 inner zinc coated steel reinforcing wires (Figure 1-3). The nominal diameters of the outer aluminum and inner steel wire strands were reported as 3.77 mm and 2.26 mm, respectively [1]. The outer aluminum wire strands for an ACSR Grackle conductor specification are manufactured from a material with a minimum aluminum content of 99.50 wt% [2,3,4]. Annex A contains the detailed data sheet for the ACSR Grackle conductor utilized by NL Hydro at Tower #1225 [1]. NL Hydro requested that Wayland Engineering provide an opinion on the mechanism(s) responsible for the failures sustained by conductor EL-1 and EL-2 from Tower #1225, which were provided for analysis.

*Table 1-1: Summary of the damage detected by the field inspection between Tower #1222 and Tower #1228 subsequent to the failure events on March 30, 2024 [1].*

<b>Tower No.</b>	<b>Description of Damage Sustained by Conductor EL-1 and EL-2</b>
1222	EL1 conductor stripped on 1221 side and birdcaged on 1223 side, EL2 Conductor complete broken on 1223 side.
1223	EL1 conductor stripped on 1222 side and birdcaged on 1224 side, EL2 Conductor complete broken on 1224 side.
1224	Both conductors stripped and birdcaged.
1225	Both conductors stripped and birdcaged.
1226	Both conductors damaged, video is not clear.
1227	Conductor severed and resting on pole conductor.
1228	EL1 conductor appears stripped and birdcaged - video not completely clear. Conductor is touching the ground.



*Figure 1-1: Google map provided by NL Hydro [1] showing the general compass directions of the segments of the transmission lines between Tower #1200 and Tower #1229. The map also shows the reported direction of the reported wind (easterly) on the day prior to and during the day of the failures [1].*



Figure 1-2: General view of suspension Tower #1225 subsequent to the line failures on March 30, 2024 [1]. The image shows the locations of conductor EL-1 and EL-2 (ellipse), which were attached to the crossarms of the tower via suspension insulators.

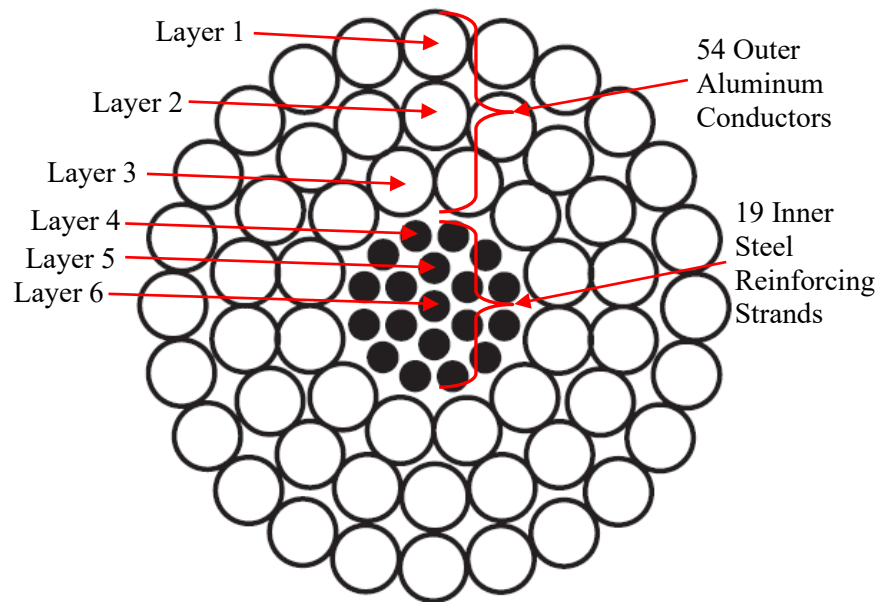


Figure 1-3: Schematic showing the general configuration of an ACSR Grackle 54/19 conductor specification.

## **2 PRELIMINARY EXAMINATION**

---

Section 2.1 and Section 2.2 detail the preliminary examination conducted for the sections of failed conductor received for analysis from line EL-1 and EL-2, respectively.

### **2.1 Preliminary Examination of Failed Conductor EL-1**

Figure 2-1 and Figure 2-2 show two views of the single section of failed conductor EL-1 provided by NL Hydro as received for analysis. The section consisted of an approximately 60 cm long length of conductor and the lower bolted wire clamp associated with the suspension insulator from Tower #1225. At one axial end of the wire clamp, evidence of severe bird-caging of the aluminum conductor strands was observed (cut end of the conductor). At the opposing axial end of the wire clamp, evidence of fractured aluminum conductor strands was observed with an approximately 15 cm long length of the steel reinforcing core extending from the failed aluminum strands. It was reported that at Tower #1225 (Table 1-1 and Figure 1-2), the EL-1 line damage consisted of stripped and birdcaged outer conductors, which suggests that the inner steel reinforcing core remained intact at the site. Figure 2-2 also shows the relative vertical position of the steel reinforcing core, which showed evidence of migration towards the lower circumferential surface of the EL-1 wire clamp.

The wire clamp was subsequently removed from the EL-1 conductor for further characterization of the damage sustained by the aluminum wire strands during the failure event. Figure 2-3 and Figure 2-4 show the upper vertical and lower vertical external circumferential surfaces of the conductor as installed in the field. On the upper circumferential surface, the ends of the aluminum wire strands were terminated by fracture failures (Figure 2-3). Figure 2-5 and Figure 2-6 show close-up views of representative examples of the fracture failure morphologies observed (subsequent to conductor disassembly). The first morphology was characterized by a tapered (necked) interval immediately adjacent to the strand fracture surface (Figure 2-5). The second morphology was characterized by an oblique fracture plane extending across the diameter of the strand (Figure 2-6).

On the lower circumferential surface, evidence of significant aluminum strand to strand fusing was observed (Figure 2-4). The extent of the fusing was observed to increase towards the outboard axial end of the wire clamp. Figure 2-7 and Figure 2-8 show close-up views of representative examples of the strand to strand fusing subsequent to conductor disassembly. Evidence of complete and/or partial fusing together of all three aluminum strand layers was observed in conductor EL-1. Section 4.1 includes the metallurgical characterization of strand fracture failures, as well as the strand to strand fusing observed in conductor EL-1.

Figure 2-9 shows a top-down view of the lower circumferential surface of the wire clamp associated with conductor EL-1. Evidence of localized brinelling (plastic deformation) was observed adjacent to the outboard axial end (on the conductor failure side) of the clamp. The brinelling was located at the approximate bottom dead center circumferential position of the clamp as installed in the field. Figure 2-10 is a close-up sectional view of the localized brinelling observed. The image shows the approximately semi-circular morphology of the damage observed at the site. Section 4.1 includes the metallurgical characterization of the localized brinelling damage observed in the conductor EL-1 wire clamp.

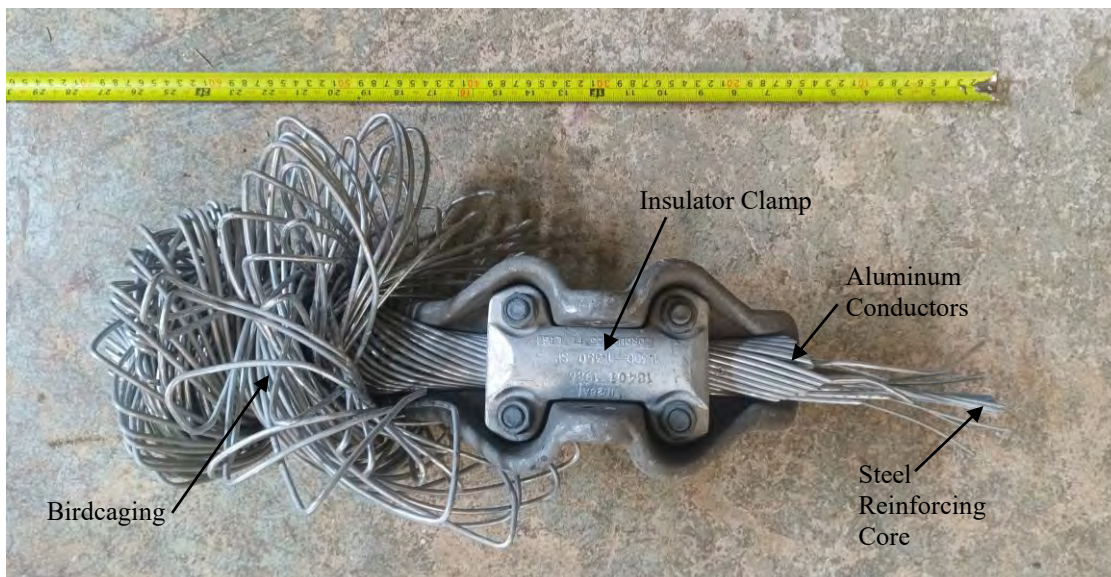


Figure 2-1: Top-down view of the wire clamp and failed section of the EL-1 conductor as received for analysis.



Figure 2-2: Side view of the wire clamp and failed section of the EL-1 conductor as received for analysis.

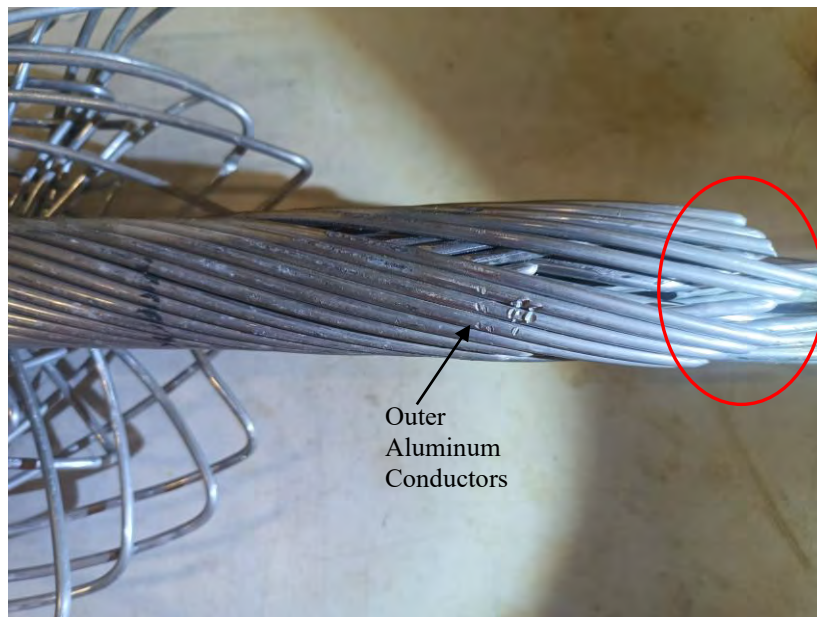


Figure 2-3: Photograph of the upper vertical external circumferential surface of conductor EL-1 as installed in the field. The image shows the fracture ends of the wire strands observed on the upper circumferential surface of the conductor (ellipse).

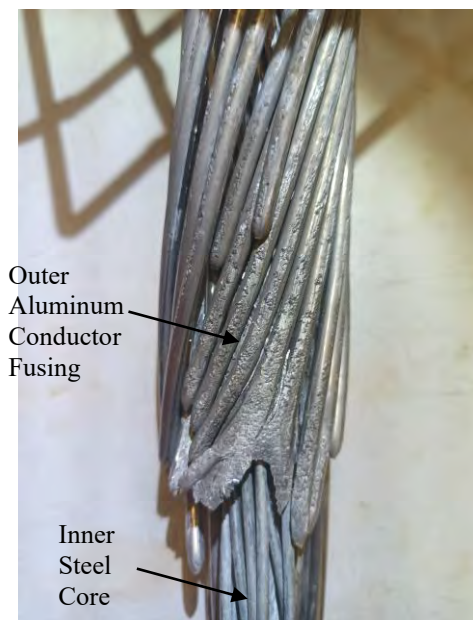
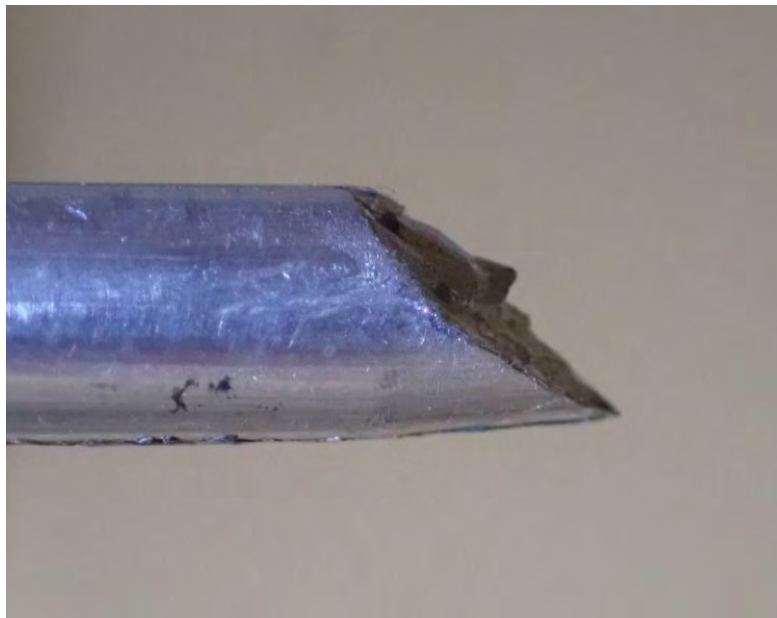


Figure 2-4: Photograph of the lower vertical external circumferential surface of conductor EL-1 as installed in the field. The image shows the significant aluminum strand to strand fusing observed on the lower circumferential surface.



*Figure 2-5: Close-up view of a representative example of the fracture failure morphologies observed for conductor EL-1 (subsequent to conductor disassembly). The first morphology was characterized by a tapered (necked) interval immediately adjacent to the strand fracture surface.*



*Figure 2-6: Close-up view of a representative example of the fracture failure morphologies observed for conductor EL-1 (subsequent to conductor disassembly). The second morphology was characterized by an oblique fracture plane extending across the diameter of the strand.*



*Figure 2-7: Close-up view of a representative example of the aluminum strand fusing observed (subsequent to conductor disassembly).*



*Figure 2-8: Close-up view of a second representative example of the aluminum strand fusing observed (subsequent to conductor disassembly).*

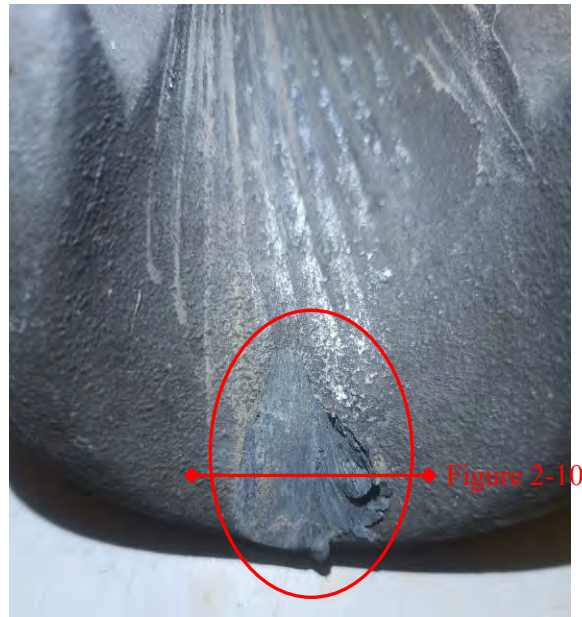


*Figure 2-9: Top-down view of the lower circumferential surface of the wire clamp associated with conductor EL-1. The image shows the localized brinelling (ellipse) observed adjacent to the outboard axial end (on the conductor failure side) of the clamp. The image also shows the approximate cutline associated with the cross-sectional view of the brinelling in Figure 2-10.*



*Figure 2-10: Close-up sectional view through the localized brinelling (arrow) shown in Figure 2-9. The image shows the approximate semi-circular morphology of the damage observed at the site (ellipse).*

## **2.2 Preliminary Examination of Failed Conductor EL-2**

Figure 2-11 through Figure 2-14 show views of the two sections of the failed conductor EL-2 provided by NL Hydro as received for analysis. The first section (Figure 2-11 and Figure 2-12) consisted of an approximately 45 cm long length of the outer aluminum conductor strands (i.e. the inner zinc coated steel reinforcing core was absent) and the lower bolted wire clamp associated with the suspension insulator from Tower #1225. At one axial end of the wire clamp, evidence of fractured aluminum conductor strands was observed. The second section of the failed conductor EL-2 (Figure 2-13 and Figure 2-14) consisted of an approximately 150 cm long length of conductor with a Stockbridge damper attached to the conductor wire. Evidence of severe bird-caging of the aluminum conductor strands was observed over the entire length of the second section of conductor EL-2 provided for analysis. At one axial end of the section with the attached Stockbridge damper, evidence of fractured aluminum conductor strands was observed. Similar to conductor EL-1, it was reported that at Tower #1225 (Table 1-1 and Figure 1-2), the EL-2 line damage consisted of stripped and birdcaged outer conductors, which suggests that the steel reinforcing core remained intact at the site.

The wire clamp and Stockbridge damper were subsequently removed from the two sections of the EL-2 conductor provided for further characterization of the damage sustained by the aluminum wire strands during the failure event. Figure 2-15 and Figure 2-16 show the upper vertical and lower vertical external circumferential surfaces of the conductor within the wire clamp section as installed in the field. On the upper circumferential surface, the ends of the aluminum wire strands were terminated by fracture failures (Figure 2-15). Figure 2-17 and Figure 2-18 show close-up views of representative examples of the fracture failure morphologies observed (subsequent to conductor disassembly). The first morphology was characterized by a tapered (necked) interval immediately adjacent to the strand fracture surface (Figure 2-17). The second morphology was characterized by an oblique fracture plane extending across the diameter of the strand (Figure 2-18).

On the lower circumferential surface, evidence of aluminum strand to strand fusing was observed (Figure 2-16). While the extent of the fusing was not as prevalent as that observed in conductor EL-1, the extent of the fusing was observed to increase towards the outboard axial end of the wire clamp. Figure 2-19 and Figure 2-20 show close-up views of representative examples of the strand to strand fusing subsequent to conductor disassembly. Similar to conductor EL-1, evidence of complete and/or partial fusing together of multiple aluminum strand layers was observed in conductor EL-2. Section 4.2 includes the metallurgical characterization of strand fracture failures, as well as the strand to strand fusing observed in conductor EL-2.

Figure 2-21 shows a top-down view of the lower circumferential surface of the wire clamp associated with conductor EL-2. Evidence of localized brinelling (plastic deformation) was observed adjacent to the outboard axial end (on the conductor failure side) of the clamp. The brinelling was located at the approximate bottom dead center circumferential position of the clamp as installed in the field. Figure 2-22 is a close-up sectional view of the localized brinelling observed. The image shows the approximately semi-circular morphology of the damage observed at the site. Section 4.2 includes the metallurgical characterization of the localized brinelling damage observed in conductor EL-2 wire clamp.



Figure 2-11: Top-down view of the wire clamp and failed section of the EL-2 conductor as received for analysis.



Figure 2-12: Side view of the wire clamp and failed section of the EL-2 conductor as received for analysis.



Figure 2-13: Photograph showing a view of the failed section of the EL-2 conductor with an attached Stockbridge damper as received for analysis.

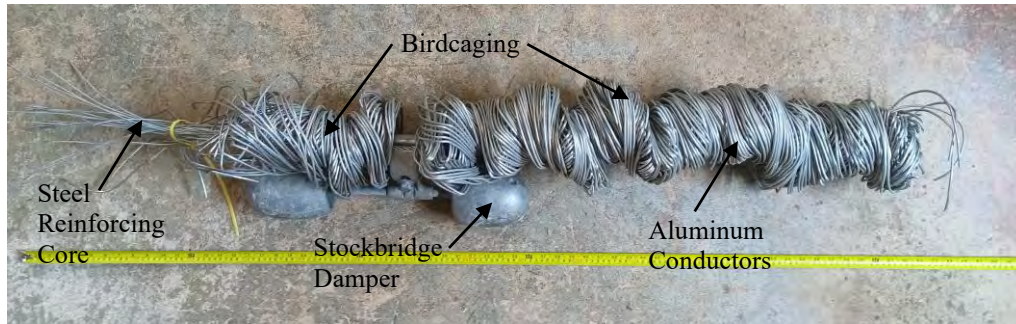
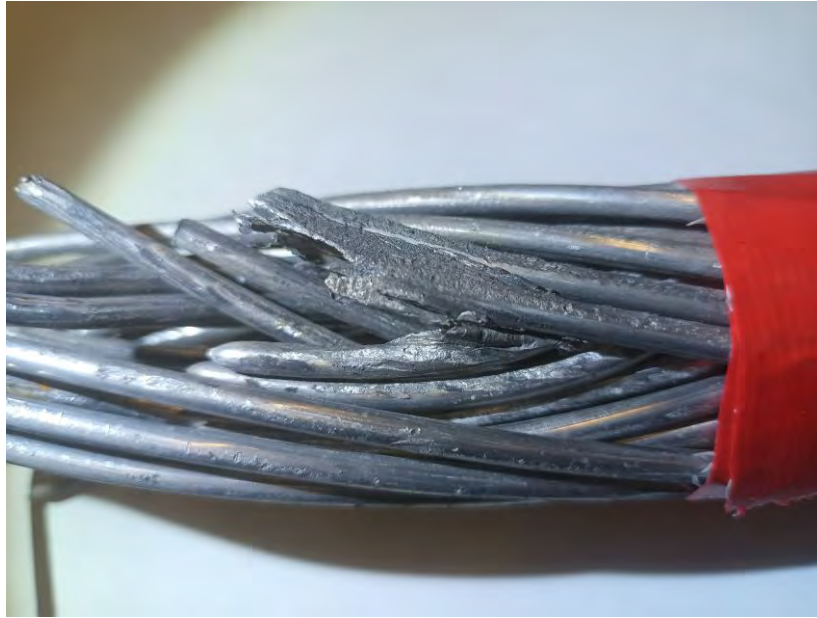


Figure 2-14: Photograph showing a second view of the failed section of the EL-2 conductor with an attached Stockbridge damper as received for analysis.



Figure 2-15: Photograph of the upper vertical external circumferential surface of conductor EL-2 as installed in the field. The image shows the fracture ends of the wire strands observed on the upper circumferential surface of the conductor.



*Figure 2-16: Photograph of the lower vertical external circumferential surface of conductor EL-2 as installed in the field. The image shows the significant aluminum strand to strand fusing observed on the lower circumferential surface.*



*Figure 2-17: Close-up view of a representative example of the fracture failure morphologies observed for conductor EL-2 (subsequent to conductor disassembly). The first morphology was characterized by a tapered (necked) interval immediately adjacent to the strand fracture surface.*



*Figure 2-18: Close-up view of a representative example of the fracture failure morphologies observed for conductor EL-2 (subsequent to conductor disassembly). The second morphology was characterized by an oblique fracture plane extending across the diameter of the strand.*



*Figure 2-19: Close-up view of a representative example of the aluminum strand fusing observed (subsequent to conductor disassembly).*



Figure 2-20: Close-up view of a second representative example of the aluminum strand fusing observed (subsequent to conductor disassembly).



Figure 2-21: Top-down view of the lower circumferential surface of the wire clamp associated with conductor EL-2. The image shows the localized brinelling (ellipse) observed adjacent to the outboard axial end (on the conductor failure side) of the clamp. The image also shows the approximate cutline associated with the cross-sectional view of the brinelling in Figure 2-22.



*Figure 2-22: Close-up sectional view through the localized brinelling (arrow) shown in Figure 2-21. The image shows the approximately semi-circular morphology of the damage observed at the site.*

### 3 EVALUATION OF THE CONDUCTOR DIMENSIONAL AND MECHANICAL PROPERTIES

---

The intervals of conductor fixed within the insulator clamps of the failed EL-1 and EL-2 sections were disassembled in order to conduct a dimensional characterization of the wire strand diameters. For the EL-1 and EL-2 strands which did not exhibit either strand to strand fusing and/or severe strand cross-sectional distortions, the diameter of the wire strand was measured at an axial distance of approximately 2 cm to 3 cm away from the terminating fracture surface associated with individual strands. An axial interval was also removed and disassembled from an intact length of service exposed (used) conductor provided by NL Hydro (Figure 3-1). The diameters of the wire strands associated with the intact service exposed conductor were also measured for comparison purposes. For the internal steel reinforcing core strands, the thickness of the protective zinc coating layer was measured on representative wire strands from the three disassembled intervals of conductor using scanning electron microscope (SEM) imaging. Section 3.1, Section 3.2 and Section 3.3 detail the results generated for the failed EL-1, failed EL-2 and intact (service exposed) conductors, respectively.

A uniaxial tension test was also conducted on a length of the intact conductor provided by NL Hydro to determine if the service exposed conductor still met the rated tensile strength requirements for a Grackle ACSR 54/19 conductor. Section 3.4 details the results of the uniaxial tension test conducted.



*Figure 3-1: Image showing the coiled length of the service exposed (used) conductor provided by NL Hydro as received for analysis.*

### 3.1 Dimensional Characterization of Failed Conductor EL-1 Wire Strands

Table 3-1 contains a summary of wire strand diameter ranges for the 6 layers associated with the failed conductor EL-1 (the detailed measurement results have been provided in Annex B). For Layer 1, Layer 2 and Layer 3 (aluminum conductor strands) the diameters ranged between 3.40 mm to 3.73 mm, 3.56 mm to 3.73 mm and 3.63 mm to 3.68 mm, respectively. For Layer 4, Layer 5 and Layer 6 (zinc coated steel reinforcing strands) the diameters ranged between 2.06 mm to 2.24 mm, 2.03 mm to 2.11 mm and 2.11 mm, respectively. The diameter ranges measured for both the aluminum conductor strands and the zinc coated steel reinforcing strands for conductor EL-1 were generally within reasonable agreement with the specified wire diameter requirements as per ASTM B-232 [2] for a Grackle ACSR 54/19 (size 1192.5 kcmil) conductor.

Figure 3-2 is a sectional SEM backscatter image of a representative example of a zinc coated steel reinforcing strand (additional representative examples are provided in Annex B). The image shows the variation in the thickness of the zinc coating observed around the circumference of the steel reinforcing strand. The minimum thickness ranged between approximately 31.86  $\mu\text{m}$  and 43.31  $\mu\text{m}$  for the strands evaluated. A range of 31.86  $\mu\text{m}$  to 43.31  $\mu\text{m}$  in zinc coating thickness equates to a layer surface density of approximately 271.9  $\text{g}/\text{m}^2$  to 404.9  $\text{g}/\text{m}^2$ , respectively. While a significant variation in the thickness of the zinc coating was observed around the circumference of individual strands, it should be noted that a breach through the coating to the steel core was not observed at the sites (i.e. the cathodic protection provided by the zinc coating remained intact).

Table 3-1: Summary of wire strand diameter ranges for the 6 layers associated with the failed conductor EL-1. The detailed measurement results have been provided in Annex B.

	Wire Strand Diameter Ranges (mm)					
	Outer Aluminum Strands			Inner Steel Strands		
	Layer 1	Layer 2	Layer 3	Layer 4	Layer 5	Layer 6
Conductor EL-1	3.40-3.73	3.56-3.73	3.63-3.68	2.06-2.24	2.03-2.11	2.11

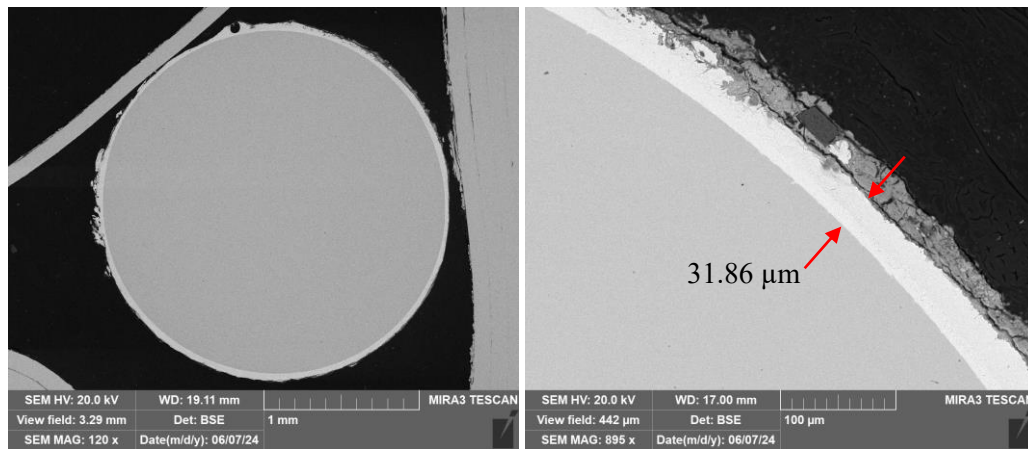


Figure 3-2: SEM backscatter image of a representative example of a zinc coated steel reinforcing strand for the failed conductor EL-1. The image shows the significant variation in the thickness of the zinc coating observed around the circumference of the steel reinforcing strand.

### 3.2 Dimensional Characterization of Failed Conductor EL-2 Wire Strands

Table 3-2 contains a summary of wire strand diameter ranges for the 6 layers associated with the failed conductor EL-2 (the detailed measurement results have been provided in Annex C). For Layer 1, Layer 2 and Layer 3 (aluminum conductor strands) the diameters ranged between 3.43 mm to 3.68 mm, 3.56 mm to 3.71 mm and 3.66 mm to 3.71 mm, respectively. For Layer 4, Layer 5 and Layer 6 (zinc coated steel reinforcing strands) the diameters ranged between 2.18 mm to 2.26 mm, 2.16 mm to 2.24 mm and 2.24 mm, respectively. The diameter ranges measured for both the aluminum conductor strands and the zinc coated steel reinforcing strands for conductor EL-2 were generally within reasonable agreement with the specified wire diameter requirements as per ASTM B-232 [2] for a Grackle ACSR 54/19 (size 1192.5 kcmil) conductor.

Figure 3-3 is a sectional SEM backscatter image of a representative example of a zinc coated steel reinforcing strand (additional representative examples are provided in Annex C). Similar to the failed conductor EL-1, the image shows the variation in the thickness of the zinc coating observed around the circumference of the steel reinforcing strand. The minimum thickness ranged between approximately 30.83  $\mu\text{m}$  and 31.57  $\mu\text{m}$  for the strands evaluated. A range of 30.83  $\mu\text{m}$  to 31.57  $\mu\text{m}$  in zinc coating thickness equates to a layer surface density of approximately 261.2  $\text{g}/\text{m}^2$  to 268.8  $\text{g}/\text{m}^2$ , respectively. While a significant variation in the thickness of the zinc coating was observed around the circumference of individual strands, it should be noted that a breach through the coating to the steel core was not observed at the sites (i.e. the cathodic protection provided by the zinc coating remained intact).

Table 3-2: Summary of wire strand diameter ranges for the 6 layers associated with the failed conductor EL-2. The detailed measurement results have been provided in Annex C.

	Wire Strand Diameter Ranges (mm)					
	Outer Aluminum Strands			Outer Aluminum Strands		
	Layer 1	Layer 2	Layer 3	Layer 4	Layer 5	Layer 6
Conductor EL-2	3.43-3.68	3.56-3.71	3.66-3.71	2.18-2.26	2.16-2.24	2.24

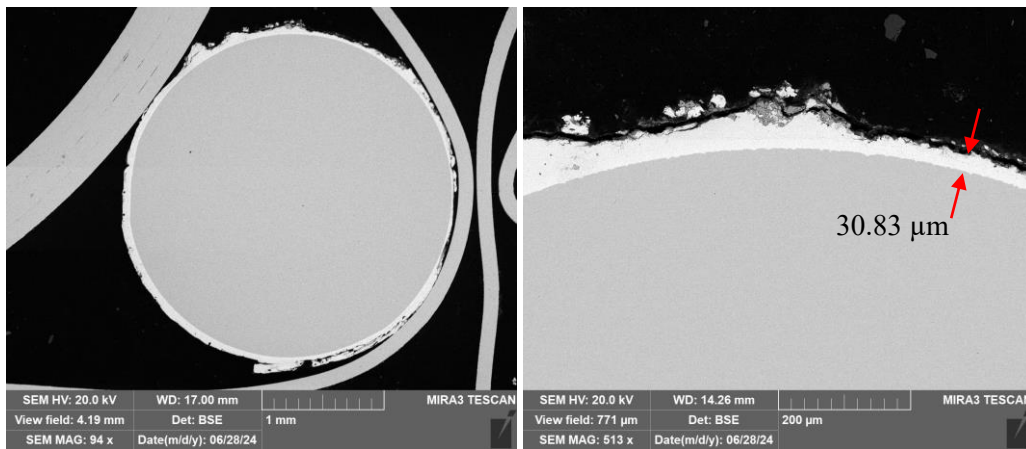


Figure 3-3: SEM backscatter image of a representative example of a zinc coated steel reinforcing strand for the failed conductor EL-2. The image shows the significant variation in the thickness of the zinc coating observed around the circumference of the steel reinforcing strand.

### 3.3 Dimensional Characterization of an Intact Service Exposed (Used) Conductor Wire Strands

Table 3-3 contains a summary of wire strand diameter ranges for the 6 layers associated with the intact service exposed conductor (the detailed measurement results have been provided in Annex D). For Layer 1, Layer 2 and Layer 3 (aluminum conductor strands) the diameters ranged between 3.71 mm to 3.76 mm, 3.71 mm to 3.76 mm and 3.71 mm to 3.73 mm, respectively. For Layer 4, Layer 5 and Layer 6 (zinc coated steel reinforcing strands) the diameters ranged between 2.21 mm to 2.24 mm, 2.21 mm to 2.24 mm and 2.21 mm, respectively. The diameter ranges measured for both the aluminum conductor strands and the zinc coated steel reinforcing strands for the service exposed conductor were generally within reasonable agreement with the specified wire diameter requirements as per ASTM B-232 [2] for a Grackle ACSR 54/19 (size 1192.5 kcmil) conductor.

Figure 3-4 is a sectional SEM backscatter image of a representative example of a zinc coated steel reinforcing strand (additional representative examples are provided in Annex D). Similar to the failed conductors EL-1 and EL-2, the image shows the variation in the thickness of the zinc coating observed around the circumference of the steel reinforcing strand. The minimum thickness ranged between approximately 21.56  $\mu\text{m}$  and 37.36  $\mu\text{m}$  for the strands evaluated. A range of 21.56  $\mu\text{m}$  to 37.36  $\mu\text{m}$  in zinc coating thickness equates to a layer surface density of approximately 171.9  $\text{g}/\text{m}^2$  to 332.3  $\text{g}/\text{m}^2$ , respectively. While a variation in the thickness of the zinc coating was observed around the circumference of individual strands, it should be noted that a breach through the coating to the steel core was not observed at the sites (i.e. the cathodic protection provided by the zinc coating remained intact).

Table 3-3: Summary of wire strand diameter ranges for the 6 layers associated with the intact service exposed conductor. The detailed measurement results have been provided in Annex D.

	Wire Strand Diameter Ranges (mm)					
	Outer Aluminum Strands			Outer Aluminum Strands		
	Layer 1	Layer 2	Layer 3	Layer 4	Layer 5	Layer 6
Intact Conductor	3.71-3.76	3.71-3.76	3.71-3.73	2.21-2.24	2.21-2.24	2.21

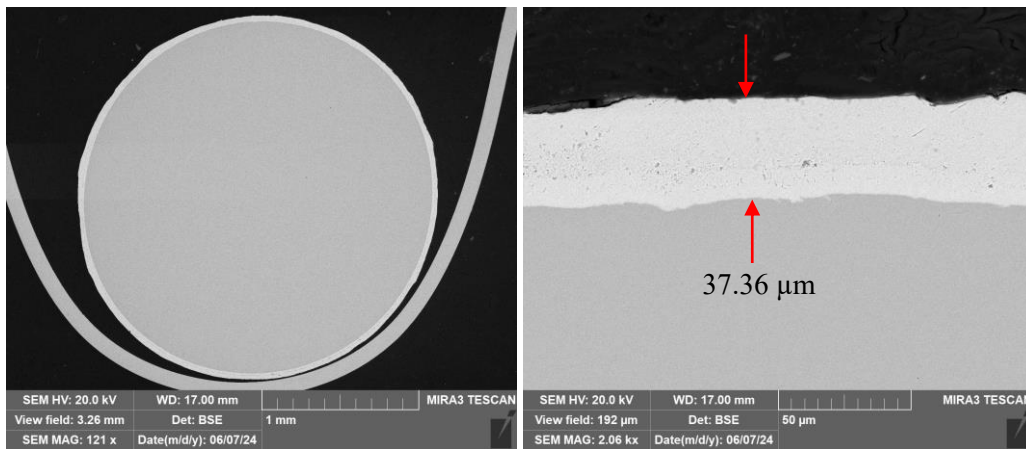


Figure 3-4: SEM backscatter image of a representative example of a zinc coated steel reinforcing strand for the intact service exposed conductor. The image shows the significant variation in the thickness of the zinc coating observed around the circumference of the steel reinforcing strand.

### **3.4 Uniaxial Tension Testing of an Intact Service Exposed (Used) Conductor**

A length of the intact service exposed (used) conductor provided by NL Hydro (Figure 3-1) was tested in uniaxial tension in accordance with the procedure specified in ASTM A931 [5]. A test sample with a gauge length of approximately 1.55 m was terminated at both ends with an epoxy filled socket fixture (Figure 3-5). Figure 3-6 shows the load train utilized to test the terminated sample. The load train was used to apply a monotonic, stroke controlled, quasi-static deflection rate to the sample until the ultimate rupture of both the outer aluminum and inner steel reinforcing wire strands occurred.

The results of the testing indicated that the applied force when the outer aluminum wire strands selectively fractured was approximately 196.6 kN. The selective fracture of the outer aluminum wire strands resulted in a reduction of the applied force to approximately 94.7 kN. With continued applied deflection to the sample, the applied force increased to approximately 114.3 kN, which resulted in the fracture failure of the inner steel reinforcing wire strands. Measurements indicated that the overall fracture failure of the conductor occurred approximately 21 cm from the beginning of one of the epoxy filled terminations (Figure 3-7).

Figure 3-8 is a close-up view of the conductor showing the relative positions of the outer aluminum and the inner steel reinforcing wire strand failures, which is consistent with that expected for the failure of a Grackle ACSR conductor. Samples of the fractured ends of the outer aluminum wire strands were removed from the failed conductor for additional analyses using SEM fractographic imaging techniques. Figure 3-9 and Figure 3-10 contain a side view and end view fractographic images of a representative example of a fractured aluminum wire strand, respectively. For Figure 3-10, image (A) shows the cup and cone failure morphology and image (B) shows the void coalescence typically associated with a ductile, limit load fracture mechanism. The cup and cone failure morphology observed was consistent with that expected for the applied uniaxial tension force generated by the test procedure. Section 4.1 and Section 4.2 include the fractographic images for the fractured aluminum wire strands from conductor EL-1 and conductor EL-2 for comparison, respectively.

It should be noted that the coil diameter of the length of service exposed conductor provided by NL Hydro was approximately 48 inches, which was below the recommended minimum diameter of 50 times the diameter of the conductor diameter (approximately 68 inches). Coiling the conductor below its recommended bend radius may result in the introduction of permanent plastic strain in the outer aluminum wire strands. In addition, the ends of the service exposed conductor were fixed with electrical tape as opposed to mechanical clamps generally recommended. Insufficient clamping pressure at the ends of the conductor may result in an axial shifting of conductor layers with respect to each other (particularly for the case where the conductor is coiled below the minimum recommended bend radius). Both induced plastic strain in the outer aluminum wire strands and a relative shift between conductor layers may result in a reduction in the ultimate breaking strength of the conductor. Thus, it is possible that the actual breaking strength of the service exposed conductor was higher than that recorded during the uniaxial tension test conducted.



Figure 3-5: Photograph showing the epoxy filled socket fixture (ellipse) utilized to terminate the conductor at both ends.



Figure 3-6: Photograph showing the load train utilized to test the intact service exposed conductor in uniaxial tension (the arrow indicates the conductor).

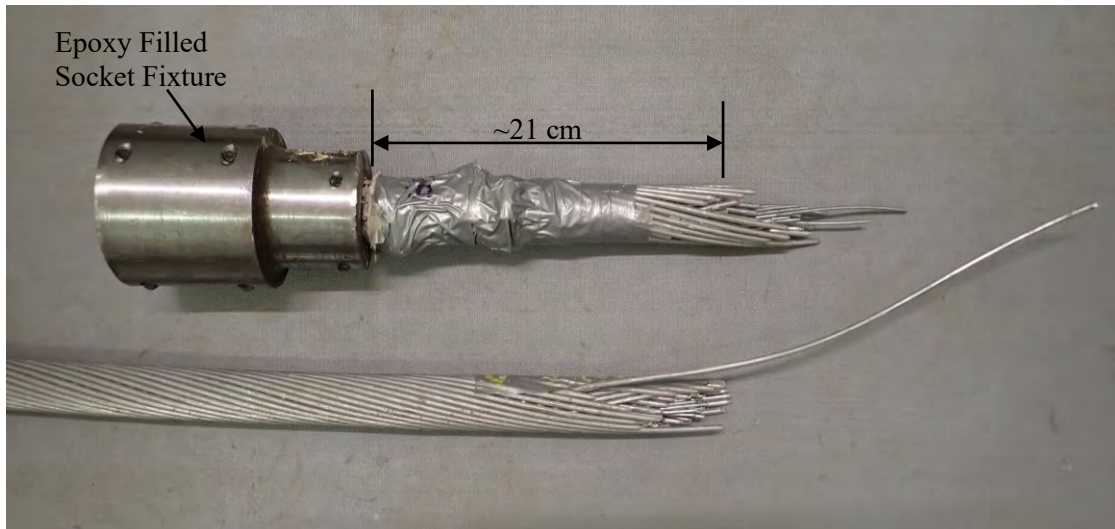


Figure 3-7: Photograph showing the service exposed conductor subsequent to failure. The axial position of the conductor failure was approximately 21 cm from the beginning of one of the epoxy filled terminations.

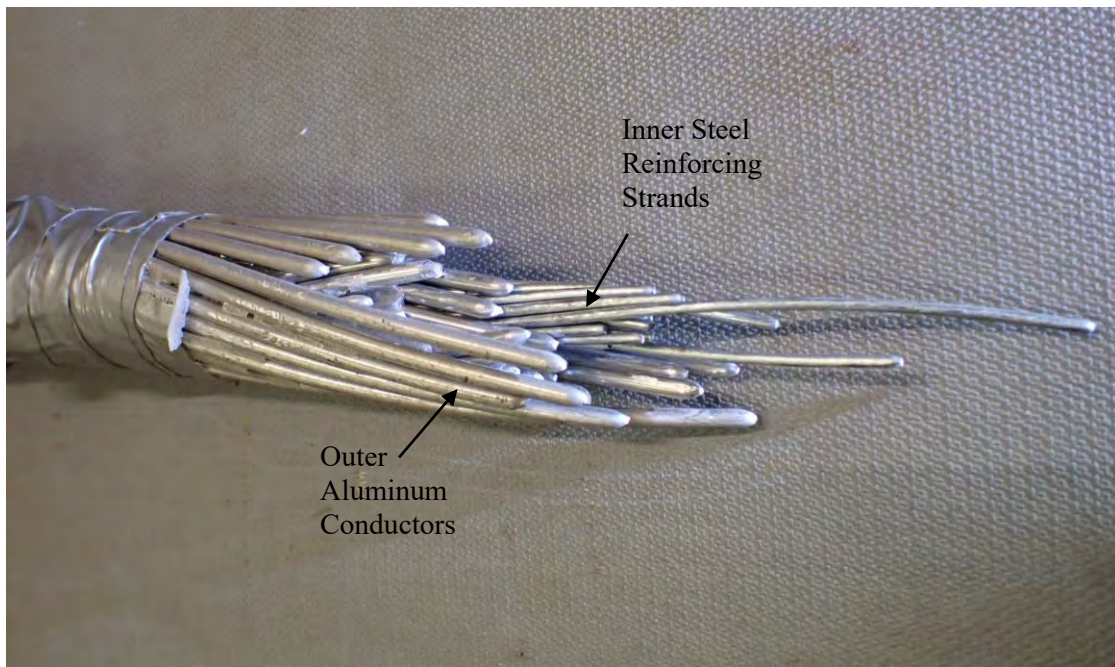


Figure 3-8: Close-up view of the conductor showing the relative positions of the outer aluminum and the inner steel reinforcing wire strand failures.



Figure 3-9: Close-up view of a representative example of the fracture failure morphology observed for the aluminum conductors associated with the uniaxial tension test. The morphology was characterized by a tapered (necked) interval immediately adjacent to the strand fracture surface.

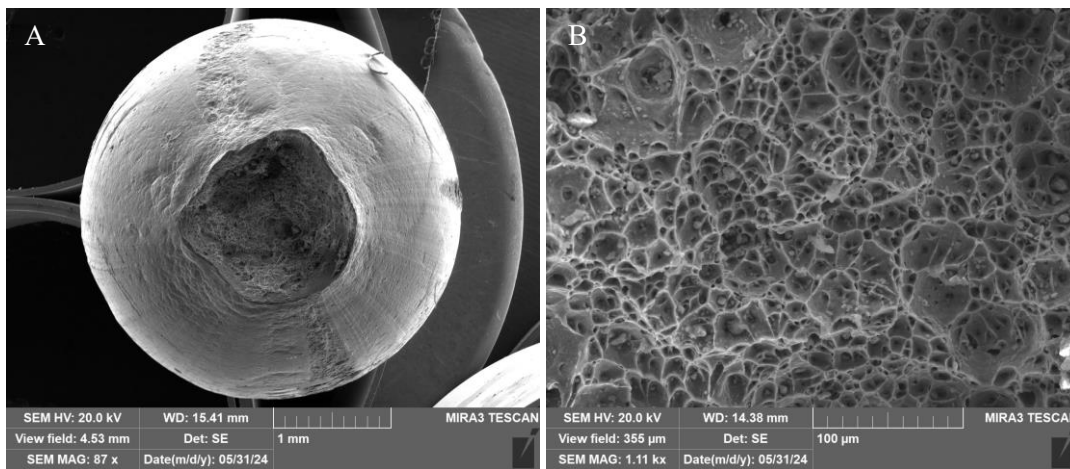


Figure 3-10: SEM fractographic images of a representative example of the fracture surface associated with the failure of the outer aluminum wire strands. The image shows the cup and cone failure (A) and the void coalescence (B) typically associated with a ductile, limit load fracture mechanism.

## **4 METALLURGICAL CHARACTERIZATION OF THE FAILED CONDUCTOR DAMAGE (EL-1 AND EL-2)**

---

Section 4.1 and Section 4.2 contain the metallurgical results characterizing the conductor and insulator wire clamp damage detected for failed conductors EL-1 and EL-2 provided for analysis respectively.

### **4.1 Metallurgical Characterization of Failed Conductor EL-1**

Samples from several of the outer aluminum wire strands, which included the fracture surface associated with the strand failure were removed from conductor EL-1. The samples were prepared for the characterization of the topological features associated with the fracture mechanism using SEM fractographic imaging techniques. Figure 4-1 is a low magnification SEM secondary image of a representative example of the fracture surface associated with the tapered-end geometry observed terminating the failed aluminum wire strands during the preliminary examination of conductor EL-1 (Figure 2-5). The image shows the general cup and cone morphology of the failed end of the wire strand. Figure 4-2 is a high magnification fractographic image within the proximity of the strand centroid showing the topological features associated with the strand fracture mechanism. The image indicates that the strand fracture mechanism was dominated by void coalescence (i.e. ductile fracture) at the site. Figure 4-3 is a low magnification SEM secondary image of a representative example of the fracture surface associated with the oblique geometry observed terminating the failed aluminum wire strands during the preliminary examination of conductor EL-1 (Figure 2-6). Figure 4-4 is a high magnification fractographic image within the proximity of the strand centroid showing the topological features associated with the strand fracture mechanism. Similar to Figure 4-2, the image suggests that the strand fracture mechanism was dominated by void coalescence (i.e. ductile fracture) at the site.

Several samples were also sectioned from the outer aluminum wire strands at locations where evidence of strand to strand fusing was observed during the preliminary examination of conductor EL-1 (Figure 2-7 and Figure 2-8). The samples were prepared for metallurgical characterization of the damage using a combination of SEM imaging and energy dispersive X-ray spectroscopy (EDS) analyses. Figure 4-5 is a sectional view SEM backscatter image of a representative example of the strand to strand fusing observed in conductor EL-1. The image shows the severe distortion of the wire strands observed, as well as the presence of a higher density phase embedded within the distorted aluminum strands. To determine the composition of the higher density phase, the material was subjected to EDS analyses. The results of the analyses (Table 4-1) indicated that the higher density phase was comprised primarily of zinc (Zn). The analyses suggest that the Zn from the outer coating associated with the steel reinforcing strands was also fusing with the outer aluminum wire strands.

Several samples were also sectioned from the insulator conductor clamp where evidence of localized brinelling was observed during the preliminary examination of conductor EL-1 (Figure 2-10). Figure 4-6 is a sectional view SEM backscatter image of a representative example of the clamp material immediately adjacent to the site of localized brinelling. Similar to Figure 4-5, the image shows the presence of a higher density phase embedded within the aluminum clamp

material. The results of the analyses (Table 4-2) indicated that the higher density phase was comprised primarily of zinc (Zn). The presence of Zn embedded within the Al clamp material suggests that the Zn coated steel reinforcing strands (from the inner conductor core) were in contact with the intrados associated with the clamp housing at the site.

*Table 4-1: Semi-quantitative SEM EDS analysis results for the strand to strand fusing observed in conductor EL-1. Figure 4-5 shows the locations of the EDS analyses.*

Position	Chemical Composition (wt%)						
	Fe	Si	Zn	Al	O	P	S
<b>A1</b>	ND	ND	93.40	3.40	3.19	ND	ND
<b>A2</b>	ND	ND	90.69	7.10	2.21	ND	ND
<b>A3</b>	ND	ND	94.26	2.82	2.92	ND	ND
<b>A4</b>	ND	ND	ND	97.65	2.35	ND	ND

Note: ND indicates that the element was not detected.

*Table 4-2: Semi-quantitative SEM EDS analysis results for the clamp material immediately adjacent to the site of localized brinelling in conductor EL-1. Figure 4-6 shows the locations of the EDS analyses.*

Position	Chemical Composition (wt%)						
	Fe	Si	Zn	Al	O	P	S
<b>B1</b>	ND	1.09	90.78	6.19	1.94	ND	ND
<b>B2</b>	ND	ND	94.81	3.36	1.83	ND	ND
<b>B3</b>	ND	ND	78.00	18.59	3.41	ND	ND
<b>B4</b>	ND	ND	92.07	3.72	4.21	ND	ND
<b>B5</b>	ND	ND	95.72	2.29	1.99	ND	ND
<b>B6</b>	ND	ND	96.53	2.00	1.47	ND	ND
<b>B7</b>	ND	11.79	ND	86.47	1.74	ND	ND

Note: ND indicates that the element was not detected.

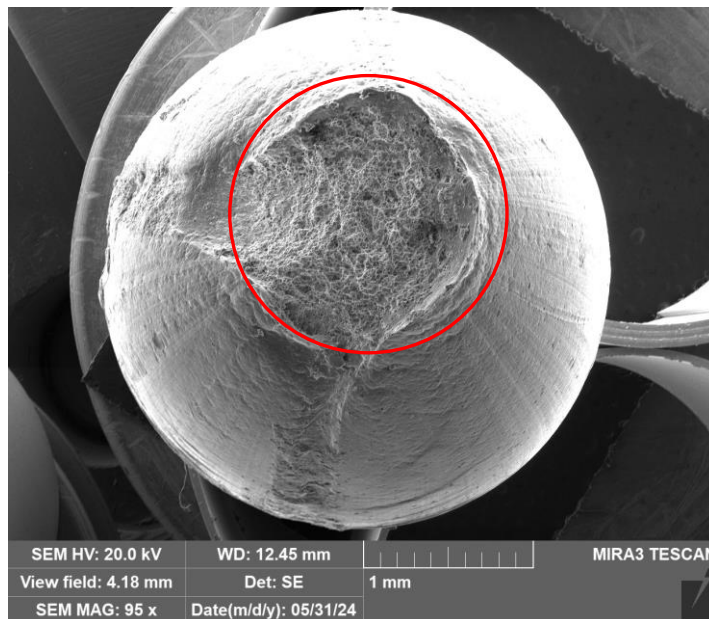


Figure 4-1: Low magnification SEM secondary image of a representative example of the fracture surface (ellipse) associated with the tapered-end (necked) geometry observed terminating the failed aluminum wire strands during the preliminary examination of conductor EL-1 (Figure 2-5). The image shows the general cup and cone morphology of the failed end of the wire strand.

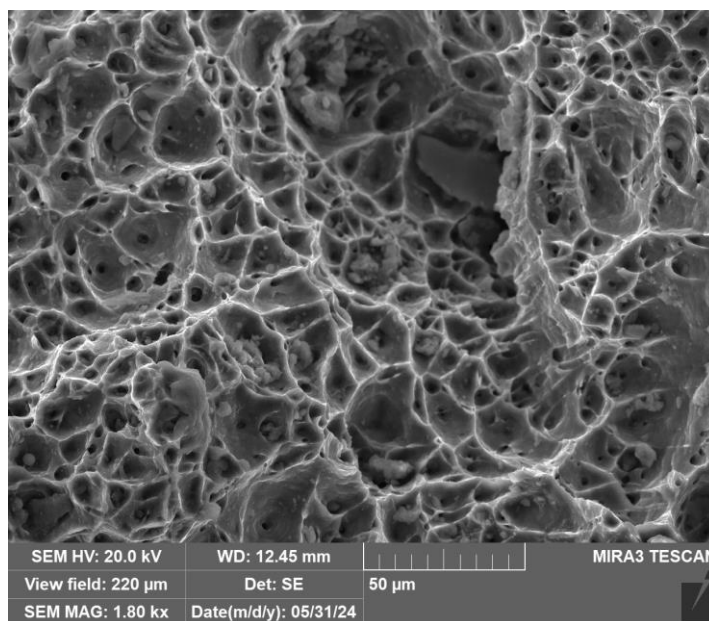


Figure 4-2: High magnification fractographic image within the proximity of the strand centroid shown in Figure 4-1. The image indicates that the strand fracture mechanism was dominated by void coalescence (i.e. ductile fracture) at the site.

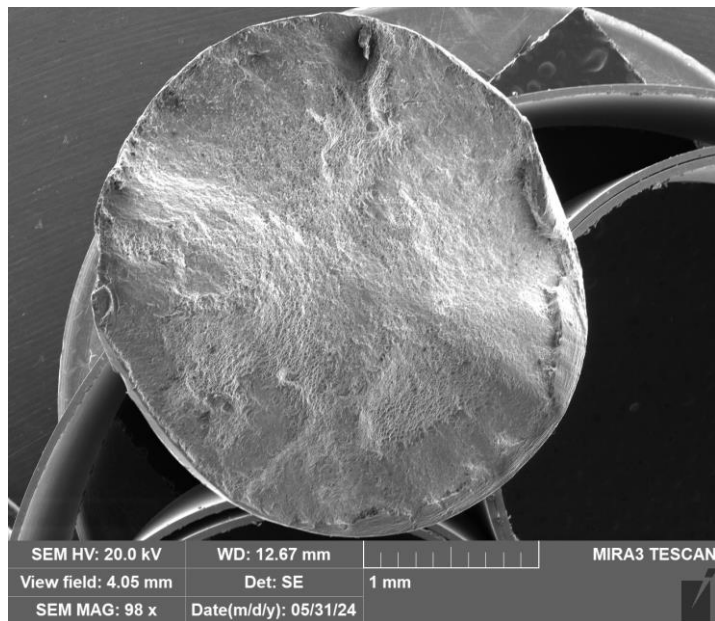


Figure 4-3: Low magnification SEM secondary image of a representative example of the fracture surface associated with the oblique geometry observed terminating the failed aluminum wire strands during the preliminary examination of conductor EL-1 (Figure 2-6).

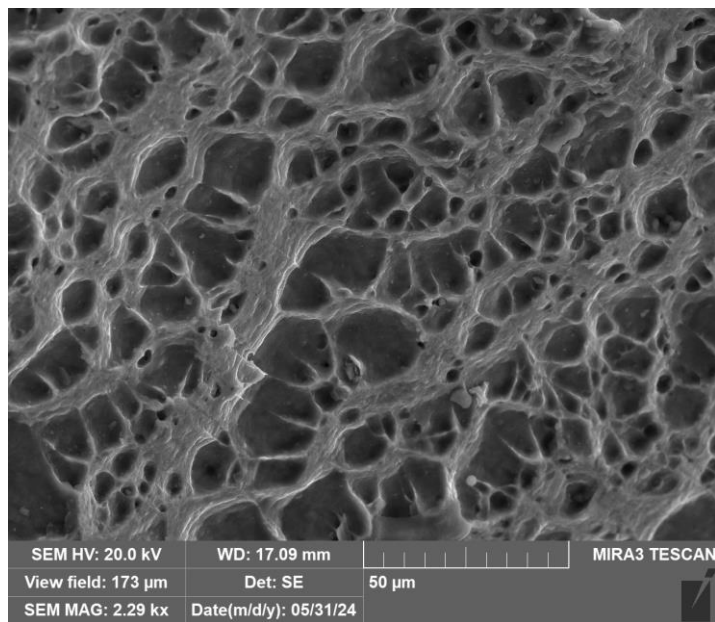


Figure 4-4: High magnification fractographic image within the proximity of the strand centroid showing the topological features associated with the strand fracture mechanism. Similar to Figure 4-2, the image suggests that the strand fracture mechanism was dominated by void coalescence (i.e. ductile fracture) at the site.

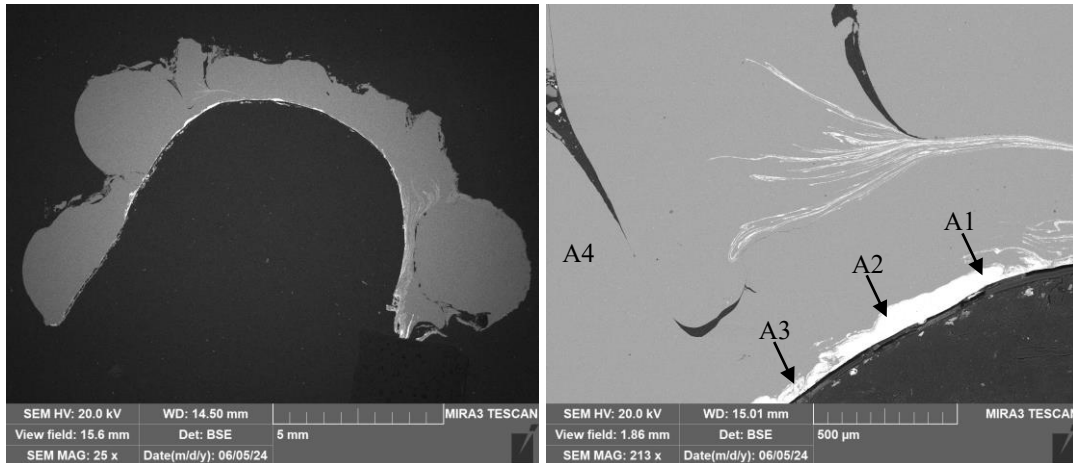


Figure 4-5: Sectional view SEM backscatter image of a representative example of the strand to strand fusing observed in conductor EL-1. The image also shows the location of the SEM EDS analyses conducted to determine the composition of the high density (light) phase observed (results are summarized in Table 4-1).

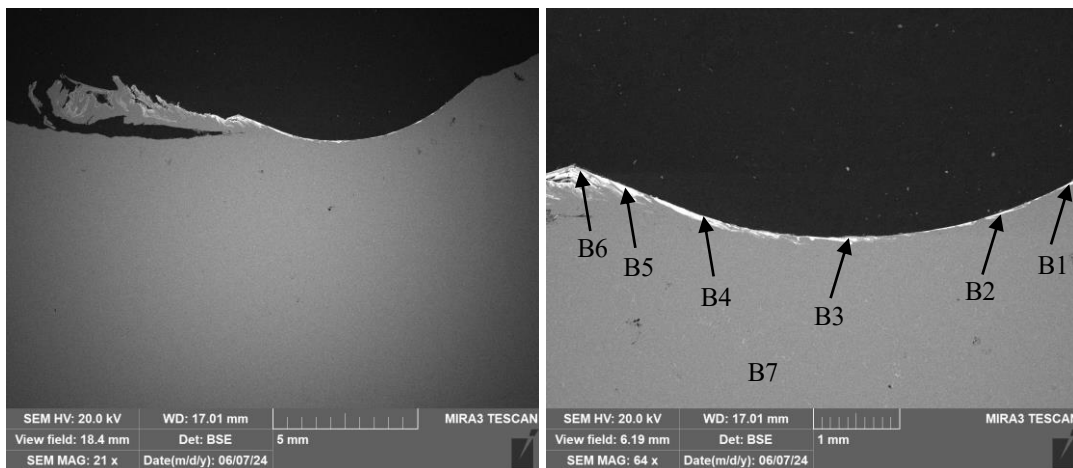


Figure 4-6: Sectional view SEM backscatter image of a representative example of the clamp material immediately adjacent to the site of localized brinelling observed. The image also shows the location of the SEM EDS analyses conducted to determine the composition of the high density (light) phase observed (results are summarized in Table 4-2).

## **4.2 Metallurgical Characterization of Failed Conductor EL-2**

Samples from several of the outer aluminum wire strands, which included the fracture surface associated with the strand failure were removed from conductor EL-2. The samples were prepared for the characterization of the topological features associated with the fracture mechanism using SEM fractographic imaging techniques. Figure 4-7 is a low magnification SEM secondary image of a representative example of the fracture surface associated with the tapered-end geometry observed terminating the failed aluminum wire strands during the preliminary examination of conductor EL-2 (Figure 2-17). The image shows the general cup and cone morphology of the failed end of the wire strand. Figure 4-8 is a high magnification fractographic image within the proximity of the strand centroid showing the topological features associated with the strand fracture mechanism. The image indicates that the strand fracture mechanism was dominated by void coalescence (i.e. ductile fracture) at the site. Figure 4-9 is a low magnification SEM secondary image of a representative example of the fracture surface associated with the oblique geometry observed terminating the failed aluminum wire strands during the preliminary examination of conductor EL-2 (Figure 2-18). Figure 4-10 is a high magnification fractographic image within the proximity of the strand centroid showing the topological features associated with the strand fracture mechanism. Similar to Figure 4-8, the image suggests that the strand fracture mechanism was dominated by void coalescence (i.e. ductile fracture) at the site.

Several samples were also sectioned from the outer aluminum wire strands at locations where evidence of strand to strand fusing was observed during the preliminary examination of conductor EL-2 (Figure 2-19 and Figure 2-20). The samples were prepared for metallurgical characterization of the damage using a combination of SEM imaging and EDS analyses. Figure 4-11 is a sectional view SEM backscatter image of a representative example of the strand to strand fusing observed in conductor EL-2. The image shows the severe distortion of the wire strands observed, as well as the presence of a higher density phase embedded within the distorted aluminum strands. To determine the composition of the higher density phase, the material was subjected to EDS analyses. The results of the analyses (Table 4-3) indicated that the higher density phase was comprised primarily of zinc (Zn). The analyses suggest that the Zn from the outer coating associated with the steel reinforcing strands was also fusing with the outer aluminum wire strands.

Several samples were also sectioned from the insulator conductor clamp where evidence of localized brinelling was observed during the preliminary examination of conductor EL-2 (Figure 2-22). Figure 4-12 is a sectional view SEM backscatter image of a representative example of the clamp material immediately adjacent to the site of localized brinelling. Similar to Figure 4-11, the image shows the presence of a higher density phase embedded within the aluminum clamp material. The results of the analyses (Table 4-4) indicated that the higher density phase was comprised primarily of zinc (Zn). The presence of Zn embedded within the Al clamp material suggests that the Zn coated steel reinforcing strands (from the inner conductor core) were in contact with the intrados associated clamp housing at the site.

*Table 4-3: Semi-quantitative SEM EDS analysis results for the strand to strand fusing observed in conductor EL-2. Figure 4-11 shows the locations of the EDS analyses.*

<b>Position</b>	<b>Chemical Composition (wt%)</b>						
	<b>Fe</b>	<b>Si</b>	<b>Zn</b>	<b>Al</b>	<b>O</b>	<b>P</b>	<b>S</b>
<b>C1</b>	ND	ND	79.55	10.26	10.20	ND	ND
<b>C2</b>	0.17	ND	32.19	54.49	12.89	0.08	0.18
<b>C3</b>	0.22	ND	95.88	1.28	2.45	0.18	ND
<b>C4</b>	0.26	ND	95.87	1.37	2.50	ND	ND
<b>C5</b>	ND	ND	87.01	7.13	5.75	0.10	ND
<b>C6</b>	ND	ND	35.66	54.43	9.90	ND	ND

Note: ND indicates that the element was not detected.

*Table 4-4: Semi-quantitative SEM EDS analysis results for the clamp material immediately adjacent to the site of localized brinelling in conductor EL-2. Figure 4-12 shows the locations of the EDS analyses.*

<b>Position</b>	<b>Chemical Composition (wt%)</b>						
	<b>Fe</b>	<b>Si</b>	<b>Zn</b>	<b>Al</b>	<b>Ti</b>	<b>Mg</b>	<b>O</b>
<b>D1</b>	ND	ND	96.21	0.98	ND	ND	2.81
<b>D2</b>	ND	ND	96.68	1.63	ND	ND	1.69
<b>D3</b>	ND	ND	97.58	ND	ND	ND	2.42
<b>D4</b>	ND	ND	97.07	1.22	ND	ND	1.70
<b>D5</b>	ND	ND	96.53	1.45	ND	ND	2.03
<b>D6</b>	ND	ND	95.35	1.99	ND	ND	2.67
<b>D7</b>	ND	ND	34.62	62.42	ND	ND	2.96
<b>D8</b>	ND	10.82	ND	86.54	0.19	0.47	1.98

Note: ND indicates that the element was not detected.

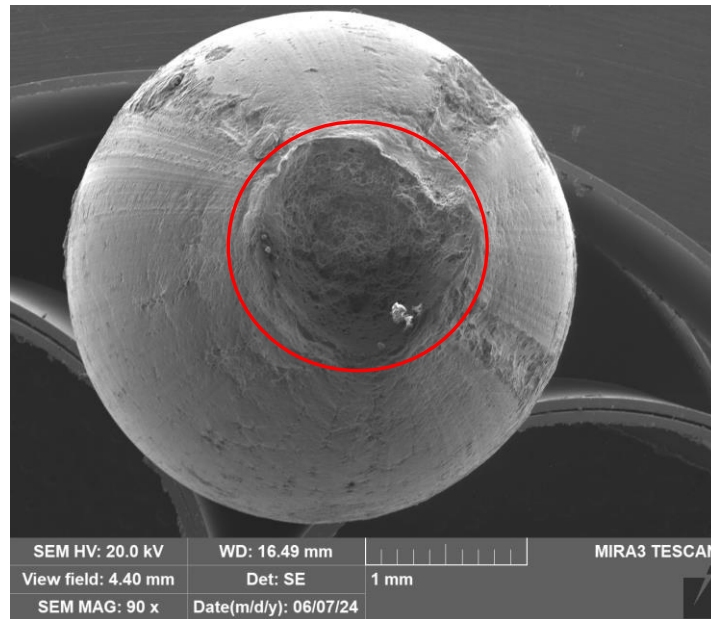


Figure 4-7: Low magnification SEM secondary image of a representative example of the fracture surface (ellipse) associated with the tapered-end (necked) geometry observed terminating the failed aluminum wire strands during the preliminary examination of conductor EL-2 (Figure 2-17). The image shows the general cup and cone morphology of the failed end of the wire strand.

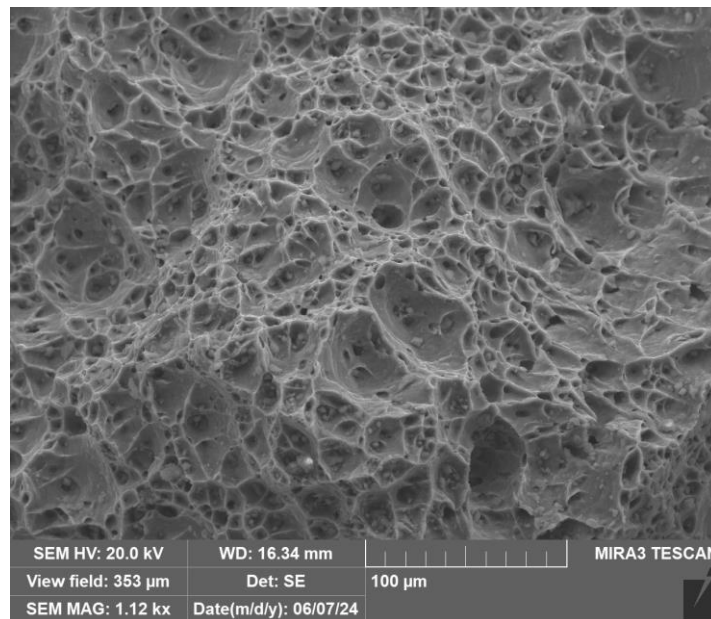


Figure 4-8: High magnification fractographic image within the proximity of the strand centroid shown in Figure 4-1. The image indicates that the strand fracture mechanism was dominated by void coalescence (i.e. ductile fracture) at the site.

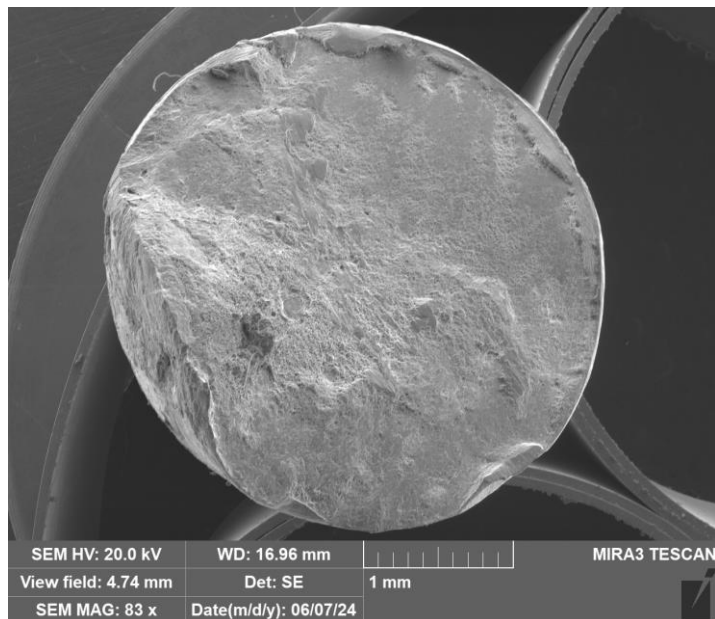


Figure 4-9: Low magnification SEM secondary image of a representative example of the fracture surface associated with the oblique geometry observed terminating the failed aluminum wire strands during the preliminary examination of conductor EL-2 (Figure 2-18).

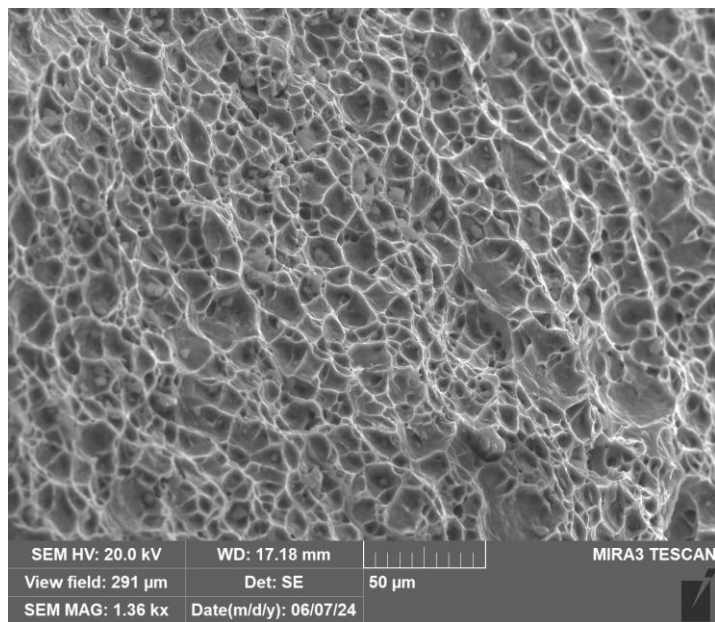


Figure 4-10: High magnification fractographic image within the proximity of the strand centroid showing the topological features associated with the strand fracture mechanism. Similar to Figure 4-8, the image suggests that the strand fracture mechanism was dominated by void coalescence (i.e. ductile fracture) at the site.

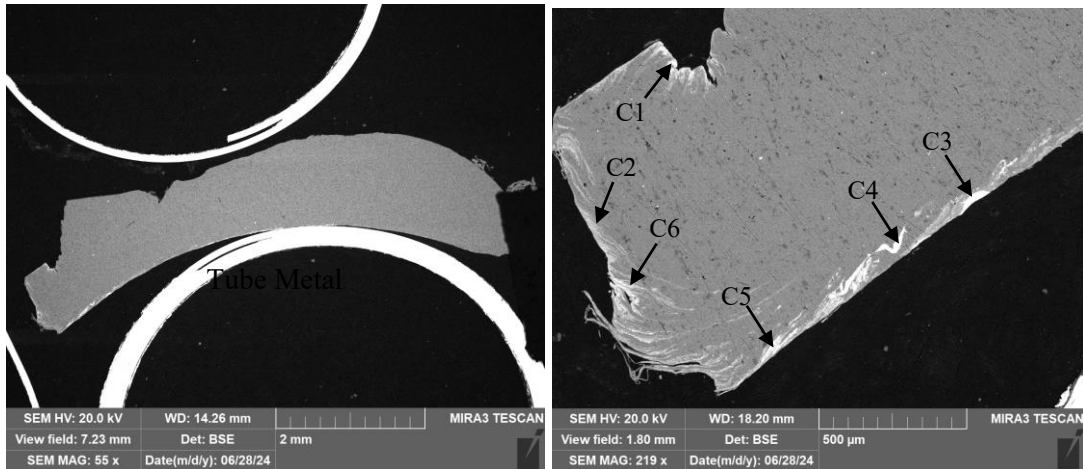


Figure 4-11: Sectional view SEM backscatter image of a representative example of the strand to strand fusing observed in conductor EL-2. The image also shows the location of the SEM EDS analyses conducted to determine the composition of the high density (light) phase observed (results are summarized in Table 4-3).

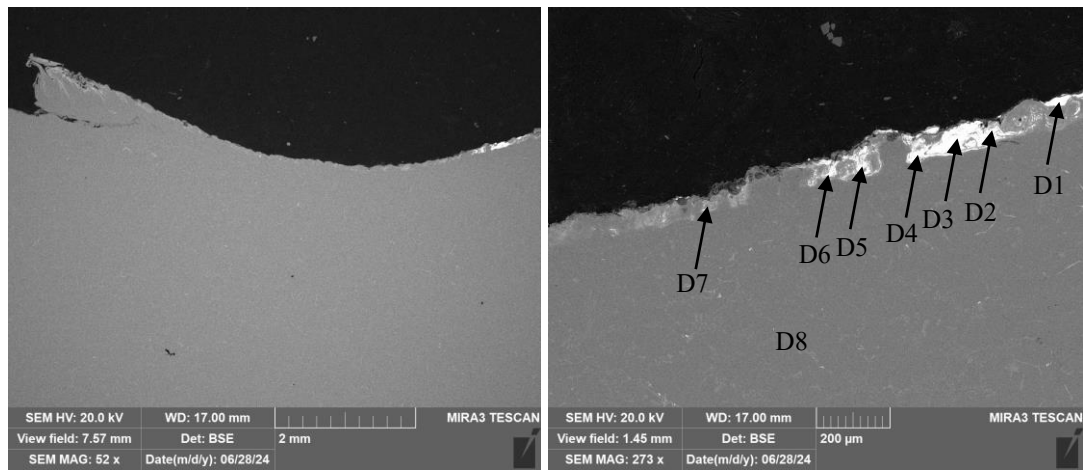


Figure 4-12: Sectional view SEM backscatter images of a representative example of the clamp material immediately adjacent to the site of localized brinelling observed. The image also shows the location of the SEM EDS analyses conducted to determine the composition of the high density (light) phase observed (results are summarized in Table 4-4).

## 5 SUMMARY AND DISCUSSION OF THE PHYSICAL EVIDENCE

---

### 5.1 Summary of the Physical Evidence

The following summarizes the physical evidence generated during the investigation for the failed sections of conductor EL-1 and EL-2 from suspension Tower #1225 provided for evaluation. Given the similarity of the physical evidence generated for conductor EL-1 and EL-2, the items below are relevant to both conductors unless otherwise noted. The physical evidence includes;

- The evidence provided by NL Hydro indicated that at Tower #1225, the line damage consisted of stripped and birdcaged outer conductors, which suggests that the inner steel reinforcing core remained intact at the tower.
- Adjacent to the termination of the insulator wire clamp, on the upper circumferential surface of the conductors, the ends of the aluminum wire strands were generally terminated by fracture failures. SEM fractographic analysis indicated that fracture surfaces associated with the failed wire strands were dominated by void coalescence (i.e. limit load ductile failure).
- Adjacent to the termination of the insulator wire clamp, on the lower circumferential half of the conductors, evidence of either severe distortion of the wire strands or strand to strand fusing was observed. SEM EDS analyses conducted for the fused wire strands detected the presence of zinc from the steel reinforcing strands embedded within the aluminum conductor material.
- Evidence of localized brinelling (plastic deformation) was observed adjacent to the lower, outboard axial end (on the conductor failure side) at the bottom dead center circumferential position of the wire clamp. The sectional profile of the brinelling was characterized by an approximately semi-circular morphology. SEM EDS analyses conducted detected the presence of zinc from the steel reinforcing strands embedded within the wire clamp material adjacent to the brinelling. The presence of the embedded zinc suggests that the steel reinforcing core was in contact with the lower surface of the wire clamp at the site.
- The wire strand diameters were measured for failed conductors EL-1 and EL-2. For conductor EL-1, the diameters of the aluminum conductor strands and the steel reinforcing strands ranged between 3.40 mm to 3.73 mm and 2.06 mm to 2.11 mm, respectively. For conductor EL-2, the diameters of the aluminum conductor strands and the steel reinforcing strands ranged between 3.43 mm to 3.71 mm and 2.16 mm to 2.26 mm, respectively. Measurements of the zinc coating thicknesses for steel reinforcing strands indicated the surface area density of the coating ranges for EL-1 and EL-2 were between 271.9 g/m<sup>2</sup> to 404.9 g/m<sup>2</sup> and between 261.2 g/m<sup>2</sup> to 268.8 g/m<sup>2</sup>, respectively.
- The wire strand diameters were also measured for a length of intact service exposed conductor provided for uniaxial tension testing. The diameters of the aluminum

conductor strands and the steel reinforcing strands ranged between 3.71 mm to 3.76 mm and 2.21 mm to 2.26 mm, respectively. Measurements of the zinc coating thicknesses for steel reinforcing strands indicated the surface area density of the coating range was between 171.9 g/m<sup>2</sup> to 332.3 g/m<sup>2</sup>.

- Uniaxial tension testing was conducted on a length of intact service exposed conductor. The results of the testing generated a breaking strength of approximately 196.6 kN, which exceeded the rated tension strength requirement of 187 kN [2].

## **5.2 General Discussion**

The physical, chemical and metallurgical evidence indicates that the mechanism responsible for the failure of conductors EL-1 and EL-2 at Tower #1225 is consistent with ductile limit load fracture of the aluminum conductor strands. It was reported that there was significant ice accumulation on the line prior to failure (estimated radial thickness of the ice was in the range between 100 – 125 mm) [1]. The wind velocity was also reported to be approximately 70 km/h and 60 km/h from an easterly direction on the day prior to and during the day of the failures, respectively [1]. It has been indicated that for a radial ice accumulation of approximately 25 mm, the design criterion for the maximum wind velocity reduces to 60 km/h [1]. The combination of the ice accumulation and wind velocities reported suggests that the line was operating in excess of the design criteria both on the day prior to and during the day of the failures. Given ice build-up and the direction of the wind reported, it is also probable that additional cyclic loading from wind induced galloping of the lines was present prior to the failures. Galloping of the conductors has been observed by NL Hydro on multiple occasions in the vicinity of Tower #1225 since the installation of the lines in 2017 [1].

The evidence also suggests that the steel reinforcing core migrated towards, and was in contact with, the lower surface of the insulator wire clamp. The downward bearing force responsible for the migration was sufficient to distort and cold pressure weld (fuse) adjacent aluminum wires together in the lower circumferential half of the conductor. It is reasonable to assume that the distortion and fusing of the aluminum strands would result in a decrease in the overall breaking strength of the conductor where it enters the wire clamp.

The evidence also suggests that the downward migration also resulted in contact between the steel reinforcing core and the bottom dead center surface of the insulator wire clamp, which, in turn, resulted in a localized area of brinelling on the surface of the wire clamp. It has been postulated that one in situ, non-destructive method of detecting steel core migration is radiographic imaging. It should be noted that if radiographic imaging is utilized, it should include a reference marker on the bottom surface of the wire clamp.

## **6 CONCLUSIONS AND RECOMMENDATIONS**

---

The conclusions and recommendations inferred by the investigation for the failed sections of conductor EL-1 and EL-2 from suspension Tower #1225 include:

- The physical, chemical and metallurgical evidence indicates that the mechanism responsible for the failure of conductors EL-1 and EL-2 at Tower #1225 is consistent with ductile limit load fracture of the aluminum conductor strands.
- The force required to precipitate a ductile limit load fracture mechanism of the aluminum conductor strands was attributed to the combination of ice accumulation and sustained wind velocities on the day prior to and during the day of the failures. It is also probable that wind induced galloping was present in the lines prior to the failures, which generated an additional cyclic force.
- The evidence suggests that the steel reinforcing core migrated towards, and was in contact with, the lower surface of the insulator wire clamp. The downward bearing force responsible for the migration was sufficient to distort and cold pressure weld (fuse) adjacent aluminum wires together in the lower circumferential half of the conductor. It is reasonable to assume that the distortion and fusing of the aluminum strands would result in a decrease in the overall breaking strength of the conductor where it enters the wire clamp.
- It has been postulated that one in situ, non-destructive method of detecting steel core migration is radiographic imaging. It should be noted that if radiographic imaging is utilized, it should include a reference marker on the bottom surface of the wire clamp. It is recommended that in consultation with experts in the field of radiography, that NL Hydro consider investigating the use of radiographic imaging to detect the presence of incipient damage in the conductors.

## **References**

---

- [1] Various E-mails provided by M. Veitch, Newfoundland and Labrador Hydro, June-September, 2024.
- [2] ASTM B232, “Standard Specification for Concentric-Lay-Stranded Aluminum Conductors, Coated Steel Reinforced (ACSR)”, ASTM International.
- [3] ASTM B230, “Standard Specification for Aluminum 1350-H19 Wire for Electrical Purposes”, ASTM International.
- [4] ASTM B233, “Standard Specification for Aluminum 1350 Drawing Stock for Electrical Purposes”, ASTM International.
- [5] ASTM A931, “Standard Test Method for Tension Testing of Wire Ropes and Strand”, ASTM International.

## Annex A Data Sheet for the ACSR Grackle (Zinc Coated) Conductor

Table A-1 is the manufactures' data sheet summary for the ACSR Grackle conductor with a zinc coated steel reinforcing core.

Table A-1: Manufactures' data sheet for the ACSR Grackle conductor (zinc coated steel reinforcing core).

ITEM	DESCRIPTION	UNIT	REQUIRED	GUARANTEED
1.0	Manufacturer Name			Midal Cables
2.0	Location of Manufacturing Plant			Bahrain
3.0	<b>Technical Characteristics</b>			
3.1	Type		ACSR	ACSR
3.2	Code name		Grackle	Grackle
3.3	Rated Tensile Strength	kN	187	194
3.4	Unit Weight of Complete Conductor	kg/m	2.28	2.271
3.4.1	Unit Weight of Aluminum	kg/km		1668.5
3.4.2	Unit Weight of Steel	kg/km		597.58
3.5	Coefficient of Thermal Expansion (Aluminum portion)	per °C	23.04 x 10 <sup>-6</sup>	23.04 x 10 <sup>-6</sup>
3.6	Modulus of Elasticity (Aluminum portion)			
3.6.1	Final	MPa	49090	49090
3.6.2	Initial Lower	MPa		36600
3.6.3	Initial Upper	MPa		36600
3.6.4	Change of Slope	MPa		NQ
3.7	Coefficient of Thermal Expansion (Steel portion)	per °C	11.52 x 10 <sup>-6</sup>	11.52 x 10 <sup>-6</sup>
3.8	Modulus of Elasticity (Steel portion)			
3.8.1	Final	MPa	21580	21580
3.8.2	Initial Lower	MPa		16090
3.8.3	Initial Upper	MPa		16090
3.8.4	Change of Slope	MPa		NQ
3.9	MaximumDC resistance at 20 °C	Ω/km	0.0472	0.0479
3.10	MaximumDC resistance at 25 °C	Ω/km		0.04887
3.11	MaximumDC resistance at 75 °C	Ω/km		0.05852
3.12	Minimum Aluminum Conductivity	% IACS		61
3.13	Emissivity Coefficient		0.5	0.5*
3.14	Solar Absorption Coefficient		0.5	0.5*
3.15	Aluminum Portion Heat Capacity	W.s/m.°C	3206.65	1537.2
3.16	Steel Portion Heat Capacity	W.s/m.°C	570.89	274.9
3.17	Nominal Cross-Sectional Area (Total)	mm <sup>2</sup>	680.64	680.07
3.18	Overall Diameter	mm	33.85	33.94
3.19	Number of Conductors per Pole	unit	1	1*
3.20	Number of Aluminum Wires (Stranding)	unit	54	54
3.21	Diameter of Aluminum Wires	mm	3.77	3.77
3.22	Type of Weld for Aluminum Wire Joint			Cold Pressure
3.23	Number of Steel Wires (Stranding)	unit	19	19
3.24	Diameter of Steel Wires	mm	2.26	2.26
3.25	Zinc Coating			
3.25.1	Thickness	g/m <sup>2</sup>		230
3.25.2	Class (as per CAN/CSA C60888)		Class A	Class A
3.26	PLS-CADD conductor file (*.wir) provided	Yes/No	Yes	Yes

**Quarterly Report on Asset Performance in Support of Resource Adequacy  
for the Twelve Months Ended March 31, 2025, Attachment 2, Appendix A, Page 48 of 54**

ISO 9001 ISO 14001 OHSAS 18001 Certified by 	<b>MIDAL CABLES LTD. (C.R.7108)</b> P.O. Box 5939, Kingdom of Bahrain Tel.: +973 17 832832 / 17 832833 Fax: +973 17 832932 / 17 832933 E-mail: midalcbl@midalcable.com Website: www.midalcable.com		شركة ميدال للكابلات المحدودة البحرين ٢٠١٤ ص.ب - ٥٩٣٩، مملكة البحرين هاتف: +٩٧٣ ١٧ ٨٣٢٨٣٢ / ١٧ ٨٣٢٨٣٣ فاكس: +٩٧٣ ١٧ ٨٣٢٩٣٢ / ١٧ ٨٣٢٩٣٣ البريد الإلكتروني: midalcbl@midalcable.com شبكة الكابلات: www.midalcable.com	
---	---	---	---	---

ITEM	DESCRIPTION	UNIT	REQUIRED	GUARANTEED
4.0	Reel			
4.1	Reel Construction	Wood/Metal	Metal	Metal
4.2	Flange	m	2.13	2.22
4.3	Traverse	m	1.47	1.25**
4.4	Drum	m	0.91	0.78
4.5	Arbor Hole	m	0.127	0.127
4.6	Drive Pin			
4.6.1	Diameter	mm		65
4.6.2	Distance Offset from Center	mm		300
4.7	Maximum Gross Reel Weight	kg		6700
4.8	Empty Reel Weight	kg		550
4.9	Nominal Conductor Length per Reel	m	2700	2700
4.10	Minimum Shipping Lots	lot		222 Reels
5.0	Lay Ratio			
5.1	Aluminum Outer Layer	max/min	14/10	14/10
5.2	Aluminum Inner Layers	max/min	16/10	16/10
5.3	12-Wire Steel Layer	max/min	20/14	20/14
5.4	6-Wire Steel Layer	max/min	26/16	26/16
6.0	Length Tolerance	%		-0/+1
6.1	Lay Direction			
6.1.1	Outer Strand of Aluminum Layer			Right Hand
6.1.2	Outer Strand of Steel Layer			Left hand

2014D91-09042014 Rev2



\*Client given data  
 \*\* Approx Overall Width Of Reel

## **Annex B Dimensional Characterization of the Failed Section of ACSR Grackle (Zinc Coated) Conductor EL-1**

---

Table B-1 summarizes the outer aluminum conductor and inner steel reinforcing wire strand diameter measurements for the failed section of conductor EL-1. Figure B-1 through Figure B-3 show representative examples of the thickness of the zinc coating present on the steel reinforcing wire strands.

*Table B-1: Summary of the outer aluminum conductor and inner steel reinforcing wire strand diameter measurements for the failed section of conductor EL-1.*

<b>Wire Strand No.</b>	<b>Wire Strand Diameter Ranges (mm)</b>					
	<b>Outer Aluminum Strands</b>			<b>Inner Steel Strands</b>		
	<b>Layer 1</b>	<b>Layer 2</b>	<b>Layer 3</b>	<b>Layer 4</b>	<b>Layer 5</b>	<b>Layer 6</b>
1	3.73	F/SD	3.68	2.18	2.08	2.11
2	3.63	3.73	3.68	2.11	2.08	
3	3.40	3.71	3.68	2.24	2.08	
4	3.43	3.56	3.68	2.13	2.11	
5	3.53	3.68	3.63	2.18	2.06	
6	F/SD	3.63	3.66	2.24	2.03	
7	3.68	3.61	F/SD	2.08		
8	3.68	3.63	F/SD	2.08		
9	3.38	3.66	F/SD	2.13		
10	3.66	3.66	F/SD	2.06		
11	3.56	3.63	F/SD	2.18		
12	3.63	3.66	F/SD	2.24		
13	3.63	3.61				
14	3.63	3.66				
15	3.63	3.66				
16	3.68					
17	3.61					
18	3.63					
19	3.63					
20	3.68					
21	3.71					
22	3.71					
23	3.68					
24	3.73					

Note 1: F/SD indicates that the wire strand was either fused to an adjacent strand or that the cross-sectional area of the strand was severely distorted.

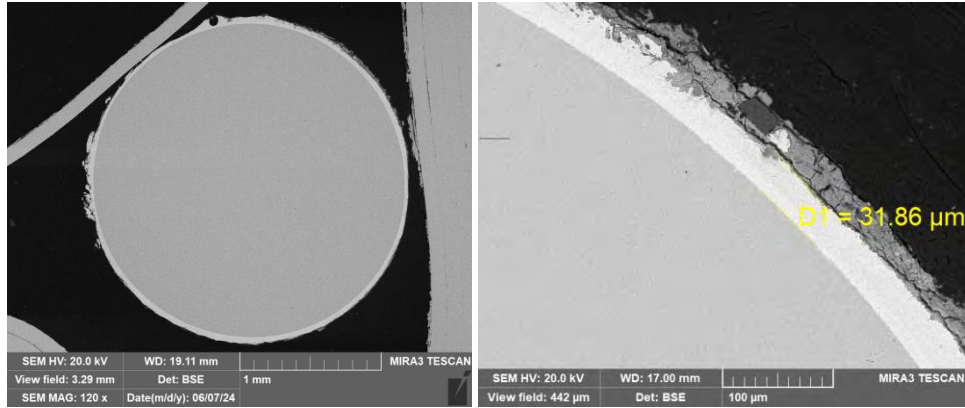


Figure B-1: SEM backscatter image of a representative example of a zinc coated steel reinforcing strand for failed conductor EL-1. The image shows the significant variation in the thickness of the zinc coating observed around the circumference of the steel reinforcing strand.

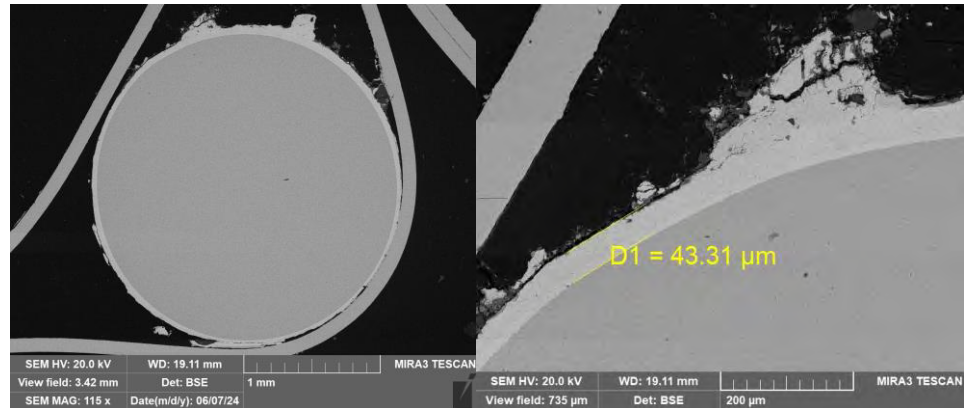


Figure B-2: SEM backscatter image of a representative example of a zinc coated steel reinforcing strand for failed conductor EL-1. The image shows the significant variation in the thickness of the zinc coating observed around the circumference of the steel reinforcing strand.

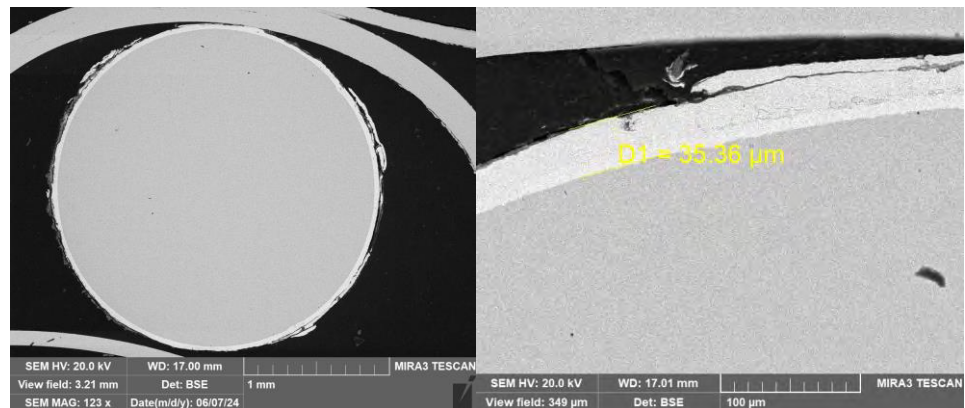


Figure B-3: SEM backscatter image of a representative example of a zinc coated steel reinforcing strand for failed conductor EL-1. The image shows the significant variation in the thickness of the zinc coating observed around the circumference of the steel reinforcing strand.

## **Annex C Dimensional Characterization of the Failed Section of ACSR Grackle (Zinc Coated) Conductor EL-2**

---

Table C-1 summarizes the outer aluminum conductor and inner steel reinforcing wire strand diameter measurements for the failed section of conductor EL-2. Figure C-1 through Figure C-3 show representative examples of the thickness of the zinc coating present on the steel reinforcing wire strands.

*Table C-1: Summary of the outer aluminum conductor and inner steel reinforcing wire strand diameter measurements for the failed section of conductor EL-2.*

<b>Wire Strand No.</b>	<b>Wire Strand Diameter Ranges (mm)</b>					
	<b>Outer Aluminum Strands</b>			<b>Inner Steel Strands</b>		
	<b>Layer 1</b>	<b>Layer 2</b>	<b>Layer 3</b>	<b>Layer 4</b>	<b>Layer 5</b>	<b>Layer 6</b>
1	3.68	3.61	3.71	2.18	2.24	2.24
2	3.61	F/SD	3.71	2.26	2.18	
3	3.58	F/SD	3.68	2.26	2.16	
4	3.43	3.66	3.71	2.21	2.21	
5	3.58	3.56	3.71	2.24	2.16	
6	3.68	3.61	3.71	2.24	2.24	
7	3.61	3.66	F/SD	2.24		
8	3.56	3.68	F/SD	2.21		
9	3.61	3.61	3.71	2.24		
10	3.66	3.68	3.66	2.26		
11	3.66	3.61	F/SD	2.26		
12	3.66	3.66	F/SD	2.26		
13	3.66	3.68				
14	3.63	3.66				
15	3.66	3.68				
16	F/SD	3.71				
17	F/SD	3.71				
18	F/SD	3.68				
19	F/SD					
20	F/SD					
21	F/SD					
22	3.68					
23	3.68					
24	F/SD					

Note 1: F/SD indicates that the wire strand was either fused to an adjacent strand or that the cross-sectional area of the strand was severely distorted.

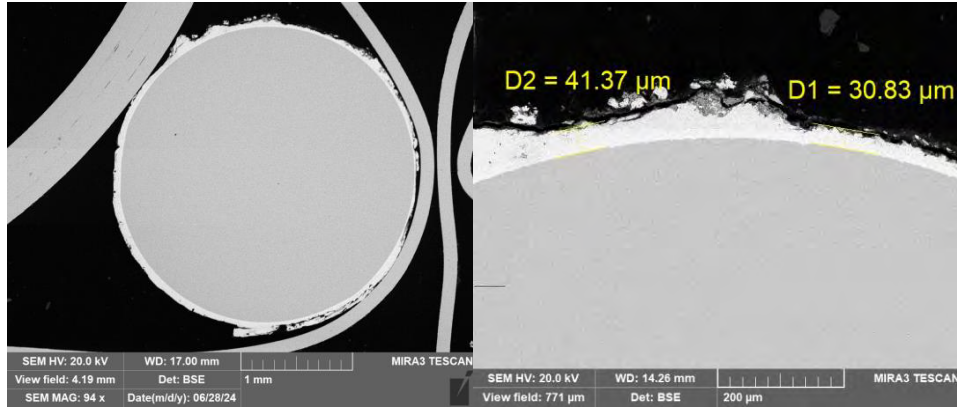


Figure C-1: SEM backscatter image of a representative example of a zinc coated steel reinforcing strand for failed conductor EL-2. The image shows the significant variation in the thickness of the zinc coating observed around the circumference of the steel reinforcing strand.

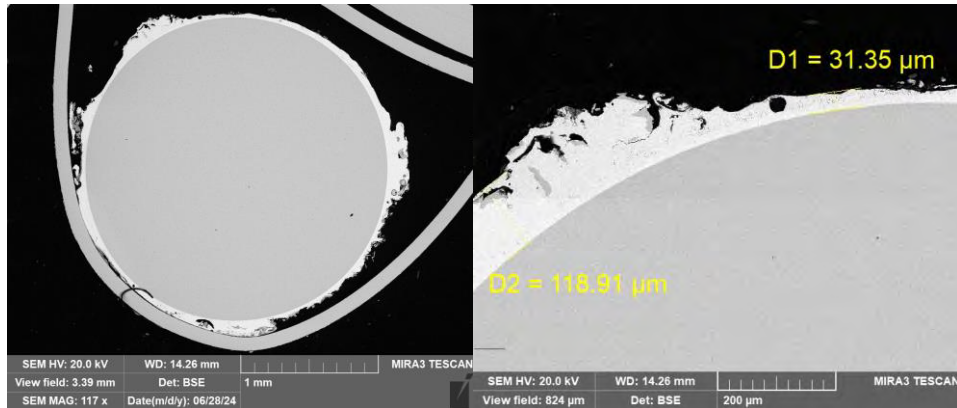


Figure C-2: SEM backscatter image of a representative example of a zinc coated steel reinforcing strand for failed conductor EL-2. The image shows the significant variation in the thickness of the zinc coating observed around the circumference of the steel reinforcing strand.

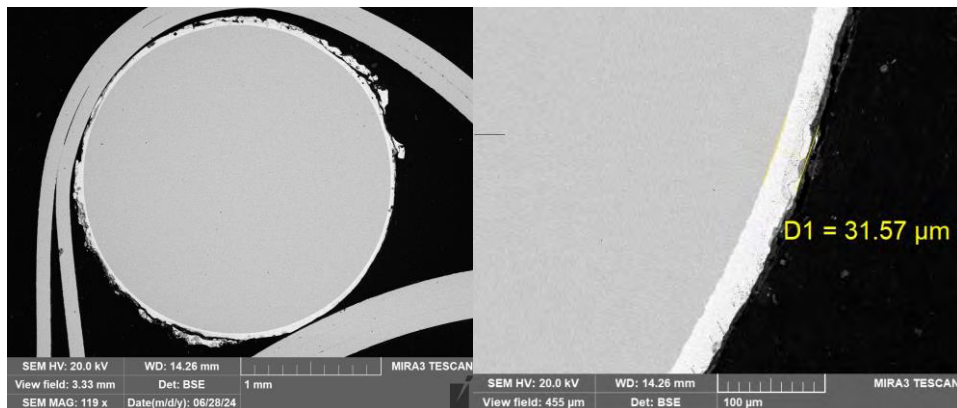


Figure C-3: SEM backscatter image of a representative example of a zinc coated steel reinforcing strand for failed conductor EL-2. The image shows the significant variation in the thickness of the zinc coating observed around the circumference of the steel reinforcing strand.

## **Annex D Dimensional Characterization of the Intact Service Exposed Section of ACSR Grackle (Zinc Coated) Conductor**

---

Table D-1 summarizes the outer aluminum conductor and inner steel reinforcing wire strand diameter measurements for the used intact conductor provided for uniaxial tension testing. Figure D-1 through Figure D-3 show representative examples of the thickness of the zinc coating present on the steel reinforcing wire strands.

*Table D-1: Summary of the outer aluminum conductor and inner steel reinforcing wire strand diameter measurements for the used intact service exposed conductor provided for uniaxial tension testing.*

<b>Wire Strand No.</b>	<b>Wire Strand Diameter Ranges (mm)</b>					
	<b>Outer Aluminum Strands</b>			<b>Inner Steel Strands</b>		
	<b>Layer 1</b>	<b>Layer 2</b>	<b>Layer 3</b>	<b>Layer 4</b>	<b>Layer 5</b>	<b>Layer 6</b>
1	3.73	3.73	3.71	2.21	2.21	2.21
2	3.71	3.71	3.71	2.24	2.21	
3	3.73	3.71	3.71	2.21	2.24	
4	3.73	3.71	3.71	2.21	2.24	
5	3.73	3.71	3.73	2.21	2.24	
6	3.71	3.73	3.71	2.21	2.21	
7	3.73	3.73	3.73	2.21		
8	3.73	3.73	3.73	2.24		
9	3.73	3.71	3.73	2.21		
10	3.73	3.73	3.73	2.21		
11	3.71	3.76	3.73	2.21		
12	3.76	3.76	3.73	2.24		
13	3.76	3.73				
14	3.76	3.73				
15	3.71	3.76				
16	3.73	3.73				
17	3.76	3.71				
18	3.76	3.71				
19	3.76					
20	3.73					
21	3.76					
22	3.76					
23	3.73					
24	3.73					

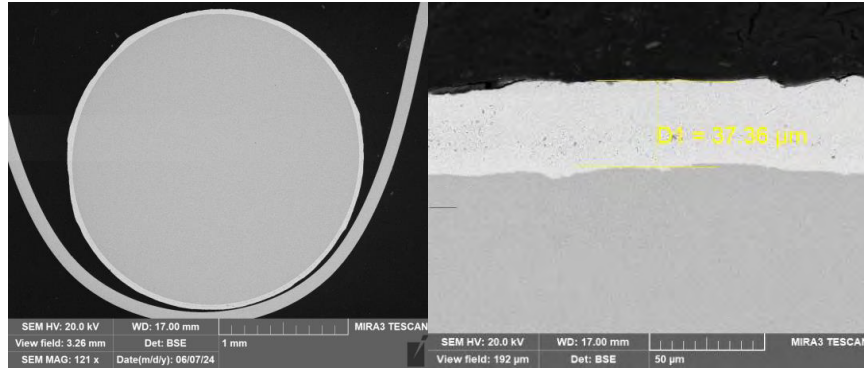


Figure D-1: SEM backscatter image of a representative example of a zinc coated steel reinforcing strand for the intact conductor. The image shows the significant variation in the thickness of the zinc coating observed around the circumference of the steel reinforcing strand.

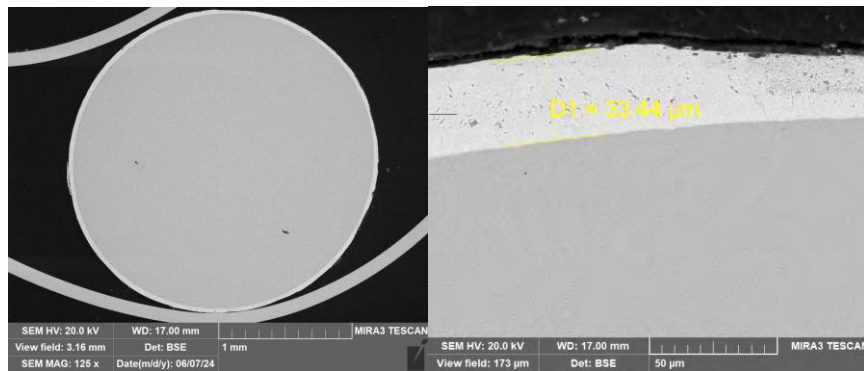


Figure D-2: SEM backscatter image of a representative example of a zinc coated steel reinforcing strand for the intact conductor. The image shows the significant variation in the thickness of the zinc coating observed around the circumference of the steel reinforcing strand.

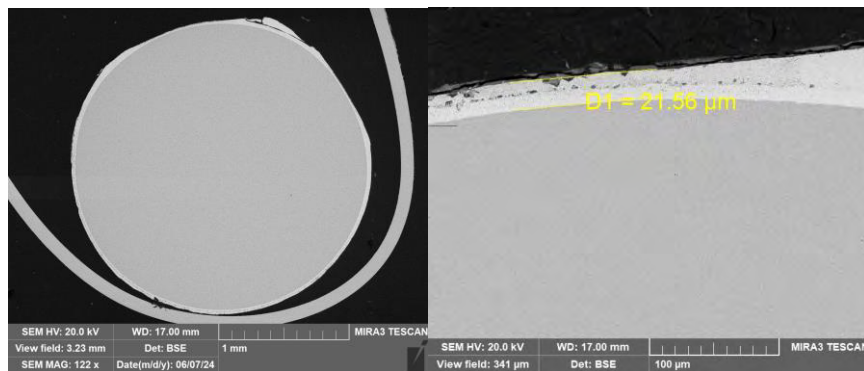


Figure D-3: SEM backscatter image of a representative example of a zinc coated steel reinforcing strand for the intact conductor. The image shows the significant variation in the thickness of the zinc coating observed around the circumference of the steel reinforcing strand.